NPL

Good Practice Guide No. 116

The Measurement of Rough Surface Topography using Coherence Scanning Interferometry

Jon Petzing, Jeremy Coupland
Loughborough University

Richard Leach
National Physical Laboratory

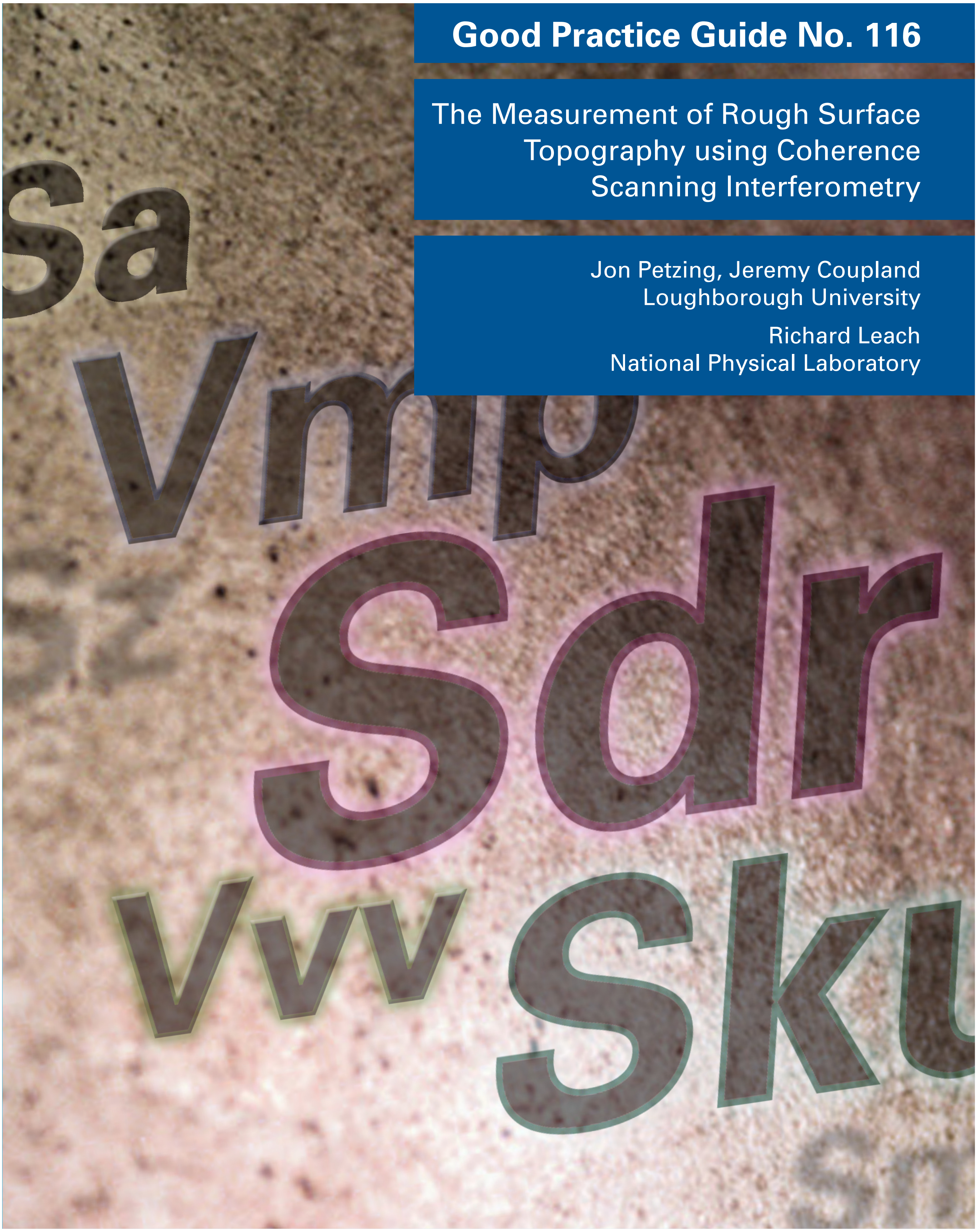

National
Measurement
System

Measurement Good Practice Guide No.116

The Measurement of Rough Surface Topography using Coherence Scanning Interferometry

Jon Petzing
Jeremy Coupland
Loughborough University

Richard Leach
National Physical Laboratory

ABSTRACT

The purpose of this guide is to describe good practice for the measurement and characterisation of rough surface topography using coherence scanning interferometry (commonly referred to as vertical scanning white light interferometry). This guide is aimed at users of coherence scanning interferometry for the optical measurement of surface texture within production and research environments. The general guidelines described herein can be applied to the measurement of rough surfaces exhibiting different types of surface topography. For the purpose of this guide, the definition of a rough surface is one that has features with heights ranging from approximately 10 nm to less than 100 µm.

ISSN 1368-6550

National Physical Laboratory
Hampton Road, Teddington, Middlesex, TW11 0LW

Acknowledgements

This Measurement Good Practice Guide has been produced and funded as part of the Engineering & Physical Sciences Research Council (EPSRC) Grand Challenge "Project 3D-Mintegration". Thanks are due to Dr Feng Gao (formerly Loughborough University), Mr Kanik Palodhi (Loughborough University) and Mr Claudiu Giusca (NPL) for their technical input, and to Mr David Flack (NPL), Dr Erik Novak (Veeco Instruments Inc.), Mr Ian Lee-Bennett (Ametek Taylor Hobson) and Dr Peter de Groot (Zygo Corporation) for reviewing the guide.

Contents

Figures

Tables

Introduction

1

IN THIS CHAPTER

- Scope of this guide
- Basic introduction to interferometry

Scope of this guide

The purpose of this good practice guide is to assist users in achieving a valid surface measurement on surfaces exhibiting roughness, texture and structures, using the technique of coherence scanning interferometry (CSI). Throughout the guide, the arbitrary definition of a rough surface is one which has features with heights ranging from approximately 10 nm to less than 100 µm. For those wishing to investigate surfaces that have heights less than 10 nm, then reference should be made to *NPL Measurement Good Practice Guide No.108 - Guide to the Measurement of Smooth Surface Topography using Coherence Scanning Interferometry*.

In 2002, the International Organization for Standardization (ISO) Technical Committee, dealing with Dimensional and Geometrical Product Specifications and Verifications (TC213), formed Working Group 16 to address standardization of areal (three dimensional) surface texture measurement methods. Working Group 16 is developing a number of draft standards (the ISO 25178 series) encompassing definitions of terms and parameters, calibration methods, file formats and characteristics of instruments. Under this process, a project team is developing standards for optical methods of areal surface texture measurement.

Where possible the terms, definitions, parameters and measurement practices that are used in the draft ISO 25178 standards have been adhered to in this guide. However, as the ISO 25178 series are draft standards, they are subject to modifications and additions. This guide will be updated to implement any changes and include any additions when the standards are formally published. The following terms that are listed in the draft standard on coherence scanning interferometry are also used to refer to CSI:

CPM coherence probe microscope
CSM coherence scanning microscope
CR coherence radar
CCI coherence correlation interferometry
MCM Mirau correlation microscope

WLI white light interferometry
WLSI white light scanning interferometry
SWLI scanning white light interferometry
VSI vertical scanning interferometry
RSP rough surface profiler
RST rough surface tester
HSI height scanning interferometer

The guide will cover the concepts of CSI, the terminology used in surface measurement with CSI, instrument set-up, calibration, uncertainty and filtering. The guide also considers the typical measurement procedures used, processing of the data using ISO standard areal roughness parameters and identifies specific limitations of CSI.

The following instruments were considered when preparing material for this guide: Taylor Hobson Talysurf CCI, Veeco NT1100, and Zygo NewView 5000 and NewView 6000. However, the guide is applicable to any CSI instrument.

Basic introduction to interferometry

CSI is a non-contacting measurement technique. It uses a broadband light source, and combines vertical (z-axis) scanning techniques with optical interferometry techniques, to achieve a three-dimensional (3D) surface measurement. To understand the above concepts an understanding of optical interferometry is desirable.

Constructive and destructive interference

Interferometry is the science and technique of superposing two or more waves, to create an output wave that differs from the input waves. Interferometry can be used to explore the differences between the input waves.

Interferometry is based on the idea that two waves with the same frequency that have the same phase will add constructively (Figure 1 – wave A combined with wave B results in wave C) whilst two waves that are out of phase by 180 º will destructively cancel each other (Figure 2 - wave A combined with wave B results in zero signal C assuming that both input waves have the same amplitude). This wave property is known as superposition and results in a set of dark and light bands known as fringes.

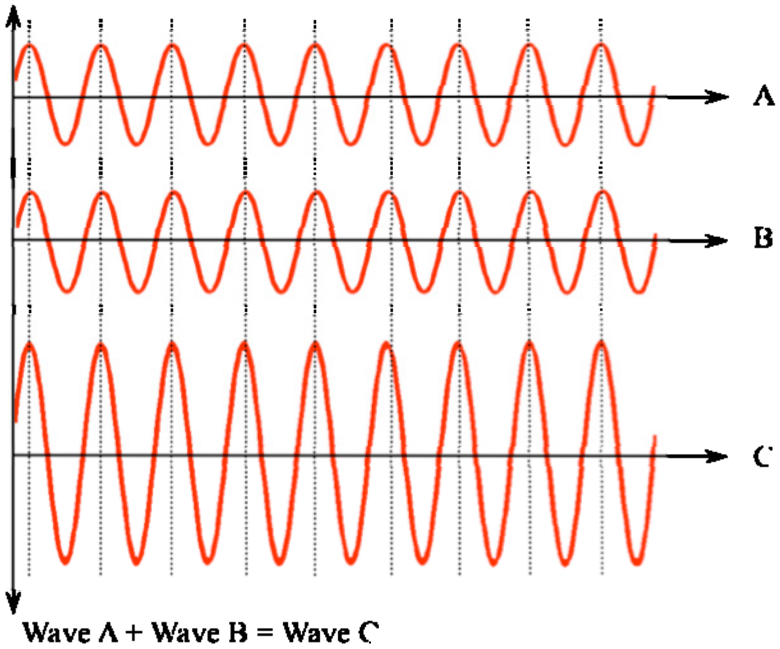

Figure 1 Graph of amplitude against time showing constructive interference

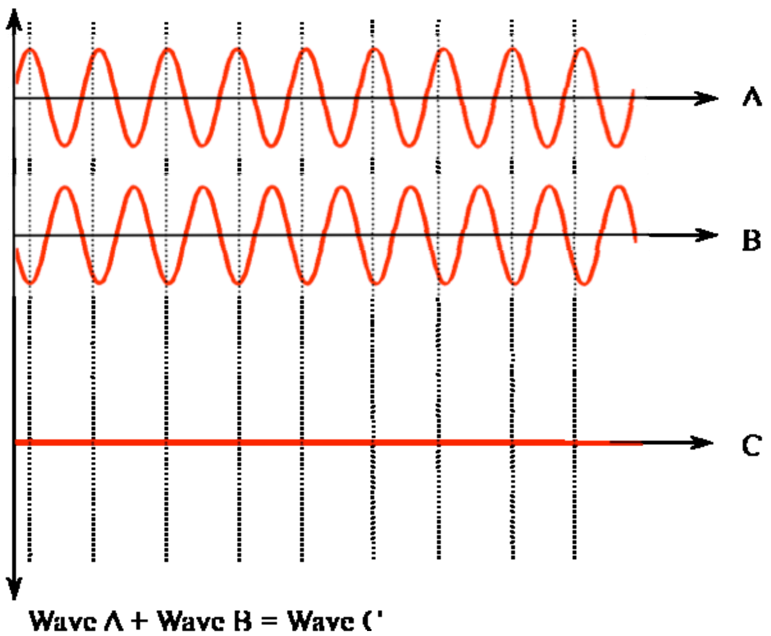

Figure 2 Graph of amplitude against time showing destructive interference

Superposition has been described mathematically in many texts. One of the core requirements for superposition to take place is that the optical wavefronts are plane waves (i.e., collimated) or, if the waves originate from a point source, the point source is sufficiently far away to approximate to a plane wave. Furthermore, it is also necessary that the polarisation vectors of the light in the two components are in the same plane, and that they are of the same frequency. The behavior of the two plane wavefronts and their interaction can be summarized as follows.

The amplitude of a plane wave at a position (x, y, z) and time, t, may be expressed as

$$E(x,y,z,t) = a\cos(\omega t - kz) \tag{1.1}$$

where a is the amplitude of the wave, $\omega = 2\pi \upsilon$ is the circular frequency (υ being the frequency of the light) and $k = 2\pi / \lambda$ is the wave number (λ being the wavelength of the light).

For more convenient mathematical manipulation, equation (1.1) can be expressed in complex exponential form as

$$E(x,y,z,t) = \mathrm{Re}\{A\exp(\omega t)\} \tag{1.2}$$

where $A = a \exp(-i\varphi)$ is the complex amplitude and $\varphi = 2\pi z / \lambda$.

Typically, in an interferometer a wave is split into two parts which travel different paths, and the waves are combined to create interference. This can be achieved using either wavefront division or amplitude division. The complex amplitude at any point in the image plane is the sum of the complex amplitudes of the two interfering wavefronts (A_1 and A_2), such that

$$A = A_1 + A_2\,. \tag{1.3}$$

Consequently, the intensity at any point in the image plane can be described as

$$
\begin{aligned}
I &= |A|^2 \\
I &= |A_1|^2 + |A_2|^2 + A_1 A_2^* + A_1^* A_2 \\
I &= I_1 + I_2 + 2\sqrt{I_1 I_2}\cos\Delta\varphi
\end{aligned}
\tag{1.4}
$$

where I_1 and I_2 are the individual intensities of the two wave components, and $\Delta\varphi = \varphi_1 - \varphi_2$ is the phase difference.

Assuming that a common source is used for the two wavefronts, then the phase difference can be related directly to the optical path difference (OPD)

$$
OPD = \left(\frac{\lambda}{2\pi}\right)\Delta\varphi . \tag{1.5}
$$

When the paths differ by an even number of half wavelengths, the superposed waves are in phase and constructive interference is observed, increasing the amplitude of the output wave. When they differ by an odd number of half wavelengths, the combined waves are 180 º out of phase and destructive interference is observed, decreasing the amplitude of the output. A schema of how the split beams produce constructive interference via amplitude division is shown in Figure 3.

In amplitude division, the two beams are derived from the same portion of the original wavefront. Beam-splitters (plates, cubes), diffraction gratings and polarising prisms can all be used to achieve amplitude division, although probably the most common optical element used is a beam-splitter.

Interferometry is also dependent on the light source used, typically either a monochromatic source or a white light source. These light sources will display different characteristics that determine aspects of the optical designs of the interferometers. These characteristics include temporal coherence, spatial coherence, wavelength and divergence.

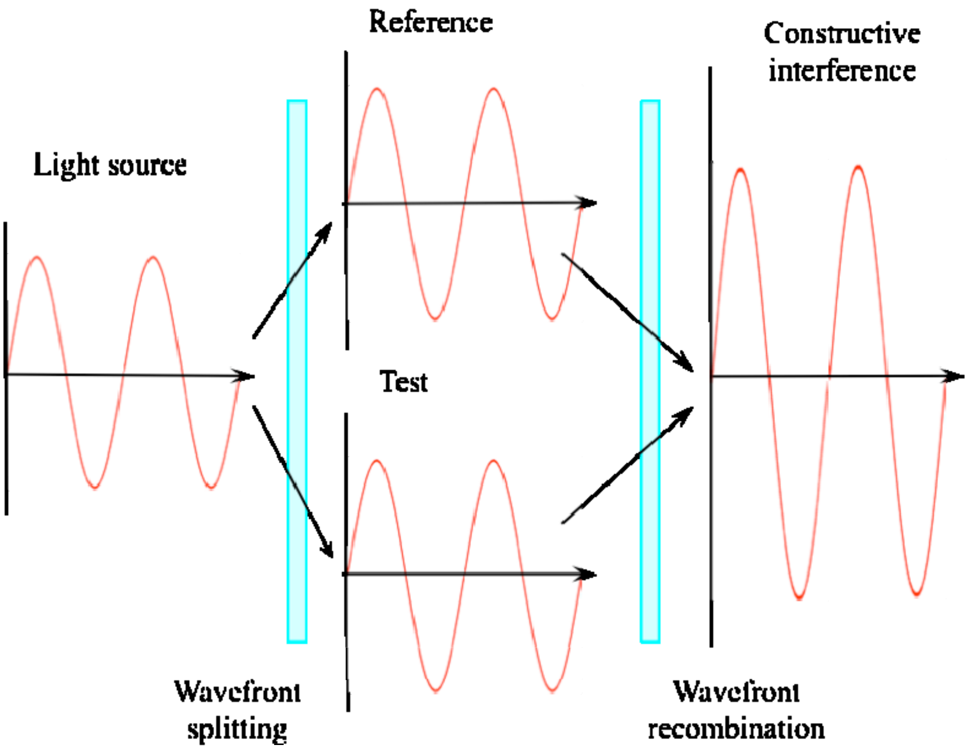

Figure 3 Constructive interference from one light source

Interferometry using monochromatic light sources

One of the most common interferometer designs is the Twyman-Green interferometer. A typical Twyman-Green interferometer will include a light source, beam-splitter, reference mirror or surface, a measured surface and an observation screen or image plane. These elements are shown in Figure 4, where the monochromatic light source is a laser.

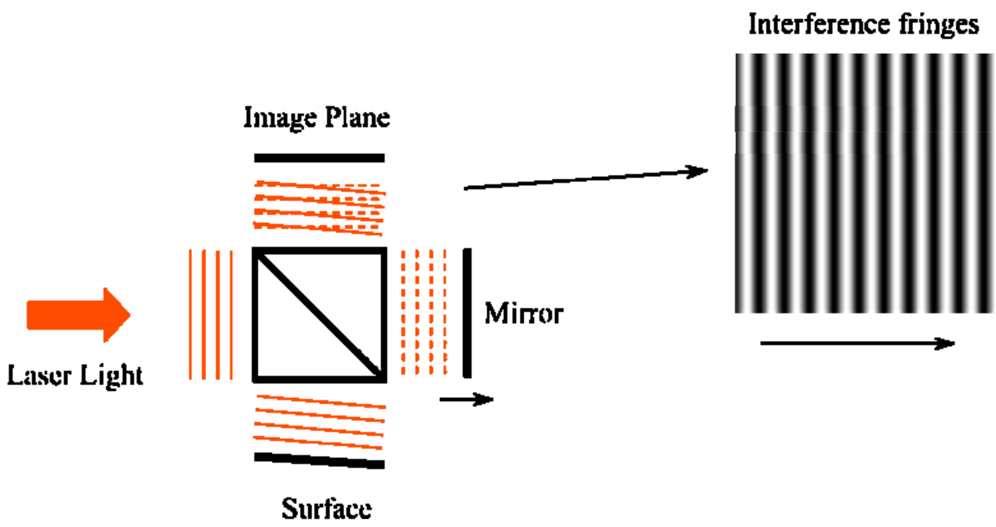

Figure 4 Twyman-Green interferometer using a laser

The light is split into two components so that one component strikes a fixed reference mirror and the second component is reflected from a test surface. When the reflected components are brought back together at an observation screen or image plane, an interference pattern results. This process assumes that any change of optical path difference between the two components is within the coherence length of the light source. For modern, single mode monochromatic laser sources, the coherence length will range from millimetres to tens of metres. Note that Temporal coherence is the measure of the average correlation between the value of a wave at any pair of times, separated by a given delay. Temporal coherence tells us how monochromatic a source is. In other words, it characterises how well a wave can interfere with itself at a different time.

If the measured surface and the reference mirror are perfectly flat and have a fixed (small) angle between them, the interference fringes formed at the image plane are a pattern of dark and light stripes. When the reference mirror is moved, as indicated in figure 5, the fringe pattern translates across the image plane.

Interferometry using white light sources

A white light interferometer uses incandescent light or polychromatic light instead of a monochromatic light source or laser. A separate set of interference fringes is simultaneously produced for each wavelength within the white light source, and consequently the intensity at any point in the image plane is a summation of these different fringe sets.

When the optical path difference of the measurement and reference wavefronts is carefully adjusted to zero at the centre of the field, a white light interference pattern will appear at the image plane, with all fringe systems derived from all of the constituent wavelengths having a maxima at this position. Because the coherence length of a white light source is typically only a few wavelengths, the interference pattern formed has different characteristics to a monochromatically derived interference pattern. Only a few fringes appear and the contrast of the fringes varies, because the fringe spacing is dependent on the wavelength.

The highest contrast fringe occurs when the optical path difference is zero. As the optical path difference increases, the interference fringes no longer coincide, resulting in a sequence of colours and a rapid decrease in contrast, as depicted in the Twyman-Green interferometer shown in Figure 5. As in the monochromatic case, if the reference mirror moves, the white light interference fringes move at the image plane.

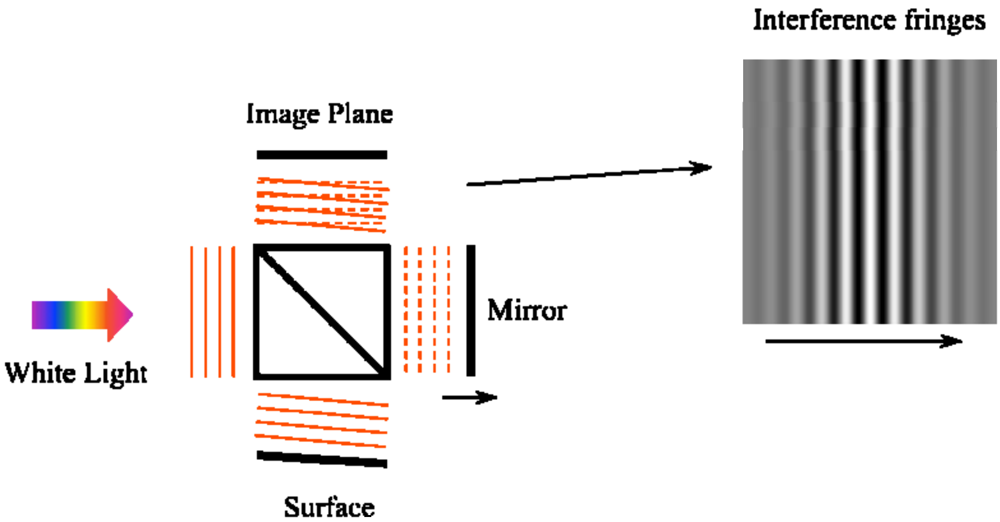

Figure 5 Twyman-Green interferometer using a white light source

Two aspects of white light interferometry make it particularly suited to surface feature analysis. Firstly, interference only occurs when the optical path difference is close to zero thus reducing any ambiguity of position. Secondly, the measurement range of a white light interferometer is limited only by the scanning range of the mechanical system that moves the reference mirror.

To extract surface topography information from interference patterns, however, requires careful interpretation of the fringe pattern, using one of a number of different techniques that are covered in chapter 2.

Coherence scanning interferometers

2

IN THIS CHAPTER

- Typical CSI instruments
- Terminology used with CSI
- Interferometric objective lenses
- Fringe formation from vertical scanning
- Analysis of the fringe data
- Peak detection methods

Coherence scanning interferometers

CSI forms the basis for a significant number of surface measuring instruments produced by a variety of instrumentation manufacturers. The purpose of this section is to allow the user to understand the operational principles of CSI and the processing methods that are used for surface measurement.

Typical CSI instruments

The use of CSI for surface measurement is based on the analysis of the interference pattern of two white light optical wavefronts, the object wavefront being reflected from the sample surface, whilst the reference wavefront is reflected from a reference mirror. As a method of distance measurement, the basis for CSI is not new. It was used by A. A. Michelson to determine the length of the International Prototype Metre in the Bureau International des Poids et Mesures in Sèvres in 1892. When augmented with modern imaging equipment and computers, CSI can be turned into a very powerful technique. Typical examples of CSI instruments produced by a range of manufacturers are shown in Figure 6.

CSI instruments typically incorporate a measurement base supported on an anti-vibration table, to negate the effect of environmental vibration sources. A translating/tilting table and a vertical column (or a bridge) are mounted onto the measurement base. The tilting table provides up to several degrees of tilt adjustment around two orthogonal axes (typically the x and y axes). A two axis stage mounted onto the tilting table provides up to several hundreds of millimetres of movement range in the two orthogonal directions.

Tilt adjustment is also provided around the x and y axes, with z axis rotation an additional option. Tilt adjustment will be necessary for fringe pattern optimization and may be necessary for specimen presentation depending on the range and slope of surface features. Stage movement and adjustment may be manually operated or motorized via a joystick control. Instruments often incorporate computer controlled motorized axes allowing for the possibility of field stitching – the building up of a patch work of images over an extended lateral range.

Figure 6 A selection of commercially available CSIs. Clockwise from bottom left: Mahr, Phase Shift, Polytec, Taylor Hobson, Veeco, Fogale and Zygo

A column (or bridge structure) supports the optical interferometry system and vertical scanning system. Some CSI instruments locate the optical source in a specially designed optical source house and light is delivered to the interferometer by an optical fibre. The electronic control and measurement systems together with a computer for data processing are included as part of the instrumentation packages. Display screens provide real-time viewing of raw interference fringe patterns, specimen monitoring and data processing.

The optical path difference change is achieved by moving the object, the scanning head, or the reference mirror at a constant speed. In a typical CSI an image sensor registers the intensity changes storing multiple frames, while the optical path difference varies in a predefined fashion. One of the most commonly used methods is to scan the head of the instrument (containing the reference mirror) in the vertical direction, resulting in one of the generic names of the technique: vertical scanning white light interferometry (VSWLI). A typical optical configuration as defined in ISO/FDIS 25178-604 (2010) is shown in Figure 7. Coarse scanning in the vertical direction (hundreds of micrometres to tens of millimetres) is often achieved using stepper motors, whilst fine scanning in the vertical direction (tens of nanometres to hundreds of micrometres) is achieved using piezo-electric actuators (PZTs) or stepper motors with nanometre steps. The scanning mechanisms are pre-calibrated to provide accurate movement and additionally may be user calibrated on a regular basis.

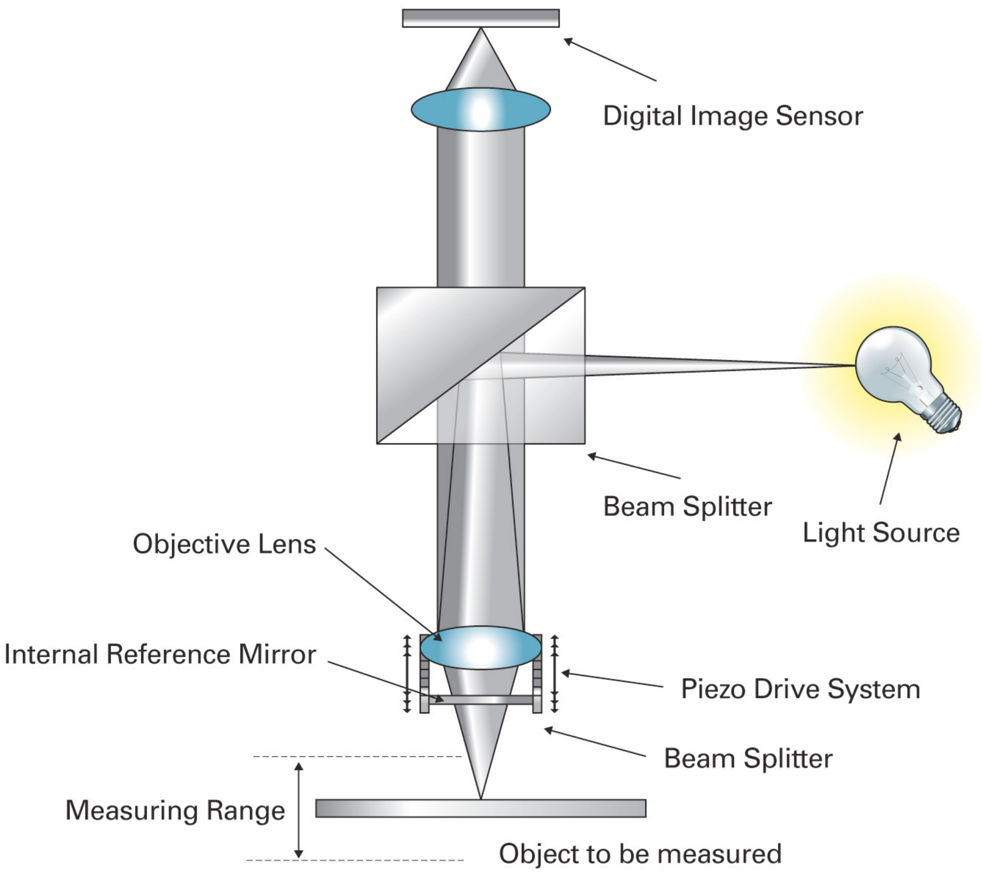

Figure 7 A typical CSI design

Terminology used with CSI

As with all measurement instruments, there are terms and phrases that are frequently used when describing aspects of instrument design or use. Some of these are given below.

Effective mean wavelength

The effective mean wavelength is the wavelength that is used in CSI and is defined as twice the period of the interference fringe closest to the modulation envelope peak. One fringe is the scanning distance of half of the effective mean wavelength. The period of an interference fringe is the scan distance separating two neighboring peaks in the CSI. The effective value of the wavelength used to measure a surface is affected by such parameters as the light source spectrum, the spectral transmission of the optical components, the tip/tilt of the surface, the numerical aperture of the microscope objective, and the spectral response of the image sensor array.

Fringe order error

Fringe order error is an error in the identification of the correct fringe when mapping heights using interference phase for surface topography calculations. Fringe order errors in CSI can be the result of errors in the analysis of the modulation envelope. They are equivalent to integer multiples of one-half the equivalent wavelength in height. They are also sometimes termed 2π errors and result in discontinuous profiles.

Instrument noise

Instrument noise is typically a small random error term superimposed on the measurement data. It is often caused by electronic noise (for example due to the imaging device, amplifiers and detectors). Some manufacturers provide software routines to directly assess instrument noise to incorporate into an error compensation file or routine.

Lateral resolution

The lateral resolution of CSI is defined as one-half the spatial period for which the instrument response (measured height map compared to the actual surface topography map) falls to 50 %. For a theoretically perfect optical system with a filled objective pupil, the lateral resolution is theoretically given by the Raleigh criterion, and is equal to 0.61 times the mean wavelength of the light source divided by the numerical aperture of the objective lens (see below). Hence lateral resolution will change with the numerical aperture of the objective lens.

Modulation envelope

The modulation envelope is the overall variation in signal strength of a CSI signal as a function of scan position. The modulation envelope is not necessarily a rigorously defined aspect of the signal. The quantitative shape of the envelope is related closely to the means by which it is calculated. The modulation envelope is most closely associated with the idea of fringe localisation, which is a basic characteristic of CSI signals. The modulation envelope is a consequence of limited optical coherence, which follows from using a spectrally broadband light source (white light), a spatially extended light source, or both.

Numerical aperture

Numerical aperture (A_N) is defined as the sine of the half aperture angle multiplied by the refractive index of the surrounding medium (most typically air at $n \approx 1$), thus

$$A_N = n \sin\theta \,. \tag{2.1}$$

The numerical aperture is also approximately equal to the objective pupil radius divided by the focal length, multiplied by the index of refraction of the surrounding medium.

Optical path length

The optical path length (OPL) is the product of the geometric length of the path light follows through the system, and the index of refraction of the medium through which it propagates.

Repeatability

Repeatability is the ability of an instrument to provide closely similar indications for repeated evaluation of the same measurement under the same conditions of measurement.

Scan increment

The scan increment is the distance traversed by the CSI scan between individual camera frames or data acquisition points. This is typically one eighth of the effective or mean wavelength of the instrument that samples the fringes at 90° increments.

Scan length

The scan length is the total range of physical path length traversed by the CSI scan. The scan length is usually synonymous with the total displacement of an interference objective mechanically translated along its optical axis during data acquisition.

Scan rate

The scan rate is the speed of vertical motion used during a vertical scan.

Spectral bandwidth

Spectral bandwidth is the spread in wavelengths of the light used to measure a surface. Instruments may be constructed with light sources (for instance light emitting diodes) with a limited spectral bandwidth and/or with additional filter elements to further limit the spectral bandwidth.

Vertical resolution

The vertical resolution of a CSI instrument is the ability of the instrument to resolve a surface profile vertically, that is in the z axis. Typically, instrument manufacturers will identify this as being 0.1 nm or less.

Interferometric objective lenses

Different designs of interferometer based microscope objectives can be used for a CSI instrument. Two of the most common are the Mirau and the Michelson objectives. In a Mirau objective the basic building blocks are a microscope objective lens, a reference surface and one semi-transparent optic (beam-splitter). These elements are configured as shown in the Figure 8.

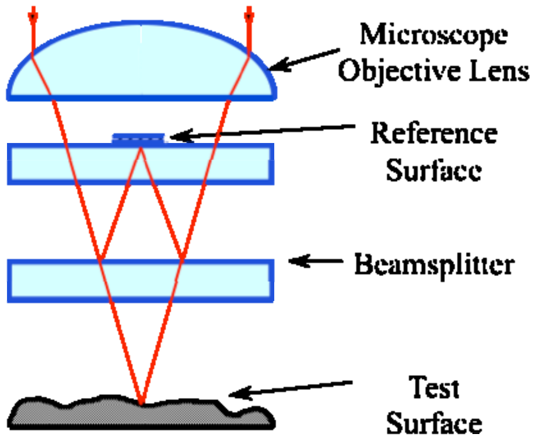

Figure 8 Schematic of a Mirau objective

There are two paths or beams from the light source to the detector. One beam reflects from the top surface of the beam-splitter, travels to the reference surface/mirror and is reflected back. It is again reflected off the beam-splitter, to the microscope objective lens and on to the detector. The other beam travels through the beam-splitter, to the test surface, reflects back to the microscope objective lens and on to the detector.

A Michelson objective (Figure 9) is configured in a similar manner to a Mirau objective but the reference surface is in a different position. This configuration is normally used for low magnification powers (less than 5×), when the reference mirror is too large to be placed in the position shown in Figure 8.

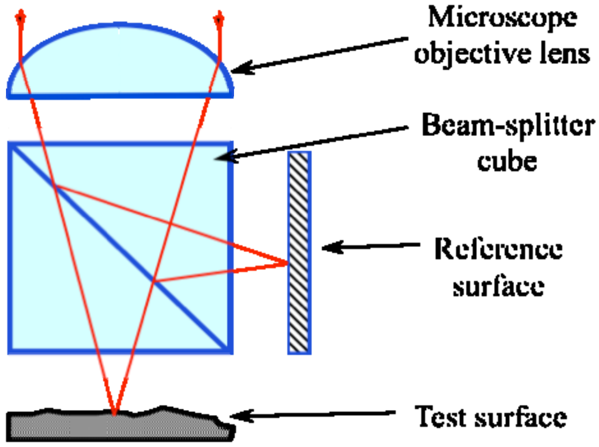

Figure 9 Schematic of a Michelson objective

Fringe formation from vertical scanning

Surface topography is deduced from the interference fringes that are observed as the object is scanned in a vertical direction. Figure 10 shows successive images from a scan of a flat polished surface, illustrating the development of fringe patterns. A similar series of images for a sphere is shown in Figure 11.

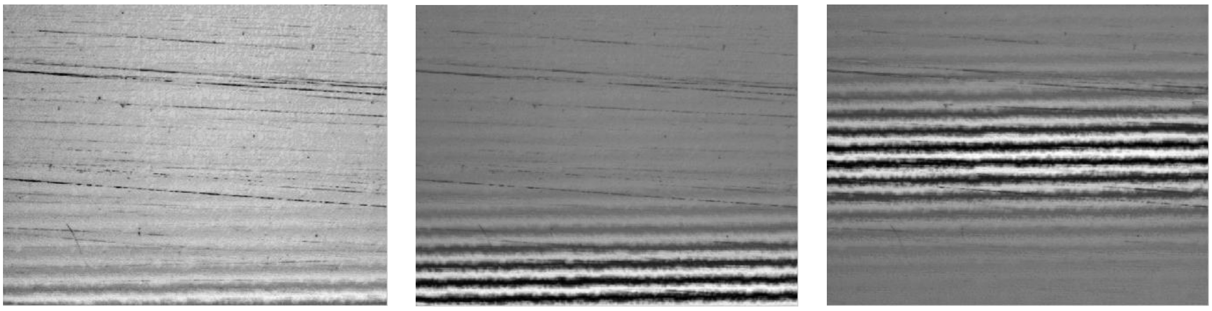

Figure 10 Successive images and fringe patterns from a flat surface

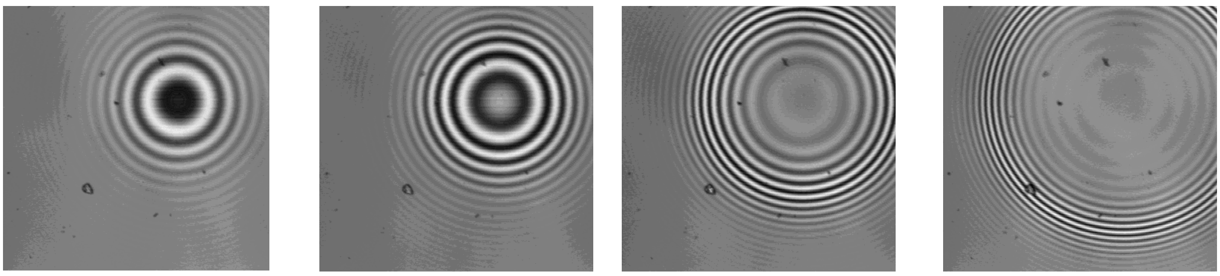

Figure 11 Successive images and fringe patterns from a sphere (courtesy of Veeco)

In Figure 10 and Figure 11, the fringes result from the interference of the field scattered from the object with that reflected from the reference surface. As the object is scanned relative to the reference surface, individual pixels within the image are seen to brighten and darken as they meet the conditions for constructive and destructive interference respectfully. Analysis of the data can be considered on a pixel basis, identifying intensity changes for each pixel on a plane by plane basis, i.e. vertically drilling down through the multiple planes of data, pixel by pixel, as shown in Figure 12.

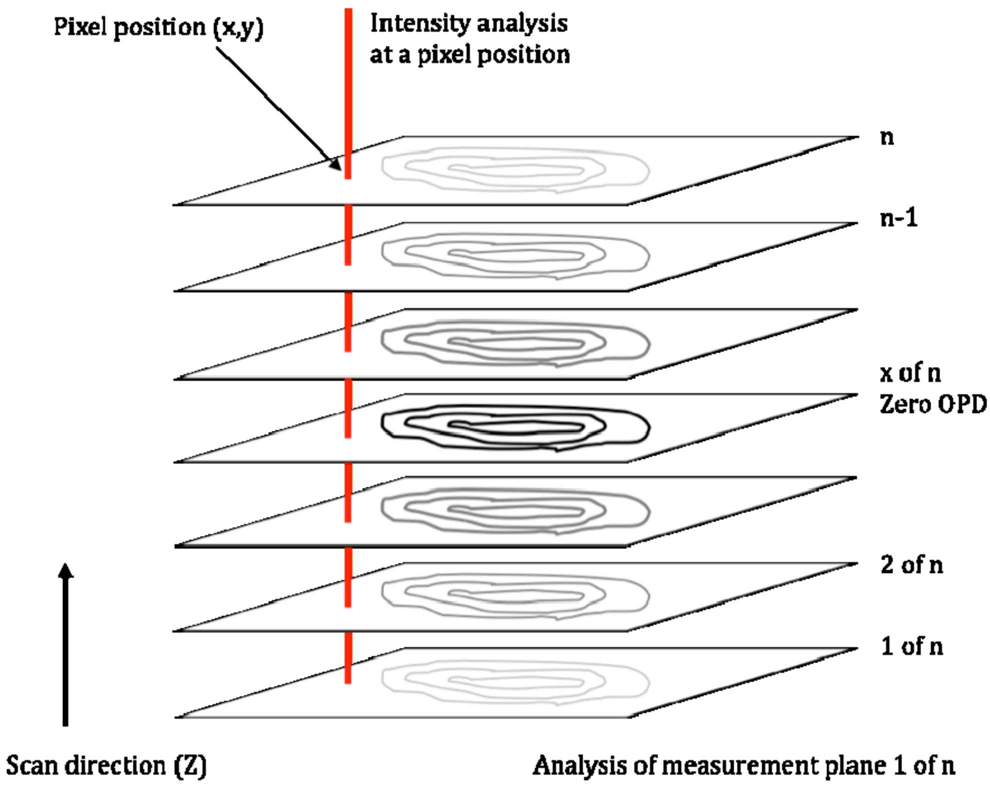

Figure 12 Intensity analysis on a pixel basis

A combination of broadband illumination and high numerical aperture means that the conditions for interference are only observed for a small part of the scan and only when the object and reference paths are closely matched. The form of the fringes can be explained in two equivalent ways. The conditions for interference require that the object and reference fields must have a degree of mutual coherence.

An incoherent (broadband and distributed) source is utilized and consequently the fields illuminating and scattered from the object and reference surfaces also have limited coherence. Unless the path lengths are closely matched the scattered and reference fields will be mutually incoherent and no interference will be observed. In this way, the envelope of the interference fringes can be thought of as a measure of the mutual coherence of the fields in the direction of the scan.

The recorded intensity can also be thought of as the superposition of the individual interference fringes due to plane wave components at different wavelengths and propagating through different angles in the interferometer. This explanation is presented in Annex B of ISO/FDIS 25178-604 where it is shown that for the case of a planar surface region that is normal to the optical axis of the instrument, the intensity, $I_{x,y}$ at a given pixel can be written in the form

$$I_{x,y}(\zeta) = I_0(\zeta) + I_{AC}\left(\zeta - h_{x,y}\right)\cos\left[K_0\left(\zeta - h_{x,y}\right)\right] \qquad (2.2)$$

where ζ and $h_{x,y}$ are the height of the reference and the object surfaces at the pixel location, I_0 is a constant offset intensity term and I_{AC} is the slowly varying modulation envelope intensity. The spatial frequency, K_0 is related to the mean effective wavelength, λ_0, such that

$$K_0 = {}^{4\pi}\!/_{\lambda_0}\,. \qquad (2.3)$$

For a low numerical aperture objective the mean effective wavelength is the arithmetic mean of the source spectrum but increases slightly from this value as the numerical aperture increases. Equation (2.2) is illustrated in Figure 13. The term $I_{AC}\left(\zeta - h_{x,y}\right)$ describes the modulation envelope and is related to the spectral bandwidth and the numerical aperture of the objective.

In the absence of dispersion the strongest interference is observed when the path length imbalance is zero and consequently the modulation envelope provides an estimate of the position of the object surface. The uncertainty in this estimate is proportional to the width of the modulation envelope. Typically this is inversely proportional to the square of the source bandwidth but as the numerical aperture of the objective is increased there is also a corresponding decrease in the width of the modulation envelope.

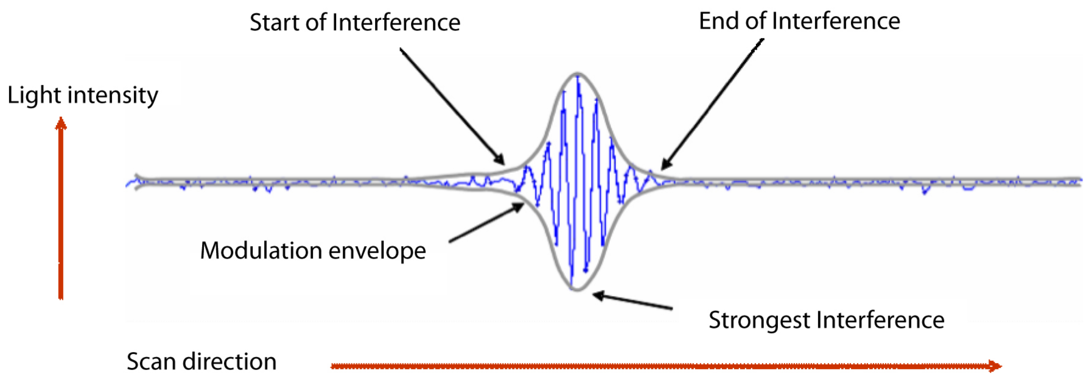

Figure 13 Pixel intensity as a function of scan direction

While the modulation envelope provides a broad estimate of the position of the object surface, the relatively high spatial frequencies within the fringe modulation provide a better measure. For this reason most CSI instrumentation uses the modulation envelope to estimate fringe order and subsequently the object surface is deduced from the phase of the underlying fringe pattern.

Analysis of the fringe data

Different fringe analysis methods are offered by different instrument manufacturers to extract surface topography data, but the methods are all similar in concept. The surface height is deduced either by detection of the modulation envelope, phase estimation or a combination of these. It is worth noting, however, that real fringe data is likely to deviate from this ideal form for reasons including aberrations and dispersion introduced by the objective lens, surface tilt, roughness and multiple scattering effects, and noise introduced during the measurement process. For these reasons robust estimators for the key fringe parameters have been devised (these are not described here).

Envelope detection

The modulation envelope is given by the term $I_{AC}\left(\zeta - h_{x,y}\right)$ in equation (2.2) (and see figure 15). Envelope detection is one of the most popular methods for the generation of surface topography data. As will be described later, the envelope term can be extracted in several ways each of which essentially demodulate the signal around the fringe frequency, K_0. In general, envelope detection is a robust technique, as it is less prone to noise than other techniques. The technique is based on estimating the surface height by fitting a curve to the envelope function or calculating the centroid rather than to rely on its peak value.

Phase estimation

The fringes themselves have a higher spatial frequency content than their envelope and for the case of smooth surfaces provide a better estimate of surface height. Although the absolute phase of the fringes depends on the complex refractive index of the surface, if the phase information is uniform the surface profile can be deduced reliably from the relative phase of the fringes.

Since phase can only be determined unambiguously over the interval zero to 2π the method can only be used in isolation if the surface deviation is less than half the mean effective wavelength of the source. In principle, phase unwrapping methods can be used for continuous surfaces, however, CSI is more generally applicable to engineering surfaces if envelope detection is used to identify the zero order fringe. For the ideal case with no dispersion the zero order fringe is the central bright fringe that corresponds to equal object and reference paths.

Envelope detection with phase estimation

Envelope detection can be combined with phase estimation. The modulation envelope is used as the means to identify the fringe order, with the phase analysis then being applied on a limited data set providing a much more detailed definition of surface height. Let us suppose that we have two sets of data, $H_{x,y}$, is a surface height estimate based on the modulation envelope while $\theta_{x,y}$ is the phase of the fringes at a height of $H_{x,y}$. It is usual to define the phase gap, $A_{x,y}$, as the difference

$$A_{x,y} = \theta_{x,y} - K_0 H_{x,y} \tag{2.4}$$

and the two sets of data may be combined to produce a map of surface elevation, $h_{x,y}$, given by

$$h_{x,y} = \frac{\theta_{x,y}}{K_0} + \frac{2\pi}{K_0} round\left(\frac{A_{x,y} - \langle A \rangle}{2\pi}\right). \tag{2.5}$$

In this expression $\langle A \rangle$ is the field average of the phase gap, $A_{x,y}$, and the function *round* () denotes the nearest integer value.

Whilst the implementation of the optical phase analysis provides better resolution of surface height, the phase analysis process by its very nature includes a cyclic fringe order ambiguity of $n2\pi$, where n is an integer number. What this means in practice, is that in certain cases, analysis is unable to determine if an optical phase jump in the data, is a function of a surface feature (step, sharp edge, high surface roughness, differing surface materials), or simply the extent of the optical phase graduations. This can consequently lead to errors in the surface height maps, known as fringe order or 2π errors that are discussed in chapter 7.

Scan domain correlation

The envelope and fringe modulation can be extracted in the scan domain or in the frequency domain. In the scan domain, one approach is to convolve the intensity data with a kernel that is matched to the CSI signal

$$S_{x,y,z} = \sum_{z'=-N'/2}^{N'/2} f_{z'} I_{x,y,z+z'} \tag{2.6}$$

where for this example the kernel $f_{z'}$ has a set of $N' + 1$ real coefficients, $c_{z'}$, and $N' + 1$ imaginary coefficients, $s_{z'}$, indexed by z', such that

$$f_{z'} = c_{z'} + js_{z'}. \tag{2.7}$$

Suitable kernels are

$$c = (0\ 2\ 0\ \text{-}2\ 0)$$
$$s = (\text{-}1\ 0\ 2\ 0\ \text{-}1).$$

Using this approach the envelope, I_{AC}, can be estimated by

$$I_{AC} \propto |S_z| = \sqrt{(2I_{z-1} - 2I_{z+1})^2 + (-I_{z-2} + 2I_z - I_{z+2})^2} \tag{2.8}$$

whilst the phase, θ, can be estimated by

$$\theta_z = \tan^{-1}\left(\frac{-I_{z-2} + 2I_z - I_{z+2}}{2I_{z-1} - 2I_{z+1}}\right). \tag{2.9}$$

It should be noted that in other texts, the scan domain correlation may be described as the coherence correlation.

Frequency domain analysis

The Fast Fourier Transform (FFT) provides a powerful tool for the envelope peak detection. By applying a FFT to the measured data series and removing the high frequency signals (by filtering) the envelope signal can be derived by applying inverse FFT (IFFT) to the filtered signal. The peak of the envelope can then be easily detected. However, this approach is still limited by the definition of the modulation envelope, and is subject to the same restrictions identified above.

Alternatively (and as identified in ISO/FDIS 25178-604), the high spatial frequency content of the signal can be directly analysed using Fourier techniques. An FFT of the intensity term $I_{x,y}$ (ξ) generates the frequency spectrum $q_{x,y}$ (K). If this function is plotted against a range of white light frequencies K, then a first estimate of the surface height at a pixel $H_{x,y}$ can be deduced from the gradient of the line of best fit, as shown in Figure 14. Note that the phase gap $A_{x,y}$ previously identified when calculating optical phase, is simply the axis intercept of the best fit line.

Consequently, the optical phase component can be calculated from

$$\theta_{x,y} = A_{x,y} + K_0 H_{x,y} \tag{2.10}$$

thus providing all of the terms to calculate the final high resolution surface height term, $H_{x,y}$.

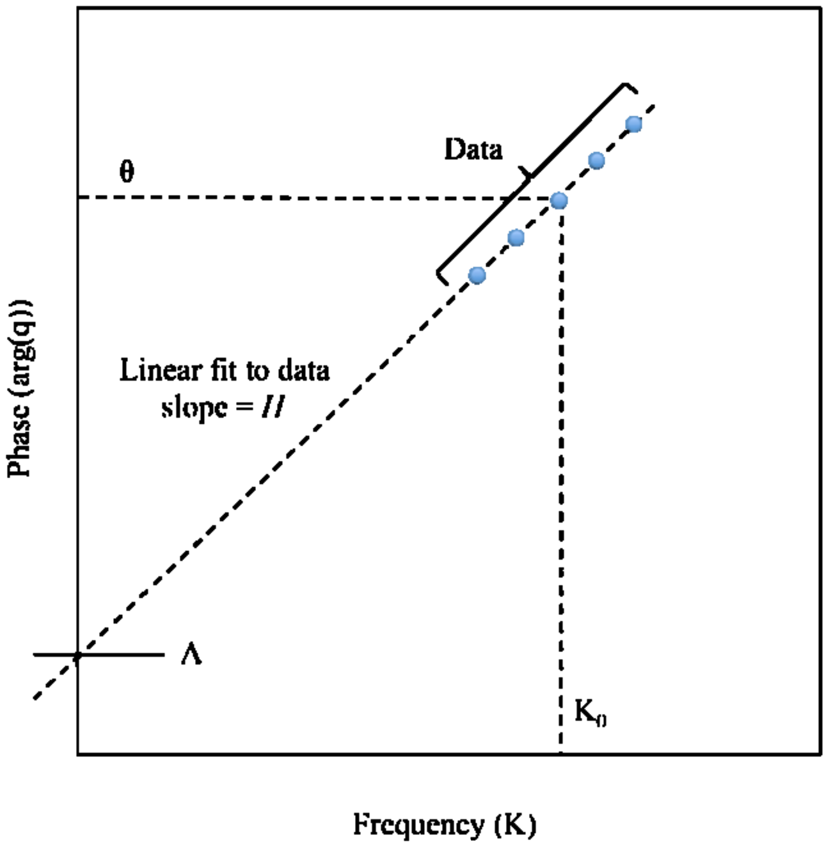

Figure 14 Frequency domain analysis (adapted from ISO/FDIS 25178-604)

Instrument setup

3

IN THIS CHAPTER

- The measuring environment
- Mode of measurement
- Camera mode selection
- Automatic gain control
- Minimal modulation
- Minimal area size
- Choice of objective lenses
- Objective mounting
- Using image zoom
- Scan length selection
- Sample preparation and handling
- Sample mounting and fixturing
- Sample replication

Instrument setup

A good instrument setup is essential for achieving a reliable measurement that is accurate, repeatable and reproducible. Different instruments may have alternative terminology and software-selectable items involved at the setup stage, so the purpose of this section is to illustrate the most important or fundamental choices that are required in order for consistent measurement to be achieved.

The measuring environment

In order to achieve measurements with the best possible repeatability, reproducibility and accuracy, appropriate environmental conditions must be maintained. As already identified, the operating principle of CSI is based on the sensitive detection of white light fringes. Fringe stability will be affected by a number of environmental parameters including (in order of priority) vibration, air turbulence and temperature.

Localized vibration may influence the integrity and stability of the CSI fringe patterns. Passive and active vibration isolation systems can be employed to reduce the influence of vibration, often caused by passing traffic or vibrating machinery. Vibration isolation systems are available from a range of third party vendors as well as the CSI manufacturing companies, although care must be taken to select an isolation system which is suited to the frequency range of damping required.

Manufacturers may specify vibration isolation requirements for specific frequency ranges, in order to guarantee performance. Acoustic noise can also be a source of vibration, though typically acoustic noise causes the part under test to vibrate unacceptably rather than causing problems with the instrument.

Consequently, the CSI instrument should be sited away from vibration or external noise sources. If this is not possible, then vibration or external noise sources may need to be turned off during measurements. It is also important to avoid moving the CSI instrument during data acquisition.

Air turbulence must also be carefully controlled for precise measurements. Airflow between the sample and objective can cause small errors in the measurement. Additionally, airflow can be a major source of vibration, particularly for the sample under test. Consequently, CSI instruments may be susceptible to air currents or draughts, causing perturbations in the white lights fringes as a function of refractive index changes. Care must be taken to avoid having air currents passing over the measurement platform, either from air conditioning plant or cooling fans from electronic equipment and computers.

A pragmatic approach may be to mount the instrument in a purpose-built cabinet, with the doors of the cabinet remaining closed while taking measurements. However, care must be taken with cabinet design because in some cases cabinet side walls can amplify airborne vibration.

Temperature stability is particularly important for the structure of the instrument and care should be taken to site the instrument in a thermally stable room away from obvious heat sources or air currents. Ideally, the room temperature should be at 20 ˚C. If this is not the case then there is the possibility that thermal compensation corrections may be required. An alternative approach is to house the CSI instrument in a localised environmental booth at 20 ˚C.

The rates of ambient temperature change are important even in controlled environments, and where possible these should be minimised. The instrument should also ideally be sited away from direct or indirect sunlight, in order to avoid solar thermal warming during operation.

Other environmental parameters may affect the performance of a CSI instrument. Elements such as changing air pressure, relative humidity and temperature will all affect the value of the refractive index of air. Some CSI instrument will allow you to input air pressure, relative humidity and temperature values, and provide compensation. This may become more relevant when measuring identical multiple components over long periods of time

An additional issue is maintaining a clean environment. Clearly some applications may require specific clean room conditions, but for those that do not, there is still a requirement to ensure that circulating environmental air does not contain particles such as dust, smoke, oil or other contaminants.

Mode of measurement

Most CSI instruments offer a number of modes of measurement within the instrument's software. The choice of modes can affect the resolution of measurement through "pixel binning" and other averaging or filtering techniques. Modes of measurement may allow the user to choose whether phase only, coherence only, intensity only or a combination, is used to create the map of the surface. The choice of measurement mode can be fairly complicated and the user should consult the instrument manual or contact the manufacturer where there is doubt. The nature of the surface being examined may determine the choice of measurement mode.

Camera mode selection

CSI instruments use a range of different analogue or digital, CCD or CMOS-TV cameras, with resolutions ranging from approximately 640 × 480 pixel array size, to megapixel arrays. The instruments may also allow the selection of a specific camera mode, thus reducing the resolution of the sensing element, but potentially decreasing processing time. Larger active array sizes typically allow the resolving of smaller details, but may increase processing time.

Common sub-array options may be 320 × 240 pixels and 160 × 120 pixels, and the user is recommended to identify the instrument's default setting. It should be noted that some manufacturers may not identify array sizes as illustrated here, but may describe the camera mode in terms of pixel count, e.g. 0.3 megapixel to 4 megapixel. Again, the more pixels involved in the analysis, the better detail produced, but the longer the computational time required.

Automatic gain control

Automatic gain control (AGC) is a common control choice for instruments using pixel array cameras. The purpose of AGC is to help to minimise saturation of image array pixels and may be a software-selectable item. Some CSI manufacturers offer AGC options within the camera controlling elements of the software packages and the appropriate manuals need to be consulted.

Minimal modulation

Minimal modulation is a criterion that defines the lowest peak signal strength deemed useable by the software for further evaluation of surface height, *i.e*. the minimum modulation necessary for a valid data point. Typically minimal modulation is a software-selectable item that sets the acceptable intensity range or minimum modulation necessary for data. Consequently, the modulation intensity is decreased to accept areas with poor fringe contrast or low reflectivity, and increased to exclude unwanted data points.

An example of this process is illustrated in Figure 15, which represents the modulation of three data points over time. Each sine wave represents the signal from a given camera pixel when the PZT (or sample) is moving during an acquisition cycle. Ideal modulation occurs when the light intensity of each data point varies from near zero to near maximum. Typically, the light intensity from each data point does not have ideal contrast, but is sufficient to provide valid data. When the modulation is insufficient, the data point is excluded as a function of the minimum modulation threshold set in software (grey zone).

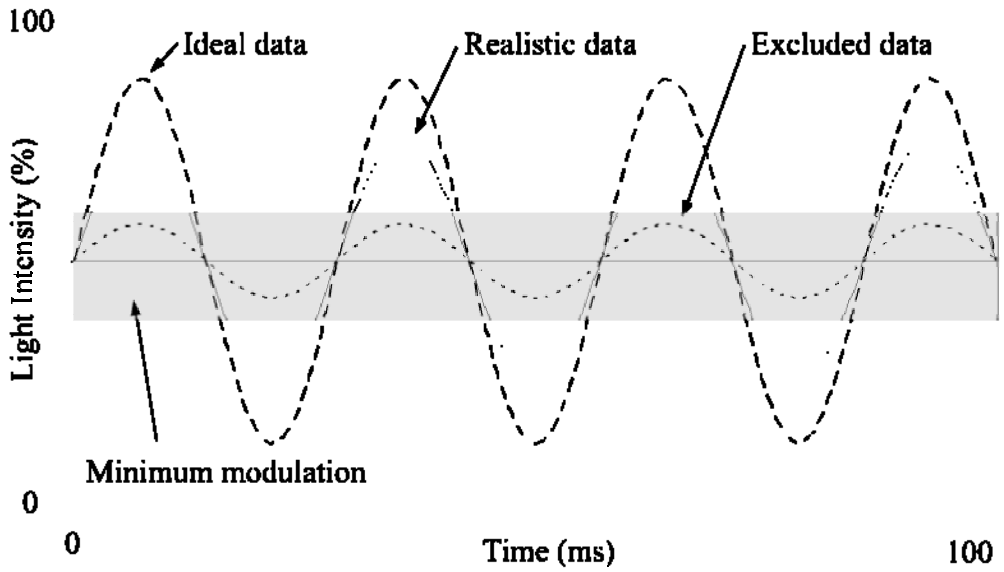

Figure 15 Modulation intensity of data as a function of time

Modulation relates the signal-to-noise ratio to repeatability. The greater the modulation of each data point, the higher the signal-to-noise ratio and the better the repeatability. As the modulation decreases, the lower the signal-to-noise ratio leading to deteriorating repeatability, and it becomes more difficult to obtain reliable data from the surface. Some CSI software will allow the user to set the modulation threshold at a value that is suitable for the surface being measured. Smooth surfaces producing high contrast fringes can have a high modulation threshold set (for instance, greater than 15 %), in order to exclude rogue data points. Rough surfaces, surfaces with high slope angles, or surfaces producing low fringe contrast may have points that cause low modulation. Reducing the modulation threshold to a lower percentage value (for instance, less than 15 %) will allow more points to pass as valid data points, but will generally increase the system noise.

Minimal area size

Some instruments allow the user to select a minimum area size in the instrument setting. This setting specifies the smallest acceptable number of neighbouring data points in a valid region of data, and acts as a high pass filter (in data point terms). This setting is useful for eliminating the effect of isolated data areas, which are not meant to be included in the measurement, negating the need for defining a mask.

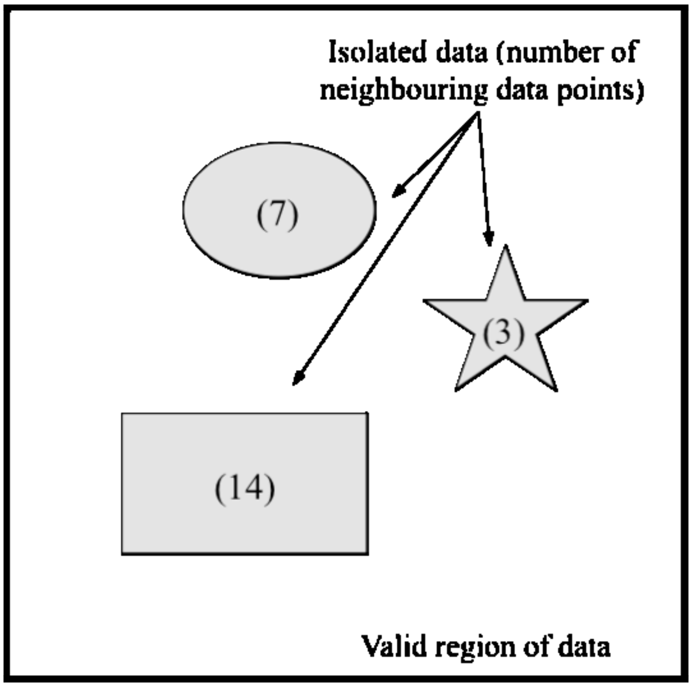

Figure 16 Isolated data within a region of valid data (adapted from Zygo Corp.)

Figure 16 shows an example with three regions of data. By setting the minimum area size to three data points, areas with three neighbouring data points (or less) would be excluded but would allow progression of areas with larger neighbouring values (those with seven and fourteen data points). As the minimum area size threshold is increased, progressively larger areas of data would be excluded.

Choice of objective lenses

Several kinds of objective lenses are used with CSI instruments, ranging from low magnification (1×) Michelson objectives to high magnification (100×) Mirau objective lenses (see chapter 2)

Manufacturers may offer parfocal and non-parfocal lenses. For microscope systems, this means that if parfocal lenses are fitted to the lens turret, then when a lens is changed (10× to 50× magnification for instance) the object still stays in focus and only requires very minimal focal adjustment. In addition some instrument manufacturers make all objectives parcentric via setup or stage automation, so that when objectives are switched features remain centred within the field of view.

Lens selection is a function of a number of competing variables. The most obvious is the area of interest on the target surface that requires investigation (the field of view). However, selecting any particular lens will have a consequence on a number of other optical and data parameters, as identified below. When attempting to measure surface roughness, lateral resolution and slope become key determining factors to the quality of the data

Lens type

Typically 1×, 1.5×, 2× and 5× magnification objective lenses will be of a Michelson based design, resulting in larger objective housings and longer working distances. Typically 10×, 20×, 50× and 100× magnification lenses will be of a Mirau (or possibly a Linnik on older instruments) based design, resulting in more compact objective housings and much shorter working distances. It should be noted that the largest lens assemblies (1× for instance) may not be compatible with a rotating lens turret and will require direct attachment to the CSI system (see Objective mounting section below). Figure 17 shows examples of four lenses used for CSI instruments.

Figure 17 Four lenses used on a CSI instrument. Clockwise from top left: 2× Michelson, 5× Michelson, 20× Mirau and 10× Mirau

Field of view

As the lens magnification factor increases, then the field of view decreases. For instance, a 1× lens may have a field of view of the order of 7 mm × 5 mm, whilst a 100× lens may have a field of view of approximately 70 µm × 50 µm. Note that these two examples are based on a rectangular aspect ratio image plane whilst other instruments may offer a square format image plane. Furthermore, the field of view may also be influenced by the lens design.

Lateral resolution

As the lens magnification factor increases, then the lateral resolution increases. For instance, a 1× lens may have a lateral resolution of the order of 10 µm, whilst a 100× lens may have a lateral resolution of approximately 0.4 µm. Reference should be made to chapter 2 when also considering the overall lateral resolution of the instrument. Furthermore, the lateral resolution had a direct influence on the resolution of the surface texture measurement and any parameter quantification.

Spatial sampling

The spatial sampling is the pixel size on the target surface and is based on the camera pixel size divided by the system magnification. Note that spatial sampling will vary as a function of the type of camera used.

Zoom multipliers

If variable or selectable zoom multipliers are used other than 1× (for instance 0.5×, 0.75×, 1.5× and 2×) then the field of view and the spatial sampling size will change.

Slope angle handling

The higher the numerical aperture of the objective, the higher the surface slope angle tolerance. The lower the numerical aperture of the objective, the lower the slope angle tolerance. If a low numerical aperture objective is used for measurement of a surface with features exhibiting significant slope, then voids may appear in the data. Consequently, the user must apply care to lens selection in order to maintain data integrity, if surface slope is an issue. This is further discussed and demonstrated in chapter 7.

Objective mounting

Most manufacturers offer the following lens mounting options, although not all lenses are suitable for turret mounting:

- single lens onto the microscope with no multi-lens turret;
- manually operated multi-lens turret; and
- automatically operated (motorised) multi-lens turret.

Care should be taken when using turrets (example shown in Figure 18) if they have a 100× lens mounted, because the working distance (from lens to target surface) is typically 2 mm or less. Consequently, it is possible that if there are raised surface feature on the target surface, the lens will come into contact with the target surface and be damaged. 100× lenses are typically the most expensive lens options available for a CSI instrument. Note that some manufacturers may specify additional adapter rings or collars (lens dependent) in order for all lenses to work correctly on one turret. Consequently significant care should be taken with lenses of this nature.

(a) Manual turret holding five objective lenses

(b) Single objective mounting on Z axis

Figure 18 Objective mounting options (courtesy of Zygo)

Using image zoom

CSI instruments often have an image zoom option. This option allows the user to automatically increase or decrease the magnification of the optical system within a limited range (0.5× to 2×) providing an ability to optimise the image detail. A zoom lens gives the benefit of versatility in the system, providing a larger range of available measurement areas and can also compensate for circumstances where there may be limited pixel count. Some instruments accomplish this function by using discrete optical elements. In this case the lateral resolution of the instrument is changed as the magnification factor is changed. Any change of magnification requires identification within the controlling software. If the setting of the software control and the optical magnification factor do not match, results will be incorrectly processed in terms of the lateral scaling of the data.

Changing the optical magnification or zoom for an instrument may be achieved in two ways. Firstly, the instrument may be fitted with continuous optics and a single graduated adjusting mechanism (possibly automatically encoded and linked to software), allowing the user to simply select the magnification factor required. Secondly, an instrument may be provided with optional individual discrete zoom elements, which have to be physically introduced into the microscope optical system by the user.

For some instruments the image magnification or zoom function is accomplished via digital techniques in software. In this case the optical lateral resolution of the instrument will not change because the zoom function is only achieved by selecting image elements that have already been correctly processed in software.

Focus

For high accuracy CSI, it is necessary that every measurement point on the sample surface passes through the focus position during the scan, and that in fact the scan starts before fringes are visible at a given point and does not end until all fringes have passed out of the depth of focus. The scan length required to achieve this is dependent on the bandwidth of the light used and the numerical aperture of the objective. When combining phase with coherence information, focus can be especially important, and some instruments use autofocus to achieve the most consistent results.

The majority of focusing is achieved manually across the range of lenses available by slow traverse movement in the vertical direction. A typical indication of when the instrument is correctly in focus, is when white light fringes are observed on the monitor screen. It should be noted that very high magnification objective lenses may have an additional focusing ring attached to the lens which aids very fine adjustment.

Scan length selection

The vertical length of the scan made by the PZT actuator (or moving sample stage) during a measurement, is generally predetermined before acquiring data. This scan length will range from tens of micrometres to millimetres. The longer the scan length, the longer the measurement time because more data are collected. Any movement of the sample during the scan period will cause errors of measurement. Consequently, good quality fixturing is important to avoid specimen movement and users should not disturb the specimen during data acquisition.

Ideally, any scan length control should be set at the minimum value, which will allow the measurement of all of the vertical features of interest on a target surface. Clearly the instrument has no *a priori* knowledge of the extent of the surface relief, and typically requires the user to manually determine the range of surface features. Further scan options may include the direction of scan and extended scans.

Unidirectional scans

Unidirectional scans will require the user to set the focal plane of the instrument either above the highest point on the surface (if the instrument scans down), or below the lowest point on the surface (if the instrument scans up).

Bipolar scans

Bipolar scans require the user to set the focal plane of the instrument at the approximate midpoint of the vertical relief of the surface. The instrument will then drop to the bottom of its scan range and scan up through the surface or *vice versa*.

Extended scans

Extended scans provide the user with an ability to significantly increase the vertical range of a scan into the millimetric range. CSI instruments use feedback controlled PZT linear actuators or precision stepper motors on the z axis for vertical movement. When using a PZT, additional z axis movement may be provided via stepper motors that allow longer travel, but with much longer measurement times and reduced vertical resolution. Stepper motor based systems typically do not suffer any measurement degradation in speed or performance over their entire scan range. The use of extended scanning is determined by the range of the surface topography or features requiring measurement.

Measurement speed

On some CSI instruments it is possible to change the speed of measurement. Changing the measurement speed can allow the under sampling of the fringe envelope, sacrificing some accuracy for measurement speed. Measurement speeds can range from approximately 5 $\mu m \cdot s^{-1}$ to 100 $\mu m \cdot s^{-1}$. Note that changing the scan speed will also affect the vertical resolution so care must be taken. Typically, the slower the vertical scan speed, the longer the data acquisition, but the better the data integrity.

Bandwidth narrowing

Most CSI instruments use a white light source with a bandwidth typically between 100 nm and 150 nm, although some manufacturers have produced instruments with narrow bandwidth laser sources. A white light source of, for instance 125 nm bandwidth, will have a coherence length of approximately 3 µm, which is appropriate for obtaining data from the majority of surfaces. However, when a surface exhibits low contrast or has high slope angles, then a CSI instrument may be prone to data dropout.

Increasing the coherence length of the system can help in these circumstances and this is often achieved through the use of bandwidth narrowing filters, which can be introduced into the optical path on an appropriate mount. For instance, typical bandwidths may be reduced to 10 nm to 50 nm, with the coherence length increasing to approximately 8 µm to 40 µm. Individual instrument manufacturers may provide guidance on these options (if available) although if the user notices significant data dropout in the processed topographical maps, then narrowing the bandwidth may help to improve data integrity.

Sample preparation and handling

When using any surface texture measuring instrument, samples for measurement must be clean and free from grease, smears, fingerprints, liquids and dust. Handling procedures must ensure that the sample is not contaminated, and handling should be kept to a minimum prior to measurement. A period of sample acclimatization may also be needed to bring the sample into thermal equilibrium with its environment. Any cleaning protocol should note that any fluids used in cleaning may contain contaminants that can leave a residue on the surface - this may affect the measurement detrimentally. Any contaminants may become part of the measured data if present on the surface, or result in missing data.

For some surfaces it may be desirable to overcoat with thin layers of vacuum coated gold or chromium. When using this method one must ensure that an even coating is deposited over the entire sample. Overcoating may be beneficial when dealing with dissimilar materials because the sample will be covered with a single material film. There is, however, an inherent danger that coating material will fill in and obscure small surface features which require measurement.

Sample mounting and fixturing

It is difficult to give comprehensive guidance on fixturing methods because solutions will depend on the geometry and mass of individual samples. Problems may be encountered by use of any method of fixturing other than the component's own mass. When using non-permanent adhesives such as adhesive tape or gels for fixturing, scope for movement during measurement is introduced through factors such as creep. When introducing external forces to aid fixturing, the possibility of sample distortion may be encountered. In addition, use of a vacuum method of fixturing may introduce vibration.

Fixturing is essential when stitching together multiple measurements to prevent movement as the translation stage is scanned. Loosely fixtured parts may also react to external vibration. Most instrument manufacturers offer a range of table mounting points and accessories, including:

- magnetic chucks/plates;
- vacuum chucks/plates;
- disk fixtures for disk media; and
- tray holders.

The use of replication compounds

Sometimes it is difficult to access a sample for measurement. For example, the sample may be too large to mount on the CSI, you may want to measure inside a cylinder or the sample may have a complex geometry that is not easily accessible by the CSI. For such samples a replication of the surface can be made using a suitable replication compound. Replication compounds are usually based on polymer material and are commercially widely available. As many of the replication samples are relatively soft polymers, care must be taken to avoid introducing unwanted form into the replica. Some studies have shown that replication compounds can reproduce the surface texture of a sample to within tens of nanometres.

Calibration and Uncertainty

4

IN THIS CHAPTER

- Instrument terminology
- Instrument calibration
- Types of calibration artefact
- System error files and error maps
- Handling of calibration artefacts
- Overview of uncertainty budgets

Calibration and uncertainty

The purpose of calibration and traceability for any measurement instrument is to provide confidence to the user that the measurement data is of good quality. The process of instrument calibration is to introduce a testing mechanism or artefact into the measurement instrumentation, which allows a comparison of the instrument output with another verified measurement of the same mechanism or artefact. This process provides a demonstrable unbroken link or chain of measurement from the instrument to the relevant primary standard, in this case the metre, which defines the traceability of the instrument.

The calibration of a CSI instrument is still an ongoing topic of research. This chapter will only discuss the background to calibration and not specific methods. A further NPL good practice guide, to be published in early 2011, will describe the calibration of the metrological characteristics of CSI.

Instrument terminology

When discussing the characteristics of measuring instruments, many terms are used to describe the quality of measurements. These terms are defined in *ISO/IEC Guide 99:2007 International Vocabulary of Metrology* and further explained in the NPL *Measurement Good Practice Guide No. 80 – Fundamental Good Practice in Dimensional Metrology*. Care must be taken when describing these terms because accurate definitions depend on whether the term is with respect to the measuring instrument, or with respect to the measurement data.

Accuracy

Accuracy is ability of a measuring instrument to give indications approximating to the true value of the quantity measured. In other words, how close to the true value will the measuring instrument measure.

Error

Error is the discrepancy between the measured value and the true value of the quantity being measured.

Precision

Precision is the measure of the dispersion of the results of a measurement instrument, *i.e*. how widely or how closely spaced are the measurements.

Repeatability

Repeatability is an indication of measurement precision under a set of repeatable conditions of measurement, *i.e*. without changing any of the process variables.

Resolution

Resolution is the smallest change in a quantity being measured that causes a perceptible change in the corresponding indication. In other words, how finely divided are the measurement scales of the instrument.

Uncertainty

The uncertainty of measurement is a non-negative parameter characterizing the dispersion of the quantity values being attributed to a measurement result, based on the information used. It is the quantification of the doubt in a measurement result.

Instrument calibration

Calibration of a CSI instrument is an important factor in producing reliable and repeatable measurements. It is important to calibrate the instrument whenever a major adjustment has been made to the instrument or to the environment in which it is housed. It is recommended that a calibration schedule be written into the overall measurement protocol for the instrument. The frequency of calibration is dependant upon a number of factors such as environment of use, instrument stability and any regulatory requirements particular to the application.

Types of calibration artifact

This section is a comprehensive but not exhaustive list of available types of calibration artefacts for various CSI instruments. It is important to note that at the time of writing of this guide only draft international standards exist for calibrating areal surface texture measuring instruments. Indeed, there is no clear route to traceability for any areal measurements. Therefore, it is only possible to check that the instrument compares to the calibration value given by the instrument manufacturer and that measurements are repeatable (but see later NPL good practice guide on calibration of CSI).

Where possible surface profile measurements can be calibrated using artefacts described in ISO 5436-1 (2002) as these measurements can be traceable to national or international standards. NPL *Measurement Good Practice Guide No. 37 – The Measurement of Surface Texture using Stylus Instruments*, describes surface profile calibration in detail for a stylus instrument but many of the calibration techniques can be applied to profiles extracted from areal measurement data.

Lateral or spatial calibration

Lateral or spatial calibration of a CSI determines the characteristics of the x axis and y axis measurement capability and allows for a correction to be applied. Lateral or spatial calibration is generally achieved by measuring a calibrated pattern on an artefact, for example a grid or series of concentric circles. For example, the measurement of a grid type calibration artefact is shown in Figure 19.

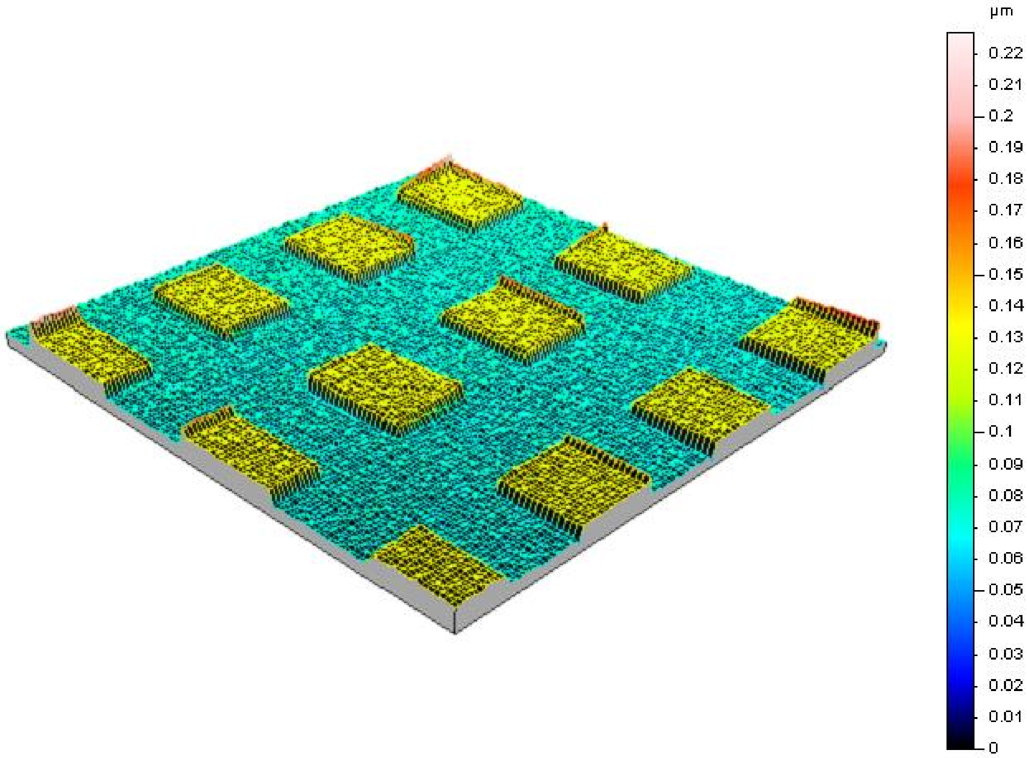

Figure 19 Measurement of a grid type calibration artefact

Vertical calibration

Vertical calibration allows for the correction of many unwanted effects in the vertical (z) measuring axis. These effects include gain errors, periodic scanner effects (such as from gears or motors) as well as overall non-linearities. Vertical calibration is generally achieved through the use of a step height of calibrated dimension. Ideally the step height used should be as close to the height that you are routinely measuring such that the calibration is localised to the operating area for any particular sample. It should be noted that some CSI instruments incorporate a separate displacement measuring interferometer to continuously measure the motion of the z axis actuator and correct for the above noted unwanted effects regardless of scan position or range. These systems should not require step calibration, although a step should ideally be used for verification purposes.

Step height artefacts are normally manufactured from quartz or silicon wafers with a positive step (etched step) or negative step (etched trench). A wide range of the step height artefacts (from tens of nanometres to several millimetres), are needed for the calibration of the CSI instruments.

Step height calibration for profile measuring instruments according to ISO specification standards is described in NPL *Measurement Good Practice Guide No. 37 - The Measurement of Surface Texture using Stylus Instruments*. This method can be applied to the vertical calibration of areal instruments, although it is better to make an areal measurement of the step rather than a single line scan. If an areal step height measurement is carried out, least squares planes need to be fitted to the data, whereas least squares lines would have been fitted for profile data. Figure 20 shows the areal measurement of a VLSI Step Height Standard composed of a grating artefact manufactured in chrome coated quartz, measured using a 50× objective with a 0.5× zoom setting.

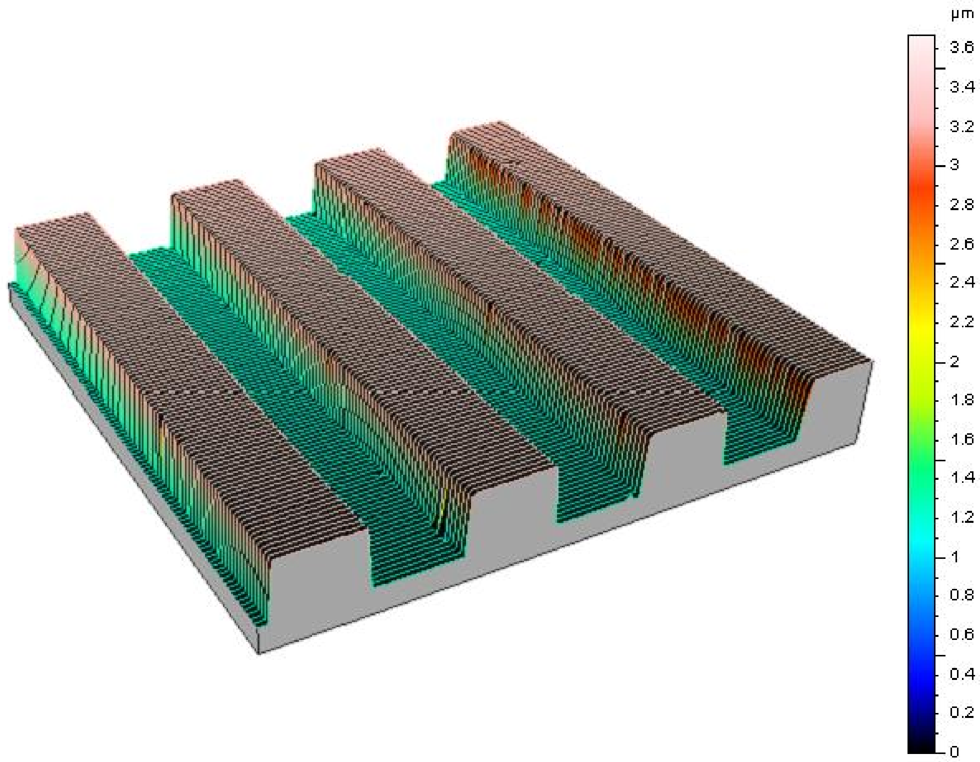

Figure 20 A measurement of a VLSI Step Height Standard

Further detail of the same step height standard is illustrated in Figure 21 showing one measured step (50× objective, 2× zoom), and a line profile taken through the step to allow calculation of step height measurement accuracy.

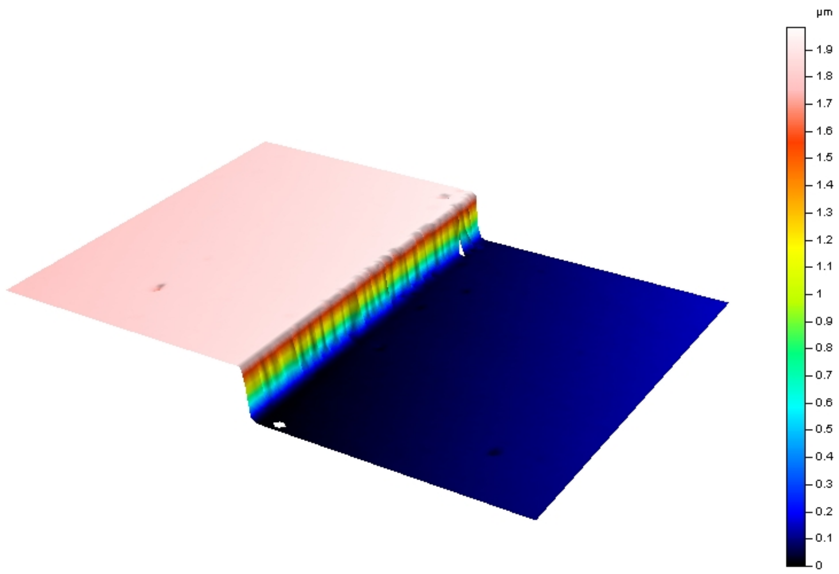

(a)

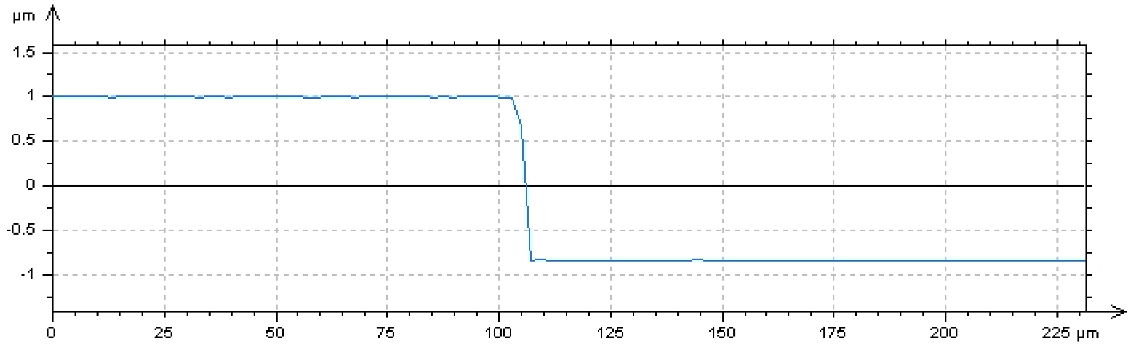

(b)

Figure 21 Detailed measurement of the VLSI Step Height Standard

System error correction

System error correction serves to correct errors associated with the reference optics, objective lens assembly and overall optical system. System error correction is generally achieved through single or multiple measurements taken of a high quality reference flat. System error correction can also be performed against spherical or cylindrical forms when those will be the primary measuring test objects, where the radii of curvature of the references should match those of the test pieces. By maximizing the area of the artefact over which measurements are taken for calibration, the effects of noise and residual contamination can be minimized, and the quality of the calibration can be enhanced.

System error files and error maps

The software associated with CSI instruments often have the ability to record and store error maps or system error files created as part of the system error correction process identified above. These files allow the operator to evaluate any objective aberrations by measuring a traceable specimen such as a reference flat, with flatness in the range of $\lambda/50$ to $\lambda/100$. The error map may then be subtracted from routine measurements when using the relevant objective and zoom settings.

Handling of calibration artefacts

Calibration artefacts should be stored and cleaned in accordance with the manufacturer’s guidelines. Cleaning methods are generally dependant upon the material of the artefacts. If there is any doubt as to the proper handling methods, advice should be sought from the manufacturer or supplier. Cleaning materials should be non-abrasive and non-corrosive to the surface. Typically a fluid such as a solvent can be used with a non-abrasive, non-shedding cloth. Note that care must be taken when selecting a solvent for use with a given substrate – seek the advice of the manufacturer of the sample or the material supplier. A clean air supply can be used to remove any loose contaminants.

Calibration artefacts should be stored alongside the instrument in a stable environment with respect to temperature and humidity. Handling of the artefacts should be kept to a minimum, and protective gloves or handling devices should be used to prevent thermal transfer and contamination.

Overview of uncertainty budgets

Every measurement is subject to some level of uncertainty. A measurement result is only traceable, if, it is accompanied by a statement of the uncertainty in the measurement result. Sources of measurement uncertainty will be inherent in the measuring instrument from; calibration uncertainties, the item being measured, the effect of the environment, the measurement process, the operator, and from other sources. Such uncertainties can potentially be estimated using statistical analysis of a set of measurements (Type A), and using other kinds of information about of the measurement process (Type B). Uncertainty budgets give the details of the uncertainties distributed around the entire measurement system.

There are established rules for calculating an overall estimate of uncertainty from these individual pieces of information as defined in ISO/IEC *Guide 98: Guide to the Expression of Uncertainty in Measurement* (*GUM*), and summarised in NPL *Measurement Good Practice Guide No. 36 – Estimating Uncertainties in Testing*. Further illustration is provided in NPL *Measurement Good Practice Guide No. 11 – A Beginner's Guide to Uncertainty in Measurement*.

It is, therefore, important to understand the uncertainties and ideally calculate the uncertainty budget for the entire instrument. This process should involve the assessment of uncertainties for each part of the measurement system and combining these contributions to create an overall system uncertainty statement. For simple measuring instruments such as micrometers or vernier callipers, this is a straightforward task. However, as the complexity of the measuring instrument increases, this task becomes evermore complex. It is common to find that this task is generally the preserve of the national measurement institute, or has yet to be attempted (or completed).

The issue of uncertainty is made more problematic by the contributions from the surface being measured, either by directly affecting the CSI measurement itself, or because the surface texture is so variable, that repeat measurements in different locations on the surface give rise to a high degree of variability. If an uncertainty calculation were to be completed for a CSI instrument, then it would still be necessary to find the uncertainty in the relevant parameter calculations. Again this is difficult in practice and often the guidelines in the GUM cannot be easily applied.

The consequence for CSI instruments is that to date there have been no published instrument uncertainty budgets, although many individual error sources have been identified and quantified, as described in chapter 7. Instrumentation manufacturers rely on statements of repeatability of step height measurement to identify instrument quality, which is valid and relevant to the user, if the user is predominantly measuring surface features that are step like. Users are, therefore, advised to apply care to their measurement procedures and methods in order to maintain data integrity, and where possible calculate and quote the standard deviation of the data. This guide will be updated in the future as calibration methods for CSI are standardized.

Typical measurement procedures

5

IN THIS CHAPTER

- Objective lens selection
- Guidance on focussing and finding fringes
- Implementing field stitching
- The importance of sample stage levelling/tilting
- Adjusting the light source intensity

Typical measurement procedures

This chapter considers the practical issues of setting up a CSI instrument in order to acquire measurement data from a surface. The assumptions made at this point are that the instrument has been correctly installed in an appropriate environment, and that appropriate calibration tasks have been completed. There are a number of variables that require the user's attention in order to maximize the quality of the measurement data.

A typical measurement procedure for a CSI instrument can be summarized as follows:

- power up the instrument and the host computer;
- run the application program on the host computer;
- select the objective lens for the measurement and identify in software;
- place the test part on the stage under the objective (adjusting the x and y axes);
- position the objective at its working distance from the part (adjusting the z axis);
- focus the microscope for a sharp image;
- adjust stage level or tilt to optimize fringe contrast/appearance;
- adjust the test part position in the x and y axes;
- minimize the number of the fringes;
- adjust the light intensity level to an optimum value;
- check correct software-selectable items;
- initiate data acquisition; and
- analyze data.

Some of these elements are described in more detail later in this chapter.

Objective lens selection

The range of lenses typically available to the user was addressed in chapter 3 (four such lenses are shown in Figure 17), along with identification of key optical characteristics and consequences of using certain lenses. From a practical viewpoint:

- higher resolution analysis, steep slopes, rough surfaces, or examining smaller areas of interest on the surface generally requires higher magnification lenses (10×, 20×, 50×, 100×);
- lower resolution analysis, flat and smooth surfaces, or examining larger areas of interest on the surface generally requires lower magnification lenses (1×, 1.5×, 2×, 2.5×, 5×);
- very large area analysis will require a field stitching function (if available); and
- magnification adjustment can be implemented using fixed or variable zoom elements.

If the instrument is supplied with parfocal and parcentric lenses, then any lens change operation will require very minimal focus or lateral adjustment. If the instrument is supplied with non-parfocal lenses, then any lens change operation will require vertical axis adjustment to move the lens to the correct focal position and potentially horizontal translations for correct spatial positioning. When a zoom/magnification setting other than 1× is used, it is likely that a software option will need to be set to identify the zoom factor for correct data processing. The use of different zoom factors is illustrated in Figure 22. Figure 22 shows three images taken from a turning operation roughness comparison specimen with a 10× objective and zoom settings of 0.5×, 1× and 2×.

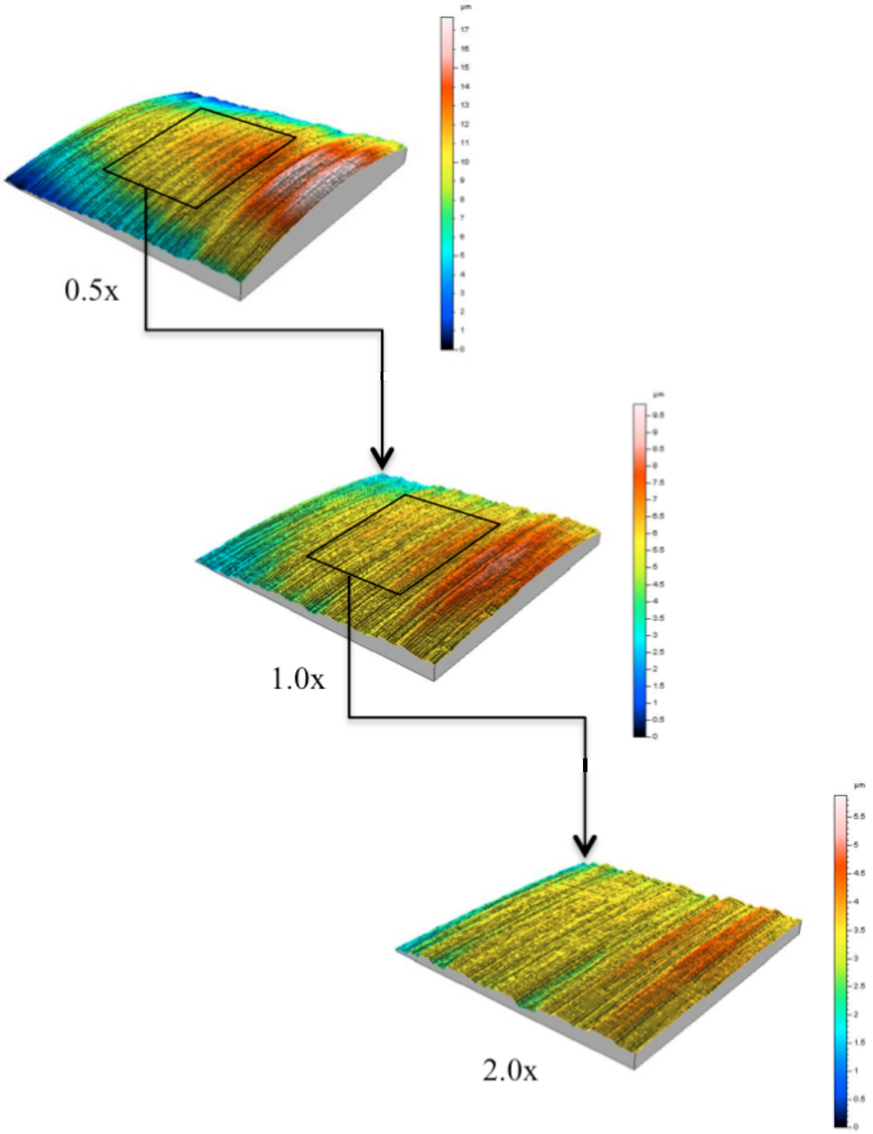

Figure 22 Change of image detail as a function of zoom setting

Guidance on focusing and locating fringes

Once the target object has been placed on the measurement stage, the focus plane of the objective lens needs to be found. This is achieved by translation of the vertical stage to bring the surface to the working distance of the objective lens. Note that, depending on the instrument design, this may be achieved either through movement of the lens assembly, or by movement of the specimen stage. Once focussed, vertical movement is completed in small increments (tens of micrometres) until fringe patterns are observed on the monitor. This process is illustrated in Figure 23 for the examination of a step height artefact.

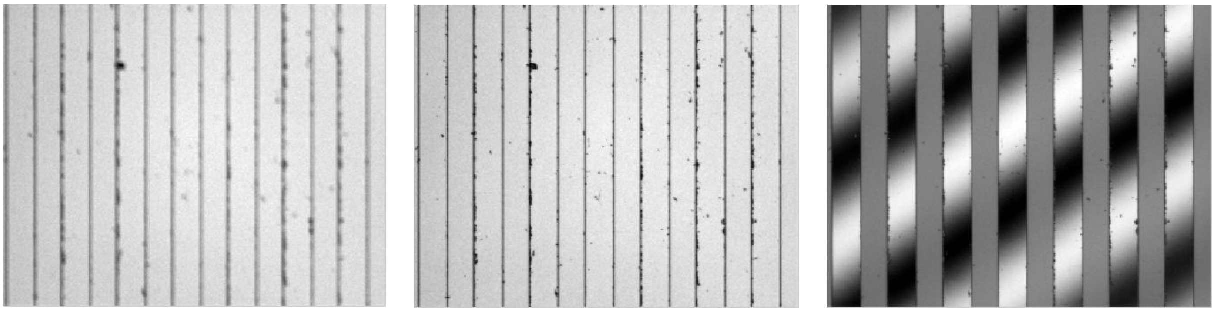

Out of focus Focussed (coarse adjustment) Focussed (fine adjustment)

Figure 23 Focussing on the surface of a step height artefact

For some types of surface and material, it is possible to find an incorrect focal plane away from the true surface, and this is a common problem when working at very high magnifications. If the surface reflectivity is high, then it is possible to image the intermediate optical surfaces within the objective lens. This incorrect focus can be identified by moving the horizontal stages laterally to determine whether the surface features appearing on the monitor screen move. If the in-focus surface features do not move as the horizontal stages are incremented, then the objective lens is not focused on the sample surface. If this is the case then the whole process of surface identification and focus needs to be repeated.

Generally, the process of finding focus on a surface is easier, when the magnification of the objective lens is reduced. This is because the depth of focus of a lens is linked directly to the numerical aperture and magnification. In general, the lower the magnification of an objective lens the larger the depth of focus. Consequently, if parfocal optics are fitted to the instrument, then it may be good practice to use a lower magnification lens first to find focus, and then change to a higher magnification lens for the final measurement.

For very high magnification lenses (50× and 100×), additional fine focus adjustment is often included on the lens assembly. This allows the user to adjust the relative focus of the object and reference.

The importance of obtaining the correct focus and the subsequent data integrity of the surface profile data is illustrated in Figure 24. Spherical and cylindrical samples have very large vertical ranges of features, with surface features (and fringes) appearing above and below the focal plane. The results in Figure 24 illustrate the measurement of a 0.3 mm diameter precision ruby sphere with five stages of focus. The central figure is a colour three dimensional profile map showing the sphere in focus, with a line section showing further surface profile detail.

In Figure 24 the CSI instrument has then been defocused in 1.8 μm steps, two steps above and two steps below the correct focal plane. The four defocused images show progressive noise (caused by 2π errors) being introduced around the sides of each image. This noise is evident in the accompanying line profiles. These plots demonstrate the narrow range in which correct focus can be achieved for some objects (and specifically higher magnification objectives), and how easy it is for parasitic noise terms to contribute to the data sets. In this example, the use of a flat reference plane set at the same height as the spherical surface can help to improve focal integrity.

Finding fringes is normally an integral part of the procedure for finding the focus. After the correct focal plane has been identified, white light fringe patterns should become apparent. If no fringes appear on the focused surface, then further focal adjustment needs to occur. For high magnification lenses, focal adjustment of the lens is often possible. For low magnification lenses, adjustment of specimen table tilt and light intensity changes can be implemented.

Implementing field stitching

When analysis is required over an area larger than the field of view of the lens (at any resolution), then field stitching is necessary. Field stitching is the process whereby a matrix of images are joined or stitched together. Realistically, this process is only viable if the CSI instrument is fitted with motorized horizontal translation stages that allow the software to accurately adjust the surface position, so that each image is correctly positioned and there is consistent overlap of images.

Overlap of the images is important because it allows the software to compare neighbouring images, and correctly correlate lateral position and consistent vertical range values. Software options will allow overlap typically ranging from 0 % to

25 %. Field stitching with a 10 % overlap on images is a common option, this being a compromise between data integrity and speed of large area data acquisition and analysis

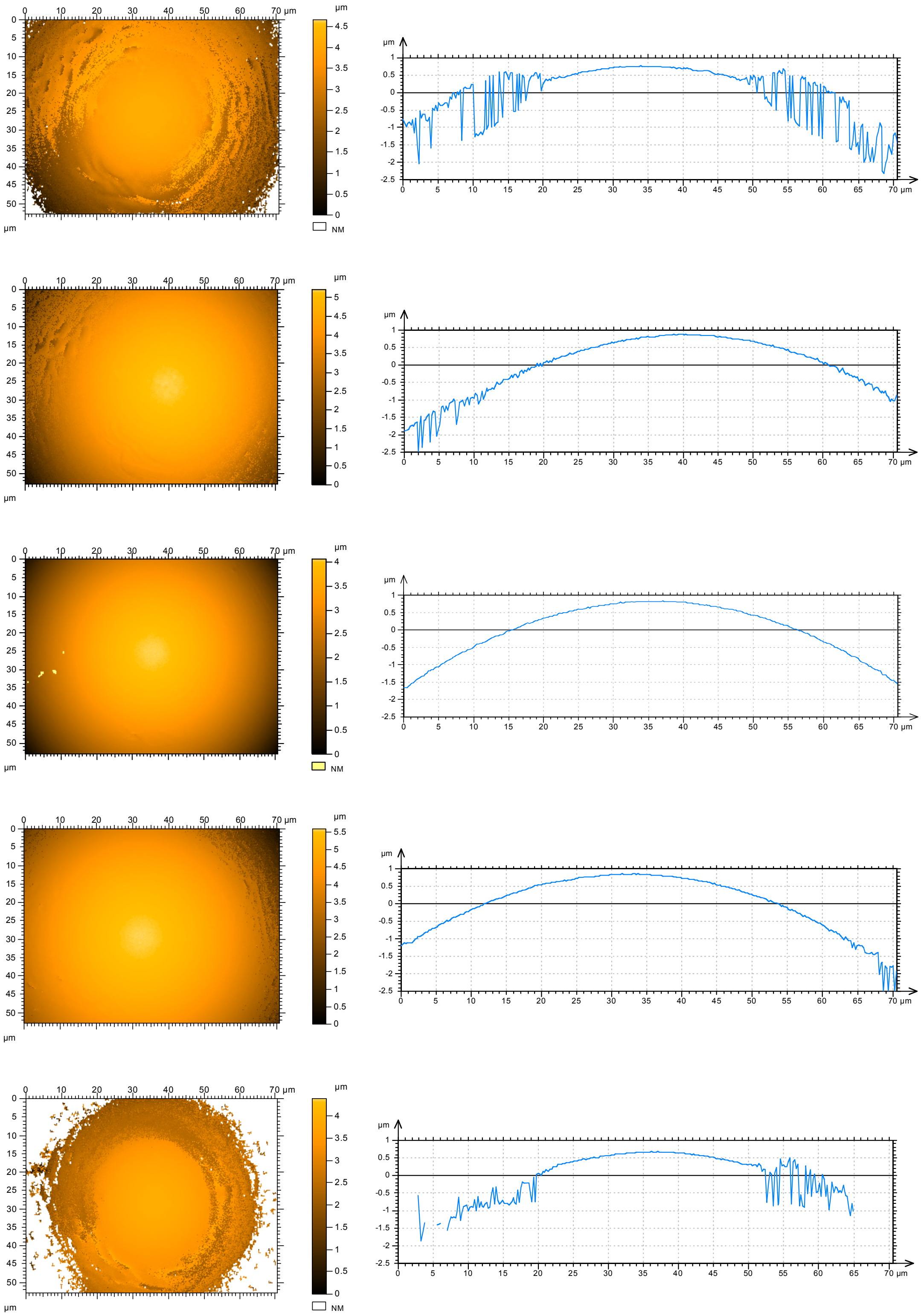

Figure 24 In-focus and out-of-focus surface data and profile

If field stitching is used there may be a number of options available to the user that will influence how the data is acquired, and the level of integrity:

- matrix shape or the pattern of images recorded by the instrument (column orientated, row orientated, circular, annulus, etc.);
- start position; and
- field overlap.

Figure 25 illustrates the use of field stitching. The first part of Figure 25 is an image (10× objective, 1× zoom setting) taken from the reverse side of a new UK five pence coin. Using the stitching function on the CSI instrument allows a four by four image stitch of a larger area, with each sub-image recorded using the same optical settings, and an image overlap of 10 %.

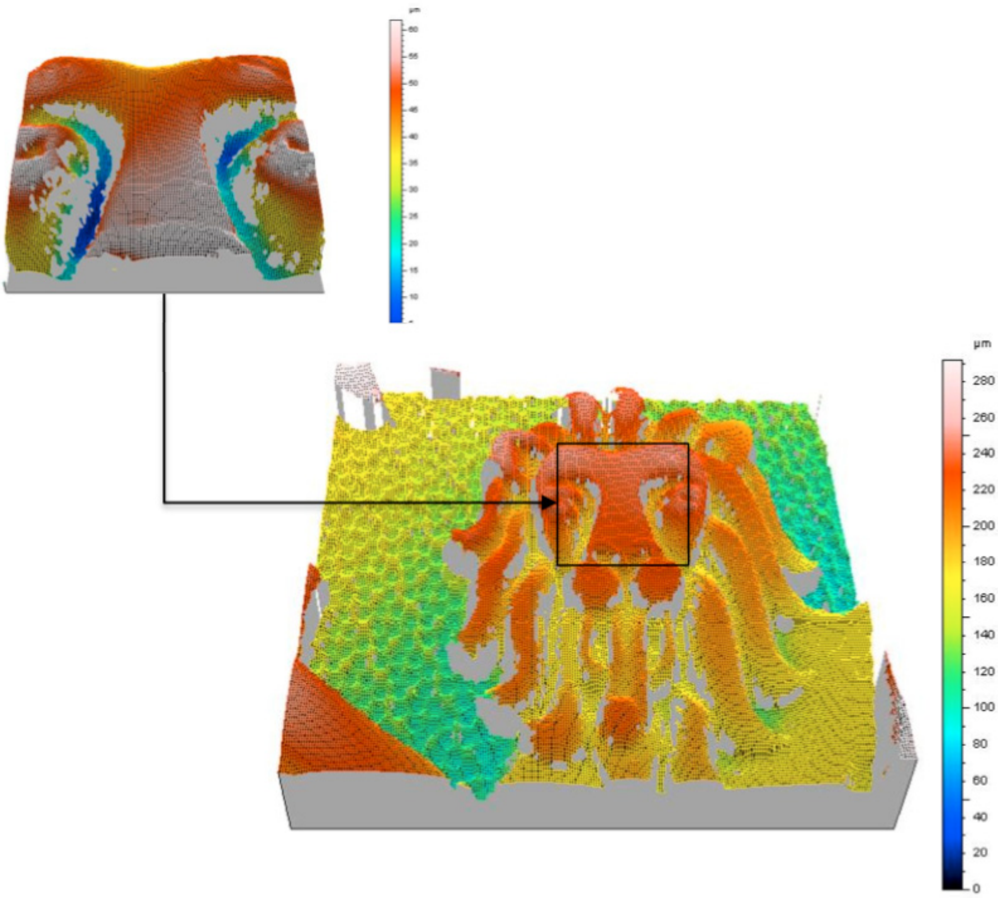

Figure 25 Imaging large areas using field stitching techniques

The importance of sample stage leveling/tilting

It is normal practice to adjust the position of the specimen surface such that the surface is normal to the optical axis (and objective lens), i.e. the surface has been levelled. The majority of CSI instruments will provide some form of tip/tilt adjustment, either manually operated or motorized. Some tip/tilt tables will also offer parcentric movement, which maintains the focussed position on the surface.

Tip/tilt adjustment can be monitored on the live image screen by observing the behaviour of the white light fringe pattern. A non-levelled specimen will exhibit a large number of densely packed fringes. As the specimen approaches a level position, the fringe spacing increases (fringe density decreases) until a point may be reached where a null fringe condition is reached. This occurs when there is one large fringe across the field of view, which will appear to blink on and off as the instrument vertically scans. It may be necessary to adjust the horizontal axes to reposition the relevant field of view, and it may also be necessary to adjust the vertical axis focus.

For surfaces that have varying surface topography, it will be possible to level the specimen with respect to the mean surface height, but it may not be possible to achieve the null fringe condition. Instead the number of observed fringes will be minimized to a certain degree, before increasing again as the table moves away from the levelled condition.

Adjusting the light source intensity

For the majority of measurements, the light source intensity should be adjusted to avoid light saturation at the image plane. This will be seen as white areas on the live image, which do not show any changes of contrast or data, and will often be coloured red in many instrument software packages to act as a visual warning of saturation. When using phase based systems, saturation during a measurement may cause a loss of data, and data holes in the final surface profiles. However it should be noted that some instruments are more tolerant to image plane saturation than others.

The effect of saturation is illustrated in Figure 26, in which three images of a section of a broaching operation roughness comparison specimen are shown, starting with good contrast and no data holes. The light intensity is increased in the second image and finally saturation in the third image leads to holes in the data file.

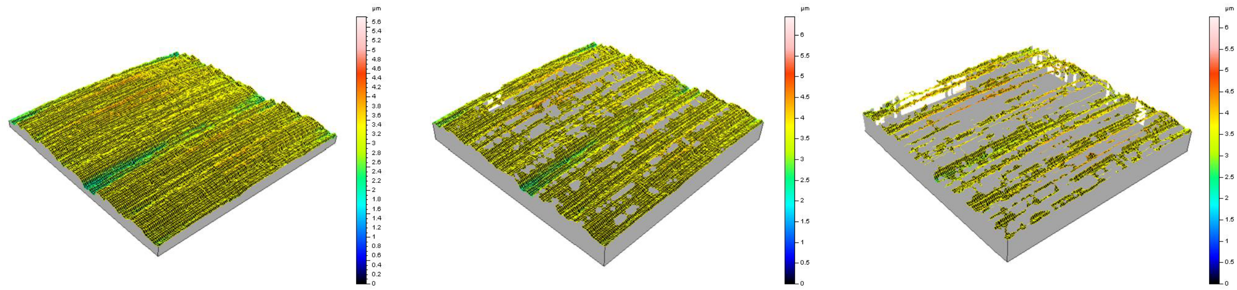

Good contrast Slight saturation Over saturated

Figure 26 Increasing image saturation leading to data holes

The majority of CSI instruments will allow adjustment of light intensity and saturation in software. Manually applied neutral density filters may also be an option. For surfaces that have uniform absorption or reflection characteristics, once the light intensity is set prior to data acquisition, saturation should not occur. For surfaces that have specularly reflective areas (mirror like) then it may be difficult to remove all saturated regions. If these are successfully removed by lowering the light intensity, then the overall contrast range may make some regions very dark, and again compromise data quality.

However, in some instances saturation may provide benefits. For rough and steep surfaces, as well as those with materials of different reflectivity, some surface measuring modes provide superior data when the bright parts of the image are saturated. Saturated parts of a surface are generally the areas of a surface that are straightforward to illuminate resulting in signal of good quality. However, more light intensity on the steep, rough, or dark portions of the sample, can significantly improve the data quality on those regions. So in these cases, the user may opt to over-saturate a portion of the field of view that has been previously measured, in order to gain data from otherwise poorly illuminated areas or features.

Processing results and interpretation

6

IN THIS CHAPTER

- The importance of filter selection
- Graphical representation
- An introduction to 2D surface texture parameters
- Areal parameters
- Example areal parameters

Processing results and interpretation

The CSI instrument produces numerical data maps of surface topography, which typically require further processing. Common operations will produce graphical representation of the data, and potentially generate numerical quantifiers of the surface, *i.e.* surface texture parameters. In this chapter, various methods and approaches to data presentation are addressed, with specific reference to filtering techniques, allowing the user to identify the range of options available. The assumptions made at this point are that the CSI instrument has been appropriately set up (see chapter 3) and the fringe patterns have been optimized as discussed in chapter 5.

The importance of filter selection

The immediate output of all CSI instruments is a raw set of quantified data, normally scaled in the range of hundreds of micrometres to tens of nanometres. These quantified maps have meaning in themselves, and graphical representation may be all that is required to solve a given problem or identify issues. In many cases, however, some form of filtering will be needed to exclude or include particular features or characteristics, or to allow the calculation of numerical surface texture parameters.

CSI instruments will often have filter options in their operational software for general data manipulation. Some of these filter types are briefly identified below.

- Low pass – low spatial frequency signal components are maintained whilst high spatial frequency signal components are rejected.
- High pass - high spatial frequency signal components are maintained whilst low spatial frequency signal components are rejected.
- Band pass – user defined band of spatial frequency signal components are maintained whilst spatial frequency components above and below the defined band are rejected. This filter can be regarded as being a combination of a low and high pass filter.
- Averaging – the combination of multiple exposures of the same region of interest.

- Median – a noise reduction technique whereby the median pixel value is chosen from the neighboring pixel values.
- Fast Fourier Transform (FFT) – a spatial frequency spectrum is generated from the data, with windowing techniques being used in the spatial frequency domain to include/exclude frequency terms.

Filter type and band selection requires the instrument user to have an understanding of the signal content of the data and the characteristics of the data required for further processing. Implementation of any of the above filter options, typically requires the user to identify appropriate frequency and/or wavelength cut-offs, in order to select/reject the correct signal frequencies. Further decisions may be required concerning edge data loss or preservation at the extremities of the filter windows, filter window sizes, and the number of filter iterations or operations.

Areal filtering

Filtering characteristics and parameters required for surface texture profile analysis have been developed over many years with specifications already defined within a number of ISO documents (ISO 4287, ISO 11562). Profile measurement filtering is discussed and summarized in NPL *Measurement Good Practice Guide No.37 - The Measurement of Surface Texture using Stylus Instruments*, and the reader should refer to this guide for further information.

Whilst profile characterization requires three groups or classes of surface description (*P, R* and *W*) areal surface characterisation does not. The meaning of the majority of the areal parameters depends on the type of scale-limited surface used. ISO/FDIS 25178 (part 3) defines two categories of filter; the S-filter and the L-filter. The S-filter is defined as a filter that removes unwanted small-scale lateral components of the measured surface such as measurement noise, spikes or functionally irrelevant small features. The L-filter is used to remove unwanted large-scale lateral components of the surface. Nominal form removal (defined as an F-operator) is achieved typically by using a least-squares method.

The scale at which the filters operate is controlled by the nesting index. The nesting index is an extension of the cut-off wavelength used in profile analysis and is suitable for all types of filters. For example, for a Gaussian filter the nesting index is equivalent to the cut-off wavelength, and for a morphological filter with a spherical structuring element, the nesting index is the radius of the spherical element. These filters are used in combination to create SF and SL surfaces.

Significant development of filter types and systems has been occurring for areal dataset applications. It has now been necessary to produce a standardised framework for filters, which gives a mathematical foundation for filtration, together with a toolbox of different filters. This framework runs parallel to, and cross-references into the ISO 25178 specifications. Information concerning these filters has been published as a series of technical specifications (ISO/TS 16610 series) with further parts still in development, to allow metrologists to assess the utility of the recommended filters according to applications. When fully published, the technical specifications will contain the classes of filters listed below.

- Linear filters - the mean line filters (M-system) belong to this class and include the Gaussian filter, spline filter and the spline-wavelet filter.
- Morphological filters - the envelope filters (E-system) belong to this class and include closing and opening filters using either a disk or a horizontal line.
- Robust filters - filters that are robust with respect to specific phenomena such as spikes, scratches and steps. These filters include the robust Gaussian filter and the robust spline filter.
- Segmentation filters - filters that partition a profile into portions according to specific rules. The motif approach belongs to this class and has now been put on a firm mathematical basis.

The Gaussian filter has become the routine standardized filter of choice for filtering of line profiles for 2D parameter generation, with both roughness and waviness surfaces acquired from a single filtering procedure with minimal phase distortion. This approach has been extended through the development of the areal Gaussian filter (and robust versions), which is now used by many instrument manufacturers, and again is being formalized in ISO 16610.

The relevance of the description of areal filtering given here is dependent on the CSI instrument being used. Users should familiarize themselves with the software options provided within the instrument, although much of the newer developments expressed in developing standards (ISO 16610 and ISO 25178) have yet to migrate to full application within CSI software.

It is clear that areal filtering is a complex subject that may be the subject of a dedicated NPL measurement good practice guide. The user should consider filtering options on a case-by-case basis with the guiding principle that if you want to compare two surface measurements, it is important that both sets use the same filtering methods and nesting indexes (or that appropriate corrections are applied).

Graphical representation

Most software applications provide a range of visualization tools for displaying CSI data, including; wire mesh, point mesh, solid rendering, photo-realistic, and contour plots, some of which are illustrated in Figure 27. Note that the 3D meshes are rendered at a mesh density of 30 % and the data have been obtained from a turning operation roughness comparison specimen.

Visualization software tools allow the user to magnify features, zoom into features, threshold aspects of the topography, rotate the data set to obtain better visualization of features, change the colour maps, etc. The range of options is dependent on the software environment. Some users may find that transferring the data into other software environments is desirable or necessary, in order to use more specialist and wider ranging graphics options, or numerical processing options.

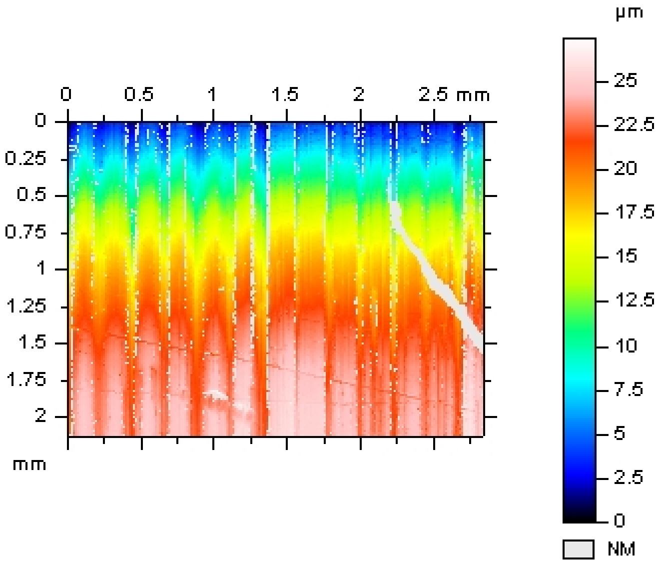

(a)

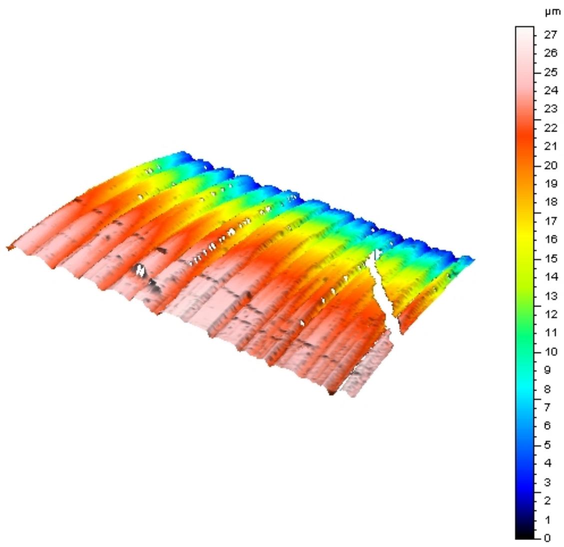

(b)

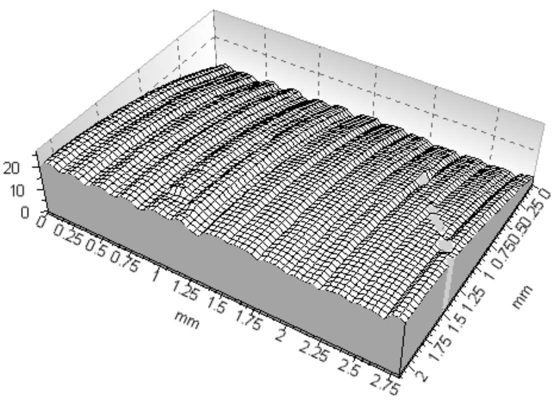

(c)

Figure 27 Examples of areal data representation

Form removal

The measurement of surface texture is carried out on surfaces with a wide variety of localized topography and overall component form, an example being the measurement of texture on a turned cylindrical billet of material. In these circumstances, the larger profile or form may mask the detail of the surface texture characteristics in question. Most software applications will allow the user to remove underlying form and perform leveling operations (which may be required for subsequent analysis routines), exposing the detail of the surface texture/characteristics.

A common approach to form removal is to fit a standard geometric form to the data and then subtract this geometric form from the data. Software selectable options will typically include standard mathematical functions that describe a cylinder, a plane and a sphere. These elements are clearly ideal when the component is cylindrical, planar or spherical in shape. For surfaces exhibiting freeform shape characteristics, further options may be available in the form of polynomial approximations. In this case the user is required to select the power or order of the polynomial (integer value often selectable between two and ten), with the coefficients of the polynomial being calculated via least-squares techniques. Care should be taken with this approach because the higher the polynomial order, the more the fitting process will remove low frequency roughness components from the data at the same time and potentially introduce minor waviness into the structure.

An example of the form removal process is shown in Figure 28, with the original data which is composed of machining marks on a cylindrical surface (Figure 28(a)), having form removal using a cylinder function results in Figure 28(b). This data is shown as a 3D mesh plot (Figure 28(c)) with the form removed version in Figure 28(d).

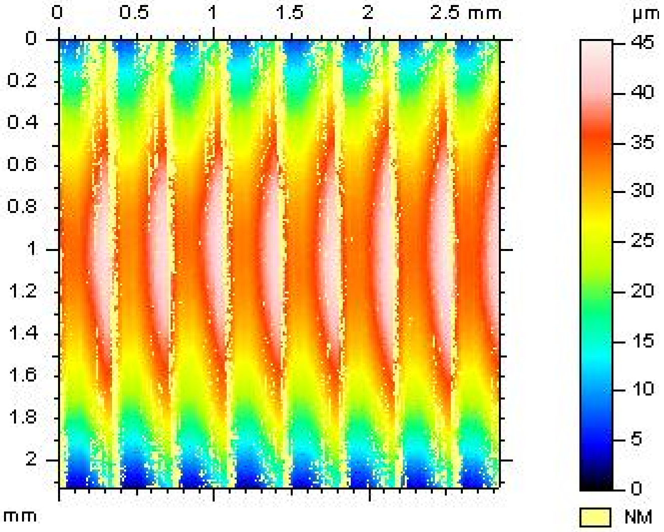

(a)

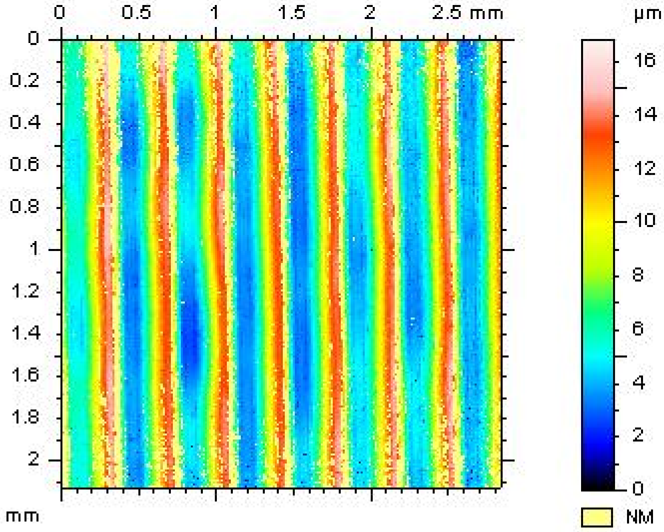

(b)

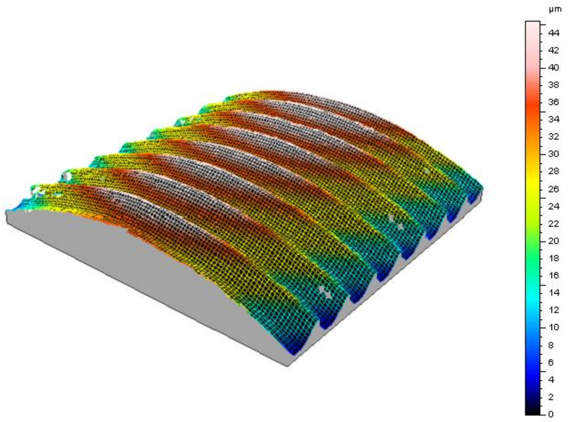

(c)

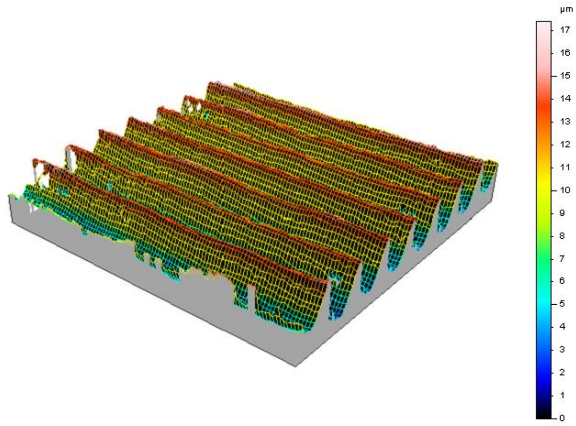

(d)

Figure 28 Areal data with and without the form removed

Data leveling

The optimization of a CSI instrument for the null fringe condition involves the manual or automatic physical leveling of the specimen (see chapter 3 and chapter 5). However, mathematical tilt removal is almost always performed before computational analysis because it is quire normal to have some imperfection in the leveling of the sample. Residual tilt in a measurement result is most often the result of alignment of the part against the test optics rather than an intrinsic property of the test piece. Slope components can mask the true extent of the surface roughness components. Typical options provided within CSI software are based on automated or manually defined least-squares plane calculation. For the least-squares approach the entire dataset may be fitted or a subset of the data may be used to calculate the least squares plane. Once calculated, this plane can then be removed from the dataset leaving the underlying roughness. The least-squares plane approach is generally recommended for surfaces with random surface texture.

Surfaces exhibiting more regular surface features may benefit from the use of manual plane definition where the user interactively selects points on the object or surface to define a plane. In this case a minimum of three points are required for plane definition. The leveling process is illustrated in Figure 29, with the original data which is composed of machining marks on a surface (Figure 29(a)), which is then leveled using a least-squares plane operation resulting in Figure 29(b). This data is shown as a 3D mesh plot (Figure 29(c)) with the mesh density increased to 100 % compared to 30 % used in Figure 29(b) and (c). Finally more detail is provided in the magnified view in Figure 29(d).

Further graphical data representation

Having the 3D data set allows the user to interrogate the information by extracting line profiles from the surface topography, which again may provide useful information. In a similar manner to the 3D data sets, users may adjust a range of viewing parameters in order to examine various aspects of the data, as demonstrated in Figure 30. This shows a line profile taken from Figure 29(a), an expanded version of the line profile (Figure 30(b)), a cumulative frequency plot (Figure 30(c)), and a material ratio curve (Figure 30(d)).

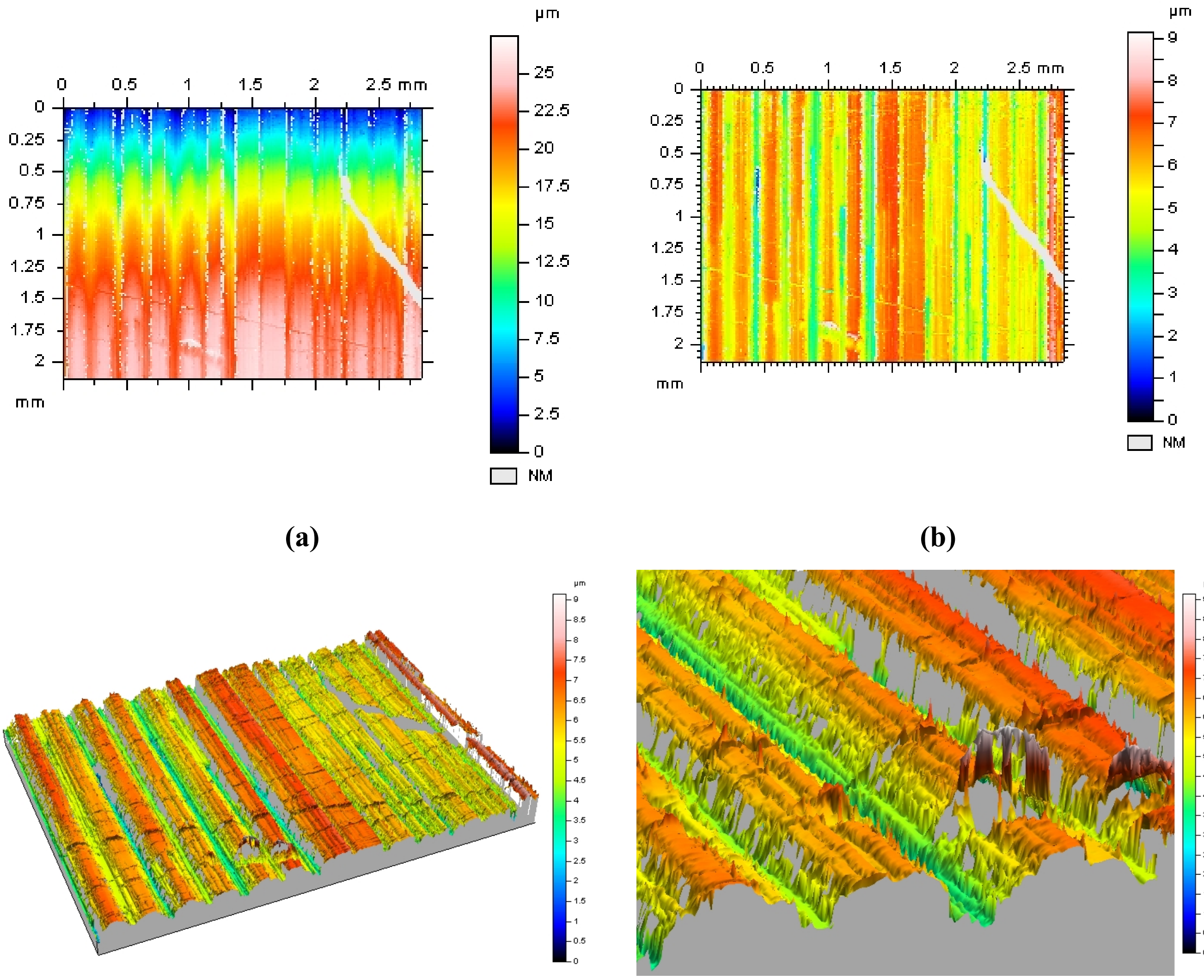

Figure 29 Areal data showing levelling of the object

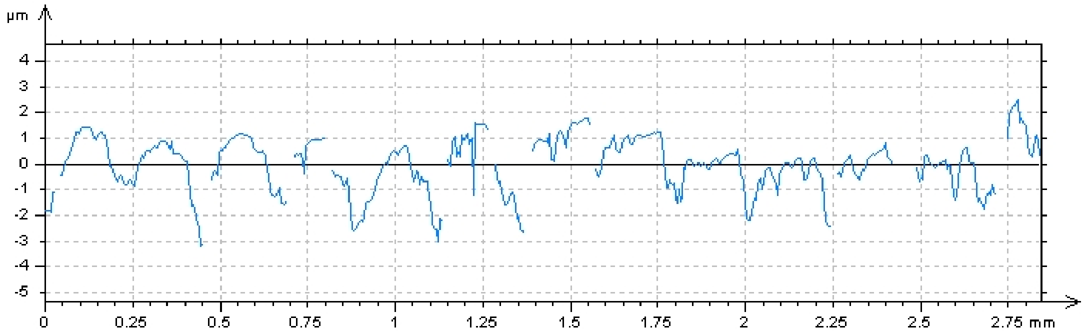

(a)

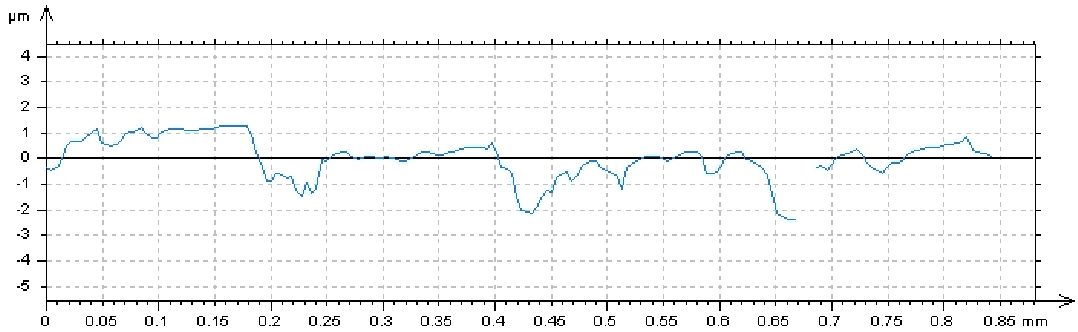

(b)

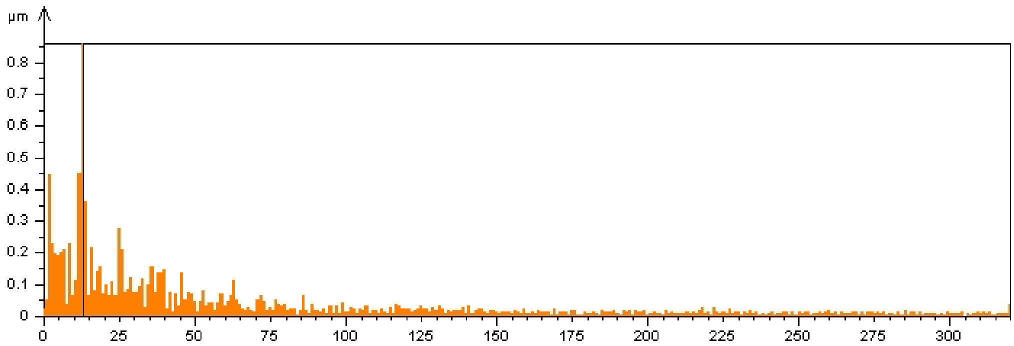

(c)

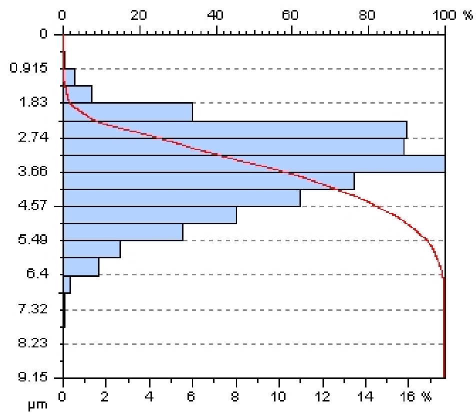

(d)

Figure 30 2D profiles and associated data representation

An introduction to 2D surface texture parameters

The 3D and 2D data sets can be used for the basis of producing numerical quantifiers or parameters, which are used to describe functionally related aspects of surfaces. At this stage it is important to identify answers to the questions listed below.

- Is there functional information and understanding about how the object operates in service?
- Is there information about the key characteristics of the surface that influence this function?
- Is there understanding of the manufacturing processes used to produce the surface?
- Are there any surface texture parameters that match the key characteristics of the surface?

The answers to these questions are important, because they can then help to select surface parameters that will be most appropriate to the function of the surface.

There are over one hundred and fifty 2D parameters in use, describing the raw data (*P* parameters), roughness (*R* parameters) and waviness (*W* parameters). The *P* parameters describe non-filtered data before wavelength cut-offs and filter profiles are applied. Roughness and waviness parameters are generated as a function of high pass and low pass filtering of the raw data respectively, and the numerical values are very dependent on the filtering parameters. Further advice is provided in NPL *Measurement Good Practice Guide No.37 - The Measurement of Surface Texture using Stylus Instruments*.

Many profile parameters have been in use for over fifty years and form the core of industrial understanding of surface texture metrology. The most commonly used parameters have been standardized in ISO 4287, with elements such as Motif parameters (ISO 12085) and parameters for stratified surfaces (ISO 13565) also being standardized. Other parameters may be industrial sector-dependant and will not necessarily be documented in standards, and some parameters may be specific to certain countries, with respect to historical development. It should be noted that the range of profile parameters available to the user will be dependent on the CSI instrument manufacturer.

There are inherent limitations with profile surface measurement and characterization. A fundamental problem is that a profile does not necessarily indicate functional aspects of the surface. For example, consider the most commonly used parameter for profile characterization, *Ra* (see NPL *Measurement Good Practice Guide No.37* for a description of the profile parameters). Figure 31 shows the profiles of two surfaces, both of which return the same *Ra* value when filtered under the same conditions. It can be apparent that the two surfaces have very different features and consequently very different functional properties.

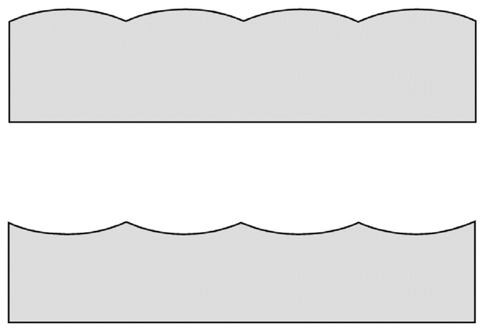

Figure 31 Profiles showing the same Ra with differing height distributions

With profile measurement and characterization it is also often difficult to determine the exact nature of a topographic feature. Figure 32 shows a profile and a 3D surface map of the same component covering the same measurement area. With the 2D profile alone a discrete pit is measured on the surface. However, when the 3D surface map is examined, it can be seen that the assumed pit is actually a valley and may have far more influence on the function of the surface than a discrete pit.

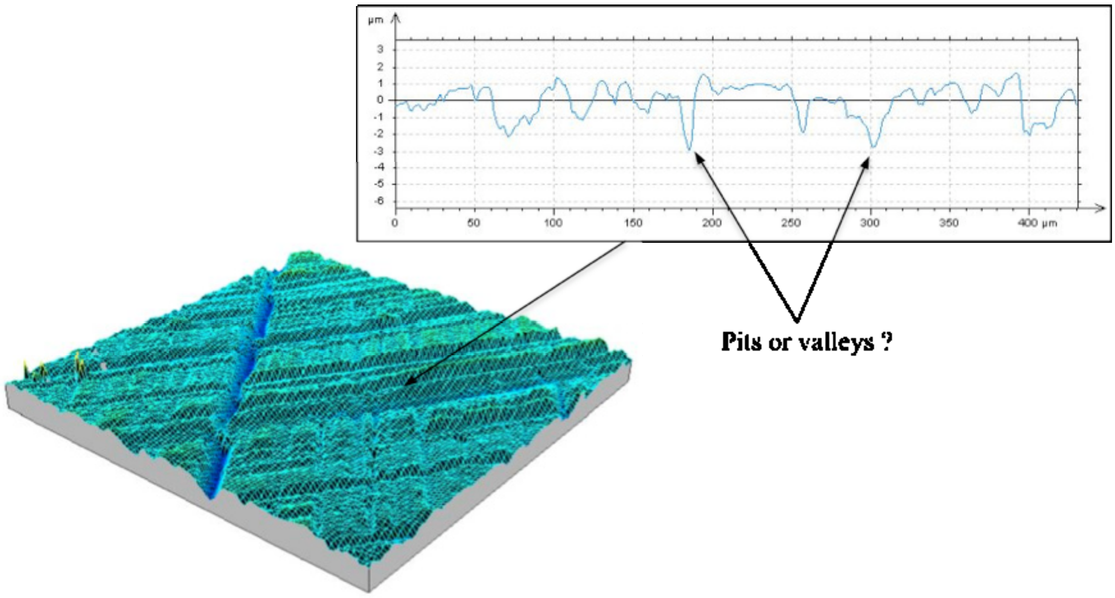

Figure 32 A profile taken from an areal measurement shows the possible ambiguity of profile measurement and characterisation

The limitations of profile measurement and characterization have brought about the development of areal surface measurement and characterization. Areal techniques give a better understanding of the surface in its functional state. In order to aid this understanding, an attempt to standardise the vocabulary of surface characteristics has been published in ISO 8785.

Areal parameters

Areal surface texture parameters have been developed over the last twenty years, in an attempt to quantify surfaces from an area viewpoint rather from a line profile viewpoint. An original set of fourteen parameters was published in 1993 by University of Birmingham as part of a European Union funded project. These parameters were re-evaluated by the University of Huddersfield, and further developed. This resulted in a redefined fifteen element strong *S* parameter set and a nine element strong *V* parameter set, documented in a recently-published textbook by one of the authors – see list of literature in the Appendix).

These parameters now form the core of the effort of Working Group 16 of ISO Technical Committee 213, which was set up to develop new a surface texture system as part of the Geometrical Product Specification (GPS) system. The prototype parameters have been further expanded through ISO committee negotiations, and have now been published (ISO 25178 part 2 is currently available from ISO). Full ISO standard publication of specifications relating to instruments, filtering and calibration details for areal surface texture measurement and characterization are expected over the next couple of years.

The challenge for the user is to identify the areal parameter or parameters that most suit the function of the surface being examined. This challenge requires an understanding of the engineering function of the object surface, or at least good communication with the surface designers. Unlike the profile parameters, the areal parameter sets do not draw any distinction between the equivalents of roughness and waviness, this distinction being a function of the recommended filtering methods. However, as with the use of the profile parameter set, the user may need to use several areal parameters to describe a surface, because one parameter may not provide sufficient description from a functional viewpoint.

A further challenge for the designer is caused by the generation of the new areal parameter specifications, from a dimensioning and tolerancing viewpoint. Whilst the rules for dimensioning and tolerancing of technical drawings include the profile parameters within the structure of ISO 1302, dimensioning and tolerancing rules for the areal parameters are only at a draft stage of formulation.

The core *S* parameters are identified in Table 1. As previously explained for the profile parameters, the range of areal parameters available to the user will be dependent on the CSI instrument manufacturer. *S* parameters have also been developed as analogies to the range of material ratio parameters defined in ISO 4287 and ISO 13565 (*Sk*, *Spk*, *Svk*, *Smr1*, *Smr2*) and ISO 13565 (*Spq*, *Svq*, *Smq*). These parameters are identified in Table 2. Where a parameter may seem mathematically complex, for example the spatial parameters, often the user only needs a good understanding of the meaning of the parameter and may not need to know its exact derivation.

Table 1 The *S* parameter set

Parameter	Description	Typical Units
Sa	Arithmetical mean height	µm
Sq	Root mean square length of the scale limited surface	µm
Ssk	Skewness of the scale limited surface	
Sku	Kurtosis of the scale limited surface	
Sp	Maximum peak height	µm
Sv	Maximum pit depth	µm
Sz	Maximum height of the scale limited surface	µm
Sal	Autocorrelation length	µm
Str	Texture aspect ratio	
Sdq	Root mean square gradient of the scale limited surface	
Sdr	Developed interfacial area ratio of the scale limited surface	
Smr(c)	Area material ratio of the scale limited surface	%
Sdc(mr)	Inverse areal material ratio of the scale limited surface	µm
Sxp	Peak extreme height	µm
Svs(s)	Volume scale function	
Srel(s)	Area scale function	
Svfc	Volume fractal complexity	
Safc	Area fractal complexity	
Std	Texture direction of the scale limited surface	degrees

Note that parameters that do not have units identified in Table 1 are of unit one by mathematical definition.

Table 2 *S* parameters as a function of material ratio

Parameter	Description	Units
Sk	Core roughness depth	μm
Spk	Reduced peak height	μm
Svk	Reduced valley depth	μm
Smr1	Material portion	%
Smr2	Material portion	%
Spq	Slope of a linear regression performed through the plateau region	μm
Svq	Slope of a linear regression performed through the valley region	μm
Smq	Relative material ratio at the plateau to valley intersection	μm

ISO 25178 part 2, linked to the new suite of standards documenting filtering - ISO 16610, also introduces some new descriptive operations for the surface data. Important elements are:

Real surface of a workpiece - set of features that physically exist and separate the entire workpiece from the surrounding medium.
Primary surface - surface portion obtained when a surface portion is represented as a specified primary mathematical model with specified nesting index.
Primary extracted surface - finite set of data points sampled from the primary surface.
Surface filter - filtration operator applied to a surface (in reality applied to the primary extracted surface).
S-filter - surface filter that removes small-scale lateral components from the surface resulting in the primary surface.
F-filter - surface filter that removes large-scale lateral components from the primary surface.

F-operator - operator that removes form from the primary surface (it should be noted that many L-filters are sensitive to form and require an F-operator first as a pre-filter before being applied).
S-F surface - surface derived from the primary surface by removing the form using an F-operator.
S-L surface - surface derived from the S-F surface by removing the large scale components using an L-filter.
Scale limited surface - S-F surface or a S-L surface.

Further definitions are used to define features on surfaces, which then link into the description of the *S* or *V* parameters:

Peak - point on the surface that is higher than all other points within a neighbourhood of that point.
Hill - region around a peak such that all maximal upward paths end at the peak.
Pit - point on the surface that is lower than all other points within a neighbourhood of that point.
Dale - region around a pit such that all maximal downward paths end at the pit.
Course line - curve separating adjacent hills.
Ridge line - curve separating adjacent dales.
Saddle - set of points on the scale limited surface where ridge lines and course lines cross.
Saddle point - saddle consisting of one point.
Areal feature – hill or dale.
Line feature - course line or ridge line.
Point feature - peak, pit or saddle point.

An additional set of descriptors has been developed to allow the user to describe the types of feature that populate a surface. These features are described in Table 3.

Table 3 Surface features

Class of limited feature	Type of scale limited feature	Designated symbol
Areal	Hill	H
	Dale	D
Line	Course Line	C
	Ridge Line	R
Point	Peak	V
	Pit	P
	Saddle Point	S

A five stage feature characterization process has been defined: selection of the type of texture feature, surface segmentation, determining significant features, selection of feature attributes, and quantification of feature attribute statistics. These features then allow the use of a range of parameters to quantify the surface, as shown in Table 4.

Table 4 Surface feature *S* parameters

Parameter	Description	Typical Units
Spd	Density of peaks	1 mm^{-2}
Spc	Arithmetic mean peak curvature	1 mm^{-1}
S10z	Ten point height of surface	µm
S5p	Five point peak height	µm
S5v	Five point pit depth	µm
Sda(c)	Closed dale area	μm^2
Sha(c)	Closed hill area	μm^2
Sdv(c)	Closed dale volume	μm^3
Shv(c)	Closed hill volume	μm^3

The final elements of the areal parameters are the *V* parameters. These parameters have been specifically developed to quantify material volume and void volume characteristics of surfaces, based on three zones or strata; the peak zone, the core zone, and the valley zone. These parameters are summarized in Table 5. It should be noted that the *S* parameters detailed in Table 2 were originally developed as a subset of the *V* parameter concept.

Table 5 The *V* parameter set

Parameter	Description	Typical Units
Vv(mr)	Void volume	ml m^{-2}
Vvv	Dale void volume of the scale limited surface	ml m^{-2}
Vvc	Core void volume of the scale limited surface	ml m^{-2}
Vm(mr)	Material volume	ml m^{-2}
Vmp	Material volume of the scale limited surface	ml m^{-2}
Vmc	Core material volume of the scale limited surface	ml m^{-2}

During the development of the areal parameters, the parameters were functionally grouped to aid selection. These functional groupings can be seen in Figure 33 and Figure 34. Note that for consistency with existing literature, the material ratio *S* parameters are included under the *V* parameter hierarchical structure.

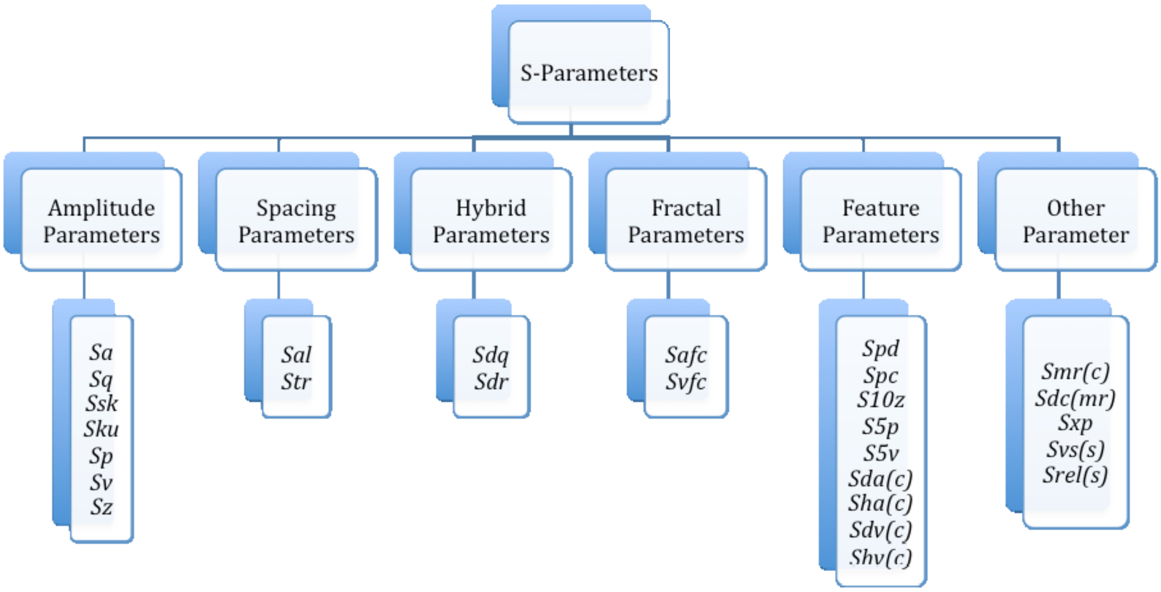

Figure 33 *S* parameters shown in a functional context

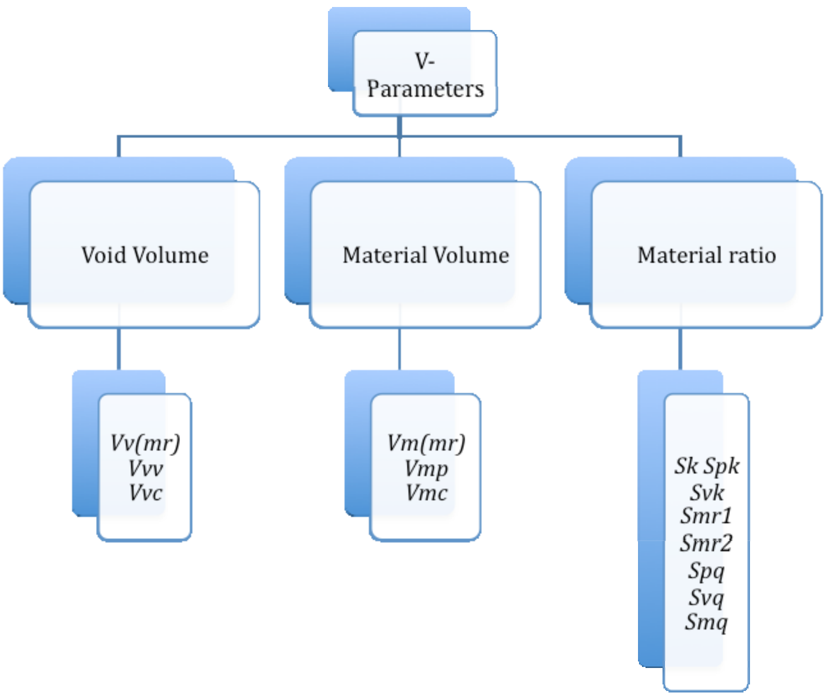

Figure 34 *V* parameters shown in functional context

Example areal parameters

The range of areal parameters available is very extensive, and the user is referred to the relevant ISO standards and user guides for more detailed descriptions. However, briefly included here, are more detailed examples of a small number of the amplitude parameters.

Amplitude parameters give information regarding the areal height deviation of the surface topography. There are seven parameters in the amplitude family that are described in this section.

The root mean square value of the ordinate values within a sampling area, Sq

The *Sq* parameter is defined as the root mean square value of the surface departures, $z(x, y)$, within the sampling area

$$Sq = \sqrt{\frac{1}{A}\iint_A z^2(x,y)\,dxdy} \tag{6.1}$$

where A is the sampling area, xy. Note that equation (6.1) is for a continuous $z\ (x, y)$ function. However, when making surface texture measurements using CSIs (or indeed any surface texture measuring instrument), $z\ (x, y)$ will be determined over a discreet number of measurement points. In this case equation (6.1) would be written as

$$Sq = \sqrt{\frac{1}{N}\frac{1}{M}\sum_{i=1}^{N}\sum_{j=1}^{M} z_{ij}^2} \tag{6.2}$$

where N is the number of points in the x direction and M is the number of points in the y direction. The equations for the other parameters below that involve an integral notation can be converted to a summation notation in a similar manner. The *Sq* parameter is the most common parameter that is used to characterize optical surfaces as it can be related to the way that light scatters from a surface.

The arithmetic mean of the absolute height, Sa

The *Sa* parameter is the arithmetic mean of the absolute value of the height within a sampling area, thus

$$Sa = \frac{1}{A} \int_{A} \left| z(x, y) \right| dx\, dy \tag{6.3}$$

The *Sa* parameter is the closest relative to the *Ra* parameter; however, they are fundamentally different and should not be directly compared. Areal, or *S* parameters, use areal filters (see later section) whereas profile, or *R* parameters, use profile filters. The *Ra* parameter is the most common profile parameter for purely historical reasons and it should be noted that *Sq* is a much more statistically significant parameter than *Sa*.

Skewness of topography height distribution, Ssk

Skewness is a measurement of the symmetry of the surface deviations about the mean reference plane and is the ratio of the mean cube value of the height values and the cube of *Sq* within a sampling area, thus

$$Ssk = \frac{1}{Sq^3} \left[\frac{1}{A} \iint_{A} z^3(x, y)\, dx\, dy \right] \tag{6.4}$$

The *Ssk* parameter describes the shape of the topography height distribution. For a surface with a random (or Gaussian) height distribution that has symmetrical topography, the skewness is zero. The skewness is derived from the amplitude distribution curve; it is the measure of the profile symmetry about the mean plane. This parameter cannot distinguish if the profile spikes are evenly distributed above or below the mean plane and is strongly influenced by isolated peaks or isolated valleys. This parameter represents the degree of bias, either in the upward or downward direction of an amplitude distribution curve.

A symmetrical profile gives an amplitude distribution curve that is symmetrical about the centre line and an unsymmetrical profile results in a skewed curve. The direction of the skew is dependent on whether the bulk of the material is above the mean plane (negative skew) or below the mean plane (positive skew). Use of this parameter can distinguish between two surfaces having the same *Sa* value.

Kurtosis of topography height distribution, Sku

The *Sku* parameter is a measure of the sharpness of the surface height distribution and is the ratio of the mean of the fourth power of the height values and the fourth power of *Sq* within the sampling area, thus

$$Sku = \frac{1}{Sq^4}\left[\frac{1}{A}\iint_A z^4(x,y)dx\,dy\right] \tag{6.5}$$

The *Sku* parameter characterizes the spread of the height distribution. A surface with a Gaussian height distribution has a kurtosis value of three. Unlike *Ssk* this parameter can not only detect whether the profile spikes are evenly distributed but also provides a measure of the spikiness of the area. A spiky surface will have a high kurtosis value and a bumpy surface will have a low kurtosis value. Note that kurtosis cannot differentiate between a hill and a valley.

The maximum surface peak height, Sp

The *Sp* parameter is defined as the largest peak height value from the mean plane within the sampling area. This parameter can be unrepresentative of a surface as its numerical value can vary so much from sample to sample. It is possible to average over several sampling areas and this will reduce the variation, but the value is often still numerically too large to be useful in many cases. However, this parameter will succeed in finding unusual conditions such as a sharp spike or burr on the surface or the presence of cracks and scratches that may be indicative of poor material or poor processing.

The maximum pit height of the surface, Sv

The *Sv* parameter is defined as the largest pit or valley depth from the mean plane within the sampling area. This parameter has the same disadvantages as the maximum surface peak height.

Maximum height of the surface, Sz

The *Sz* parameter is defined as the sum of the largest peak height value and largest pit or valley depth value within the sampling area.

The *Sp, Sv* and *Sz* parameters give absolute values for features on the surface. They can be useful independently, but also can be used in conjunction with other parameters to describe surface topography more comprehensively. For instance, by examining both the *Sq* value and the *Sz* value, it may be possible to indicate whether the apparent roughness is due to isolated features or the overall surface roughness.

Parameter generation from data

Figure 35, Figure 36 and Figure 37 serve to illustrate the generation of areal quantified data from typical surfaces. In all cases, the data has not had any form of numerical/data filling, to fill in non-measured points of data voids caused by the limitations of the CSI instrument. Filling non-measured data points has consequences on data integrity that will be demonstrated in chapter 7. Where required the data sets have had leveling operations performed (least-squares planes via subtraction) and the option of form removal. All figures show examples of less and more extensive surface roughness for similar surface treatments, with an accompanying range of basic *S* parameters.

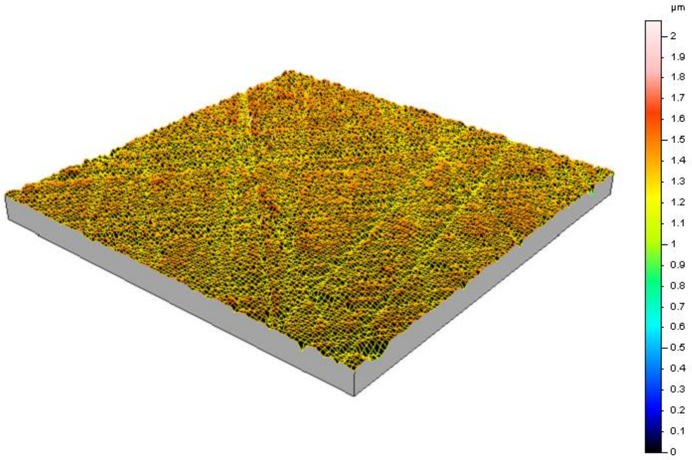

Parameter	**Value**
Sa	0.058 µm
Sq	0.082 µm
Sp	0.682 µm
Sv	1.390 µm
St	2.070 µm
Sz	1.980 µm
Ssk	-2.13
Sku	21.70

(a)

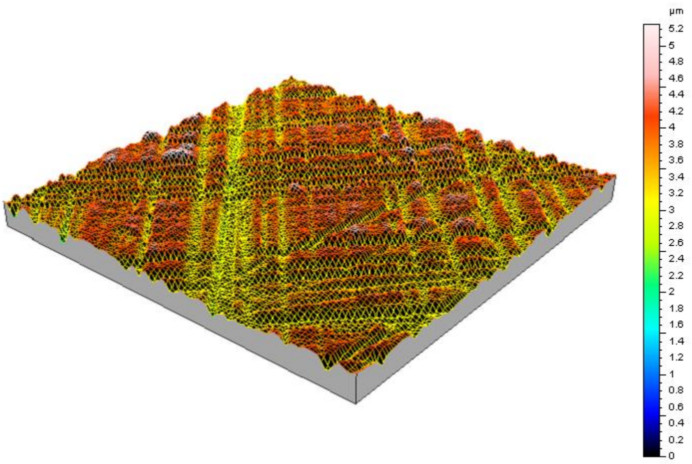

Parameter	**Value**
Sa	0.492 µm
Sq	0.621 µm
Sp	1.720 µm
Sv	3.540 µm
St	5.260 µm
Sz	4.970 µm
Ssk	-0.95
Sku	3.91

(b)

Figure 35 Analysis of honed surfaces

The honed surfaces (Figure 35) required a least-squares leveling operation using a plane subtraction technique. The dominating cylindrical forms of the two datasets were removed using a third order polynomial form removal operation. *S* parameters were generated without any further filtering of the datasets.

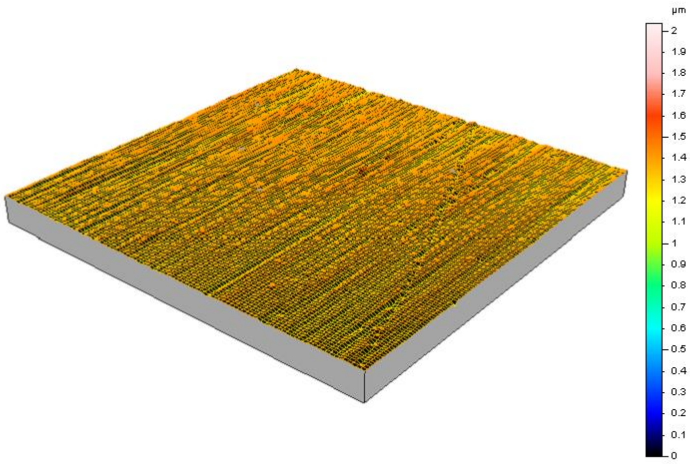

Parameter	Value
Sa	0.033 µm
Sq	0.046 µm
Sp	0.633 µm
Sv	1.400 µm
St	2.040 µm
Sz	1.780 µm
Ssk	-1.98
Sku	35.30

(a)

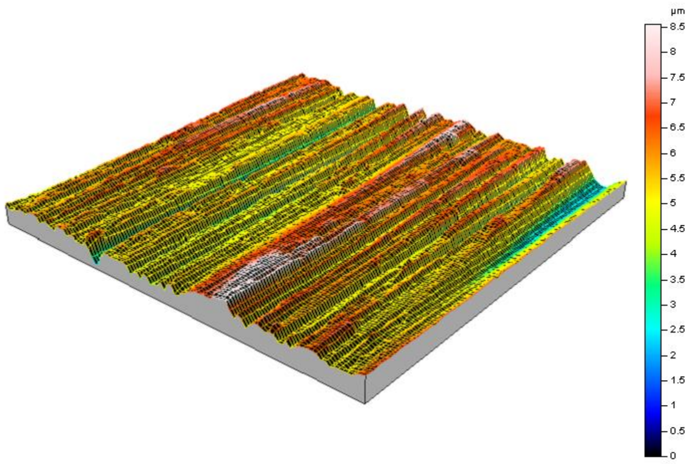

Parameter	Value
Sa	0.898 µm
Sq	1.190 µm
Sp	3.030 µm
Sv	5.530 µm
St	8.560 µm
Sz	7.950 µm
Ssk	-0.86
Sku	3.91

(b)

Figure 36 Analysis of ground surfaces

The ground surfaces (Figure 36) required a least-squares leveling operation using a plane subtraction technique. The initially flat substrates did not require any further form removal. *S* parameters were generated without any further filtering of the datasets.

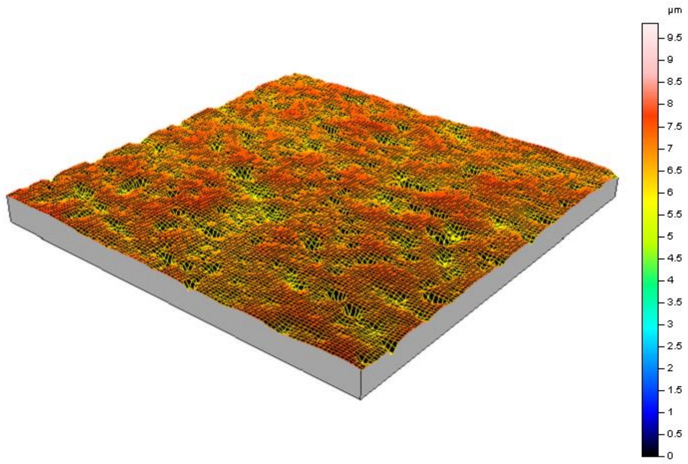

Parameter	Value
Sa	0.355 μm
Sq	0.539 μm
Sp	2.840 μm
Sv	7.010 μm
St	9.850 μm
Sz	7.820 μm
Ssk	-2.87
Sku	16.80

(a)

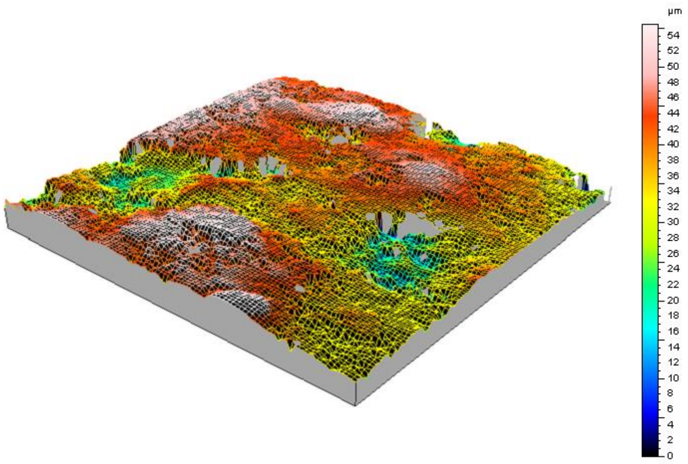

Parameter	Value
Sa	6.560 μm
Sq	8.300 μm
Sp	16.700 μm
Sv	38.900 μm
St	55.600 μm
Sz	49.700 μm
Ssk	-0.832
Sku	3.44

(b)

Figure 37 Analysis of shot blasted surfaces

The shot blasted surfaces (Figure 37) required a least-squares leveling operation using a plane subtraction technique. The initially flat substrates did not require any further form removal. *S* parameters were generated without any further filtering of the datasets.

Limitations of CSI

7

IN THIS CHAPTER

- Data dropout
- Re-entrant features
- Effect of surface gradient
- Fringe order errors
- Dissimilar materials
- Films
- The batwing effect
- Pitch related errors
- Multiple scattering
- Consequences of error sources

Limitations of CSI

CSI is a powerful technique but can have its limitations. For example, the data shown in chapter 6 demonstrate the ability of CSI to generate large data sets and to provide quantitative estimates of surface texture parameters. In the measurement of step artefacts with smooth surfaces such as those used to calibrate CSI instrumentation, it is possible to make traceable measurements with uncertainties of the order of a few nanometers (see chapter 4). It is tempting to assume that this level of accuracy is routinely achievable, however, for the case of machined engineering surfaces, it is found that the measurement uncertainty depends on both the form and the roughness the surface itself as well as the scan algorithm, illumination bandwidth, and measurement speed.

Because the accuracy of CSI is dependent on the surface itself it is not possible to make a general statement of measurement uncertainty. If the general limitations of CSI are understood however, it is possible to identify when CSI would be expected to work at its best and when errors are likely to occur. This chapter the limitations of CSI will be highlighted, including some of the more obvious effects of multiple scattering, and illustrate how errors can be identified and estimated in practice.

From a user's perspective, performing the same task with objective lenses of different numerical aperture or source filters of different bandwidth, can sometimes produce quite different results. The most obvious difference is usually the degree of data dropout or voids in the reported data set. Data dropout occurs when the quality of the fringe data (from which all the surface quantified data and hence parameters are derived) falls below a certain threshold. It is usually a sign that an instrument is working near to or sometimes beyond, the limits of its specification and measurements close to an area of dropout should be treated with caution.

It is possible to reduce dropout rates by changing certain instrument parameters. CSI software usually allows the user to define a minimum fringe modulation threshold and a minimum area over which the fringe data must be of sufficient quality for surface measurements to be reported (see chapter 3). In general reducing the bandwidth of the light source also increases the fringe modulation and consequently reduces the dropout rate. When these adjustments are made, in phase-based methods the user frequently observes abrupt jumps in the data that most often correspond to a height of one half of the mean illuminating wavelength, or equivalently a phase error of 2π radians. Accordingly, jumps of this kind are commonly referred to as fringe order or 2π errors and are another sign that the instrument is working at the limits of its specification.

Very occasionally good quality fringe data masks gross measurement errors. Grooved surfaces are examples of coherent structures that often yield some quite unexpected results but more random scored surfaces can also exhibit errors. This type of error is caused by multiple scattering and this represents a fundamental limitation to CSI.

With this approach we will address three key issues for the CSI user; to assess whether errors are present and if so, to assess whether they are significant, and finally to understand the effect errors may have on derived surface parameters.

Data dropout

Data dropout is a common problem that is frequently observed when CSI is used to characterize engineering surfaces. It is usually a sign that the surface gradient is approaching or has gone beyond the acceptable range for a CSI instrument but can also be indicative of improper focus or a poorly aligned source. Figure 38(a) and Figure 38(b) show data dropout occurring when examining a machined cast iron surface that exhibits voids as a function of the iron-carbon matrix. Figure 38(b) shows the detail of the pit in the surface in the larger image (Figure 38(a)).

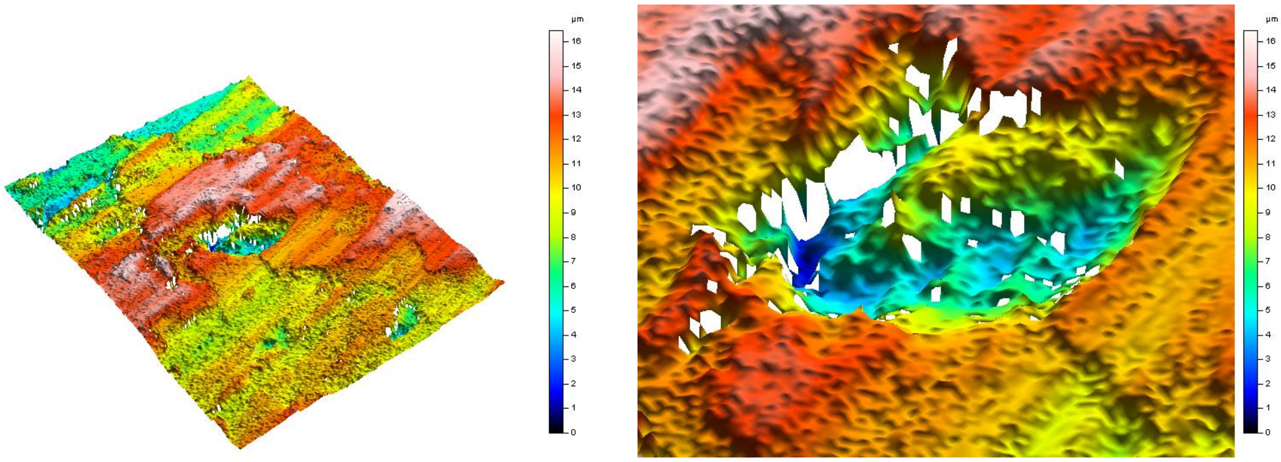

(a) (b)

Figure 38 Data dropout in the measurement of a cast iron surface

It can be seen that the data dropout occurs in well defined regions where the surface gradient is large. On a superficial level, data dropout ruins the appearance of the measured surface image, but it also has more fundamental consequences. Because data dropout is well correlated with surface gradient, simply ignoring its existence will lead to biased estimates of the surface parameters. For example if data dropouts are omitted from calculations, mid-height samples will be under-represented and surface parameters such as *Sa* and *Sq* will be underestimated.

As identified in chapter 6, various software tools exist to allow the user to ‘fill in’ these data voids. As a cosmetic operation this is acceptable, but once again care should be taken if statistical parameters are to be estimated. For example, if linear interpolation is used to fill in the data, mid-height samples will generally be over represented and in this case the *Sa* and *Sq* parameters will be overestimated. It is therefore advisable to process data without filling the data voids, unless it is absolutely necessary to fill the voids.

Re-entrant features

Data dropout occurs for many reasons. Most obviously, data dropout will almost certainly occur if a sample containing re-entrant features is measured. A re-entrant feature is illustrated in Figure 39, and is typified by an oblique pocket in the surface.

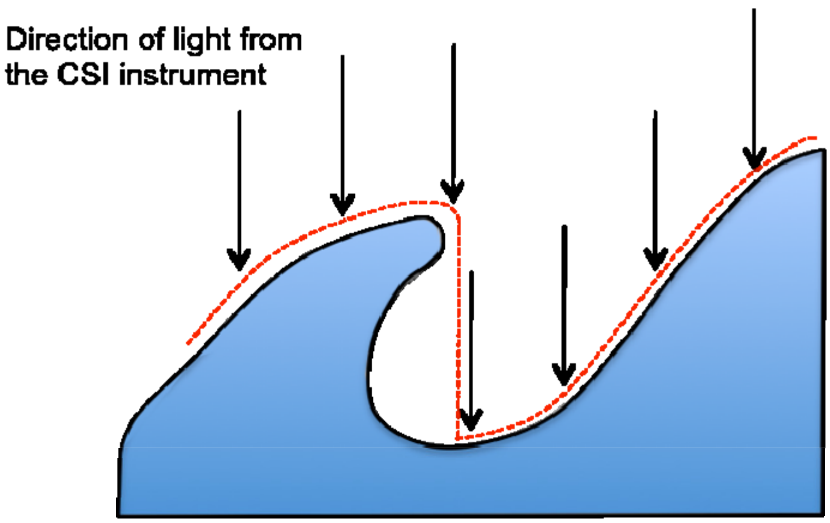

Figure 39 A re-entrant feature on a surface (based on an image from Taylor Hobson Ltd)

Re-entrant features present a challenge to all types of contacting or non-contacting surface texture measuring equipment. The optical path of a non-contact analysis (instrument independent) is illustrated by the black arrows in Figure 39. As the surface is translated from left to right, the return signal and surface profile trace (red dashed line) follows the surface until the point it enters the pocket in the surface.

The line-of-sight nature of current optical sensors typically results in the re-entrant aspect of the pocket (obscured void on the left of the pocket) not being measured properly. The surface profile trace is re-established at the bottom of the pocket and will continue along and out of the pocket. A similar effect occurs with very tall step-like features, where a shadowing effect may not allow for enough light to be reflected back to the objective from the bottom of the step close to the edge.

Effect of surface gradient

For the case of smooth surfaces there is a clear limit to the surface tilt that is acceptable to a CSI instrument. The effect of surface gradient can be seen in Figure 40. This figure shows a measurement of a precision sapphire ball (diameter = 500 µm ± 2 µm) measured with a 50× objective with numerical aperture 0.55. In this measurement, useful data is observed until the surface gradient is greater than 23 degrees where the fringe modulation falls bellow 1 %. The visual result is an incomplete data mesh below 10 µm in Figure 40.

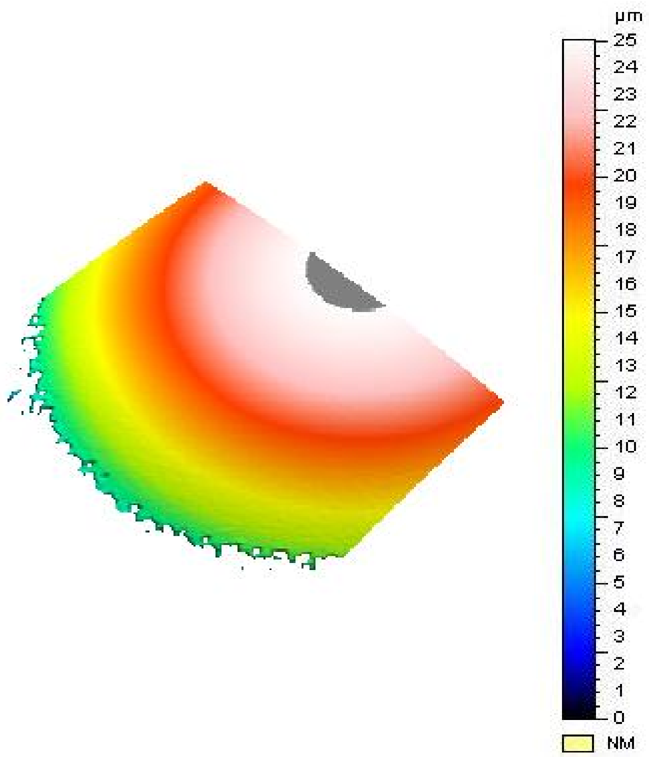

Figure 40 Measurement of a precision sapphire sphere

One reason for the loss of modulation is that at large tilt angles fewer rays will be collected by the objective. Figure 41 shows a tilted specimen and the cone of rays that illuminate the specimen (shown red) and those, after reflection (shown blue).

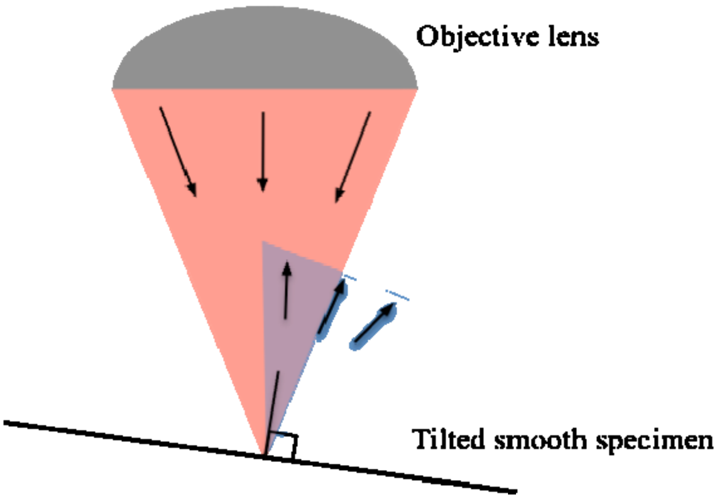

Figure 41 Cones of rays illuminating and reflected from a tilted smooth specimen

As tilt increases, progressively less of the rays that are reflected by the specimen are collected by the aperture of the objective lens. Consequently the signal level decreases and measurement noise increases. If the surface is tilted beyond a certain angle no rays will be accepted by the objective. The cut-off angle θ_{max} is given by,

$$\theta_{\max} = \sin^{-1}(A_N / n) \tag{7.1}$$

where A_N is the numerical aperture and n is the refractive index of the ambient medium (usually air). For a high power 50× objective with a typical A_N = 0.55 operating in ambient air, the maximum tilt angle is approximately 33 degrees, however, fringe modulation often rolls off before this limit is reached.

Figure 42 shows the relative fringe modulation observed when measuring a plane, tilted specimen using 5× (Michelson), 10× (Mirau) and 50× (Mirau) objectives of differing numerical aperture. Experimental data (ex) is compared with theoretical predictions (th).

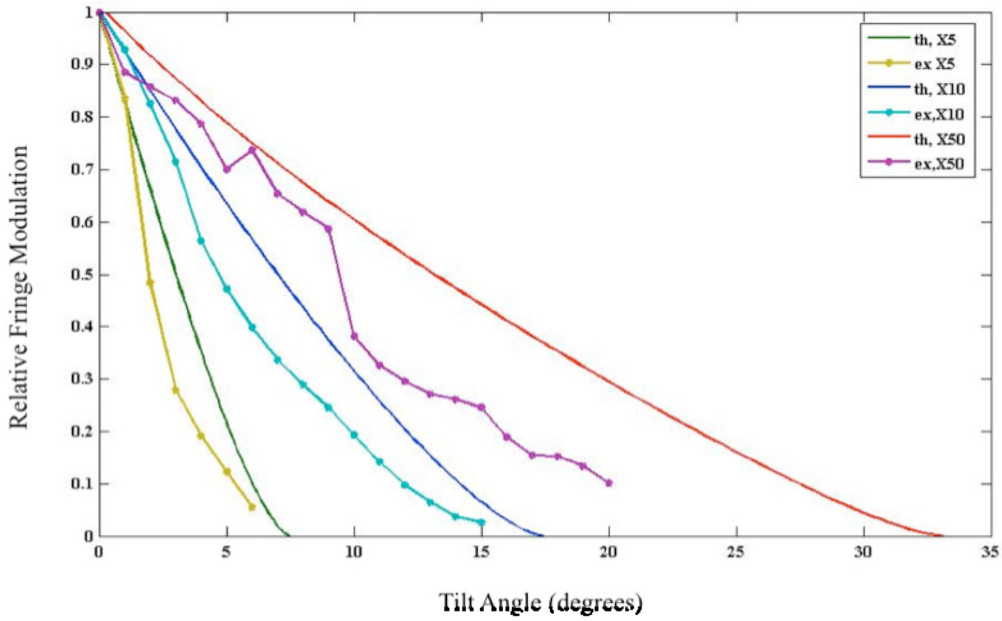

Figure 42 Relative fringe modulation as a function of specimen tilt

In each case the fringe modulation has been normalized to be unity at zero tilt. For the case of low power low numerical aperture objectives, the measured data tends to closely follow the theoretical curves that correspond to the fraction of the incident intensity collected by the objective as illustrated in Figure 41. For the case of the 50× objective with a significantly higher $A_N = 0.55$ the fringe modulation rolls off slightly quicker than is expected.

The results presented in Figure 42 show that for the case high numerical aperture objectives, the roll off in fringe modulation as a function of surface tilt cannot be explained purely in terms of the loss of rays collected by the lens. Close inspection of the fringe data shows that in general the fringe envelope also broadens as the specimen is tilted and this further reduces the fringe modulation. In principle, this effect diminishes as the bandwidth of the source increases, however, the fringe modulation is also affected by residual chromatic aberration in the objective lens that has the opposite effect.

Surface tilt and rough surfaces

Rough surfaces behave in a different manner. There are two separate cases to consider. Surfaces such as that shown in Figure 43 can be considered to be smooth on a piecewise basis. That is, the lateral scale of the rough surface features is greater than the lateral resolution of the objective. In this case we can expect the modulation of the fringes recorded at a given location to roll off as a function of gradient in the same way as a smooth surface. If, however, the scale of the surface roughness is smaller than the lateral resolution of the objective then the situation is quite different. If the surface features are not resolved by the objective then the spatial statistics of the scattered field must be considered carefully.

When the roughness parameter (Ra) is greater or comparable to the mean effective wavelength then the surface can be considered to consist of an infinite number of point-scatterers. In general a rough surface with these characteristics will scatter in all directions and the objective will collect a proportion of this as shown in Figure 42.

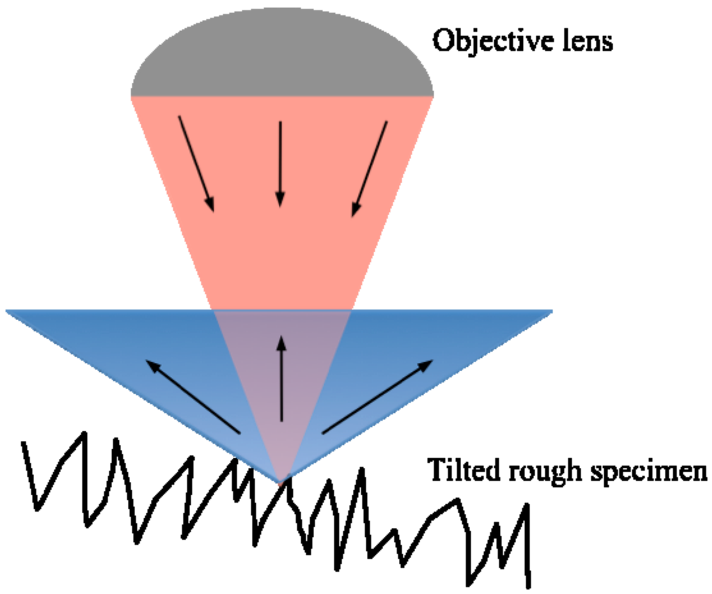

Figure 43 Cones of rays illuminating and reflected from a tilted rough specimen

Because the light is scattered more or less isotropically it is possible to measure rough surfaces with gradients that exceed θ_{max}. Figure 44 is an example of a measurement of a surface tilted at a measured angle of 23.5 degrees. The surface measurement was made with a 10× objective (numerical aperture 0.3) and no measurement (NM) is reported below a modulation threshold value of 8 %.

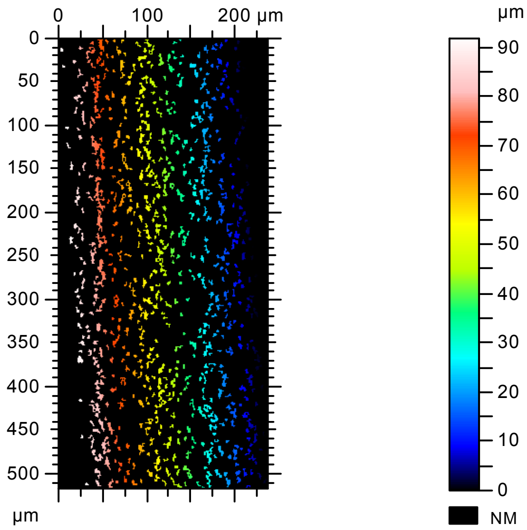

Figure 44 Measurement of a rough tilted surface with a 10× objective

Although the surface tilt is significantly more than the cut-off (θ_{max} = 19 degrees) the surface tilt can clearly be seen. There is however, a significant amount of data dropout. By considering the reflected field to be the superposition of the fields generated by random sources, these observations can be explained. In this case the image of given area of the surface will only appear bright if the contributing sources interfere constructively. In general the criteria for constructive interference will be a function of wavelength and it is possible for parts of the surface to scatter strongly over some parts of the spectrum and less so in others. Moreover, the phase of the various scattered components will also be a function of wavelength, having the effect of reducing the fringe modulation and consequently increasing the dropout rate.

Bandwidth narrowed source

For the case of rough surfaces data dropout can be reduced by narrowing the bandwidth of the source spectrum. Many instruments supply an interference filter for this purpose or use multiple sources of differing bandwidths. Figure 45 shows the same measurement as Figure 44 but now using a filter of 40 nm bandwidth (rather than the full original instrument bandwidth which can be up to 300 nm). Once again, no measurement (NM) is reported below a fringe modulation threshold value of 8 %.

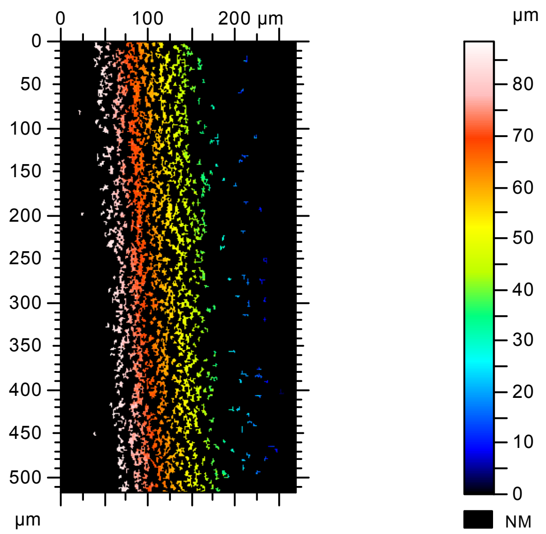

Figure 45 Re-measurement of surface in Figure 44 using line narrowing filters

In this case the rate of data dropout has clearly reduced. This is because an interference filter increases the coherence length of the source and will, in general, broaden the fringe envelope. Its effect will depend on the surface roughness (*Ra*) parameter. As a rule of thumb the filter will reduce data dropout if the surface roughness, *Ra,* is less than the coherence of the source, or equivalently, the axial extent of the fringe envelope such that,

$$Ra < \frac{\bar{\lambda}^2}{2\Delta\lambda} \tag{7.2}$$

Where $\bar{\lambda}$ is the mean effective wavelength and $\Delta\lambda$ is the wavelength range transmitted by the filter. It should be noted, however, that as the fringe envelope broadens the detection of its centroid is less precise. The use of a line narrowed source therefore reduces data dropout but increases uncertainty.

Finally, it is important to realize that when measuring rough surfaces with roughness parameters greater than one half of the mean wavelength of the source and at scales less than the lateral resolution of the microscope objective, the phase of the fringe data does not correlate well with the surface profile and random phase jumps are observed in the fringe data. Because of this, the extra resolution afforded by phase measurement cannot be exploited in this regime and for this reason measurements based on the position of the fringe envelope should always be used. It should also be noted that roughness parameters from steep, rough surfaces that are beyond the normal slope limitation of the objective should be treated with caution. In these cases the form information may be treated with more confidence.

Fringe order errors

In many cases, jumps in the data that correspond to one fringe or half the mean effective wavelength of the illuminating light, are observed when using techniques that combine phase and the position of the fringe envelope. These are generally referred to as fringe order or 2π errors. The origins of this type of error are varied and depend on the type of processing that is applied to the fringe data.

A good example of fringe order errors is shown in Figure 46. In this case the sample is a sinusoidal profile grating with an amplitude of approximately 200 nm and was measured using a 50× objective with a numerical aperture of 0.55. Although the parts of the profile that have small gradients have been characterized well, jumps corresponding to approximately 300 nm are evident in areas of increased slope.

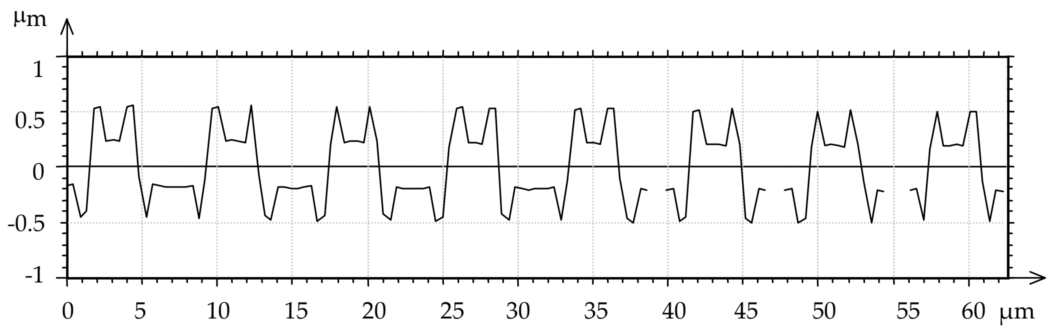

Figure 46 2π or fringe order errors observed in the measurement of a sinusoidal grating

In practice, it is found that fringe order errors can occur when the surface gradient is considerably smaller than the cut-off angle θ_{max}. Figure 47 shows the effect of the numerical aperture of the lens and is illustrated when examining a material measure. Here, the artefact has been measured using a 5× lens (Figure 47(a)) with a numerical aperture value of 0.13, with a 10× lens (Figure 47(b)) with a numerical aperture value of 0.3 and a 50× lens (Figure 47(c)) with a numerical aperture value of 0.55. In the first example, it is clear that the artefact surface contains data voids where the gradient is largest, in the second example the data voids are substantially reduced and in the third example the data set is almost complete.

(a)

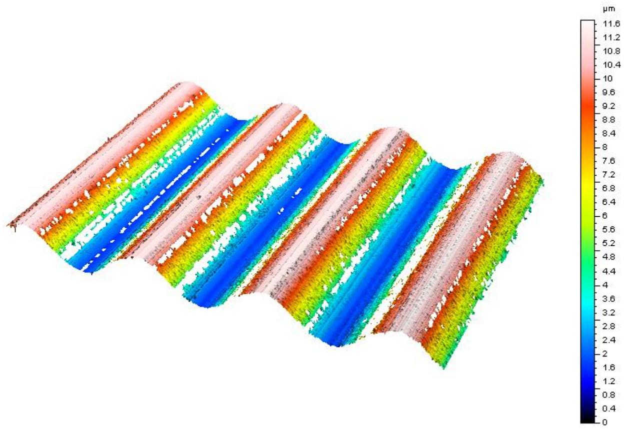

(b)

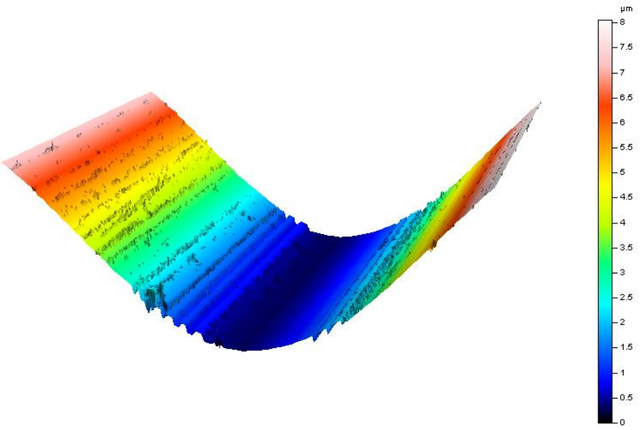

(c)

Figure 47 Material measure measured with three different objectives (5×, 10× and 50×)

In Figure 47(c) periodic "ripples" of 300 nm steps in the data corresponding to half the mean effective wavelength can be observed and these are immediately recognized as fringe order errors. In principle fringe order errors can be removed by adding or subtracting integer multiples of 2π radians to the phase to minimize the occurrence of discontinuities in the profile, however, this approach is only applicable if the surface is known to be continuous.

Ghost steps

An extreme example of fringe order errors are the so-called ghost steps that have been reported when measuring perfectly flat objects. Ghost steps again only occur with certain measurement techniques, and can be triggered by a field dependent aberration. They are generally a sign that the instrument is not properly aligned. Aberration causes the analysis software to 'switch' to a higher (or lower) order fringe resulting in a discontinuity of half the mean effective wavelength in the estimate of surface profile.

Dissimilar materials

If a substrate is composed of different materials (such as chrome layer deposited on a glass substrate), each material will affect a different phase change on reflection. This phase change will add or subtract to that resulting from the change in profile. Figure 48 shows the CSI measurement image of a NPL chrome line width standard, previously measured as being 60.8 nm high using a contact stylus instrument. Low contrast interference fringes can be seen on the left and right of the image, on top of the glass substrate. High contrast interference fringes can be seen down the middle of the image, on top of the deposited chrome.

The optical phase change effect can be seen as a mismatch in fringe position between the glass and the chrome. Repeated CSI measurements recorded the height of the chrome to be 37.3 nm, *i.e*. 23.5 nm lower than the stylus instrument results. A theoretical calculation shows that the expected phase change across the two materials should produce a step deviation of at least 19.5 nm, which agrees well with the error of measurement from the CSI results.

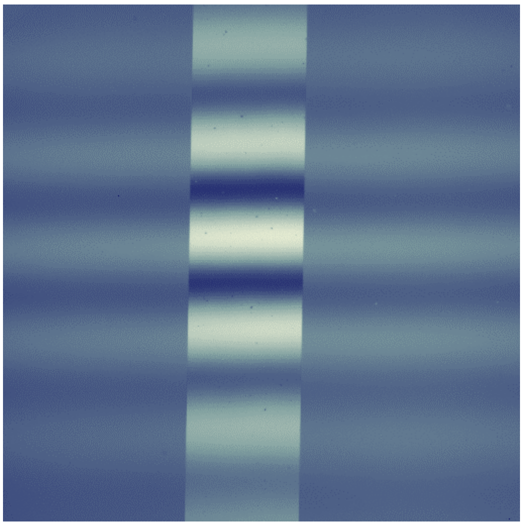

Figure 48 NPL chrome line width standard showing area of measurement

Phase changes are typically less than 45 degrees and correspond to surface height errors of less than 30 nm. If the user has knowledge of the optical properties of the materials under investigation and the materials are opaque, then it is possible to correct for this behaviour. Corrections or verification can possibly be achieved using alternative measurement techniques.

Films

If a sample has a transparent film on it, of thickness less than the total scan distance of the instrument, the air-film boundary and film-substrate boundary can both contribute to the overall measurement result. This can lead to inaccurate height information, and may sometimes even cause tall features to report as lower in height than their surroundings. Some instruments have a film mode that can separate out the signals and provide topographic and thickness information on each of the layers. For thin films (those less than about 2 μm in thickness), or films with widely varying index of refraction across the film, this is often not possible. Whenever measuring films, care must be taken when interpreting the results. Gold coating a representative sample, such that it is opaque across its entire surface, can often be employed to see what the effect of the film is and if it is significant.

The batwing effect

The batwing effect is a well known example of an error that is observed around a step discontinuity in a surface especially for the case of a step height that is less than the coherence length of the light source. This problem is called the batwing effect because of the shape of the error, and is usually explained as the interference between reflections of waves normally incident on the top and bottom surfaces following diffraction from the edge. Figure 49 shows the batwing effect when a 5 μm pitch square wave grating with 185 nm step height is measured using a CSI instrument. The ideal grating profile is illustrated with the dashed line.

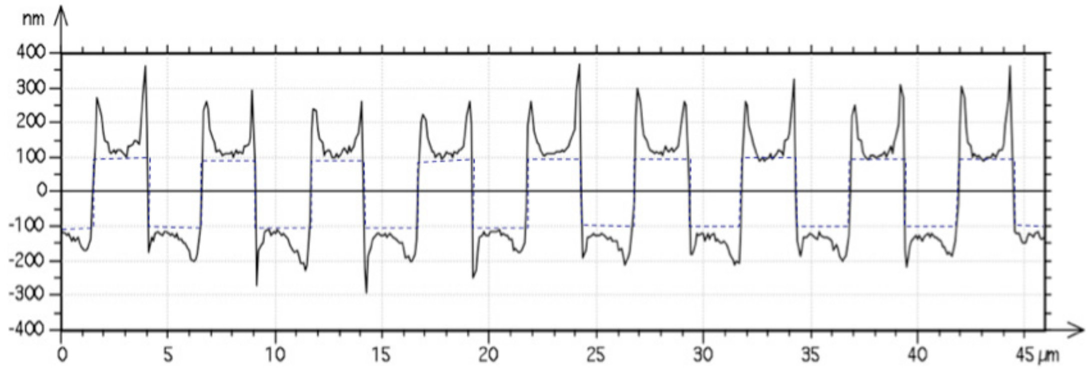

Figure 49 Example of the batwing effect

An additional issue is that a CSI instrument does not give the correct surface height at the positions close to the step even if the step height is significantly greater than the coherence length. This is caused by a combination of both shadowing and the way in which the optical field diffracts around the discontinuity. In this case the measurement error is small but still significant compared to the instrument resolution

Pitch related errors

It is generally found that errors (particularly fringe order errors) increase in frequency as the scale of surface features approach the mean effective wavelength of the instrument. For instance, for a white light source the mean effective wavelength is approximately 500 nm with pitch errors starting to become an issue below approximately 1.5 µm. This is illustrated in Figure 50 that shows the measurement of a star pattern etched in silicon using a 50× objective lens and a zoom setting of 0.4×, 1× and 2× respectively.

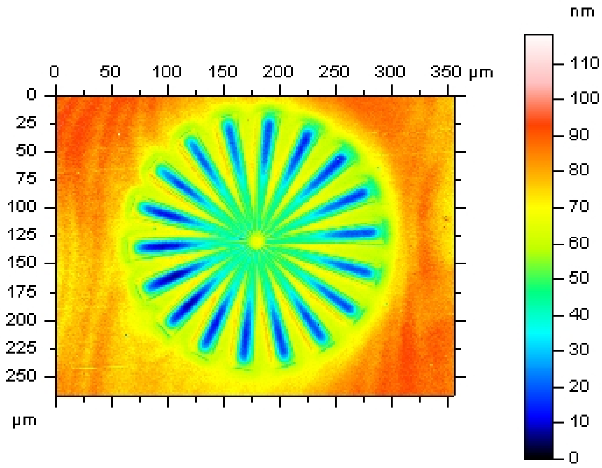

(a)

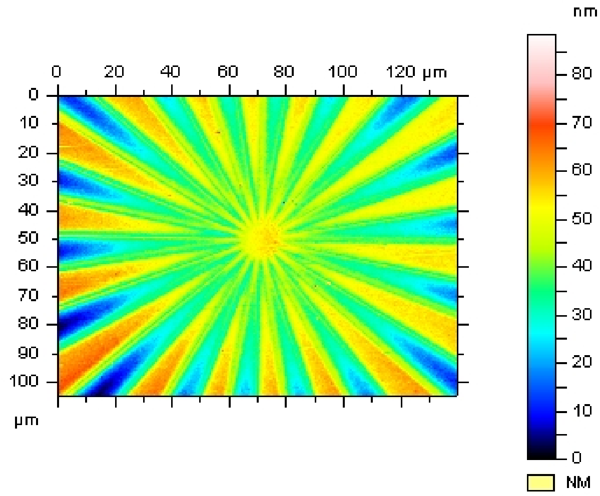

(b)

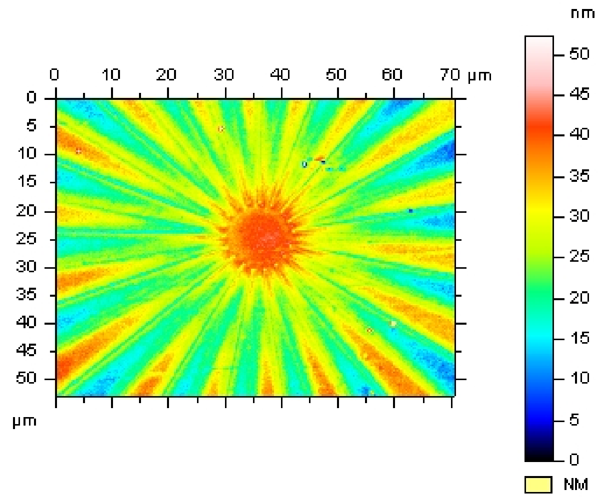

(c)

Figure 50 Analysis of an etched star pattern using

The star pattern provides an indication of the CSI capability over a range of different and reducing spatial frequencies. Generally the upper and lower surfaces of the etched star pattern are correctly located, although frequent fringe order errors occur at the step discontinuities and these errors increase toward the centre where the pitch spacing reduces to approximately 1.75 µm. These plots show that when the pitch of the artefact approaches the lateral resolution of the objective lens, errors are more likely to occur. Errors depend strongly on the type of processing used (CSI or PSI/CSI) and on aberrations introduced by the objective lens. It is also possible that some errors are introduced by multiple scattering of the illumination around the discontinuities. This is discussed in more detail in the following section.

Multiple scattering

Although in general CSI is unlikely to report measurements when the surface gradient is greater than the cut off angle of the objective, this is not always the case. As we have seen, rough surfaces can provide data in this instance but this is usually accompanied by low fringe modulation and high levels of data dropout. In certain circumstances, however, high modulation fringes can be observed beyond the cut off angle and seemingly good quality but nevertheless erroneous measurements are reported.

If a 70 degree silicon V-groove is measured, for example, a clear peak can be seen at the bottom of the profile due to multiple reflections (scattering) as shown in the 2D cross-section in Figure 51.

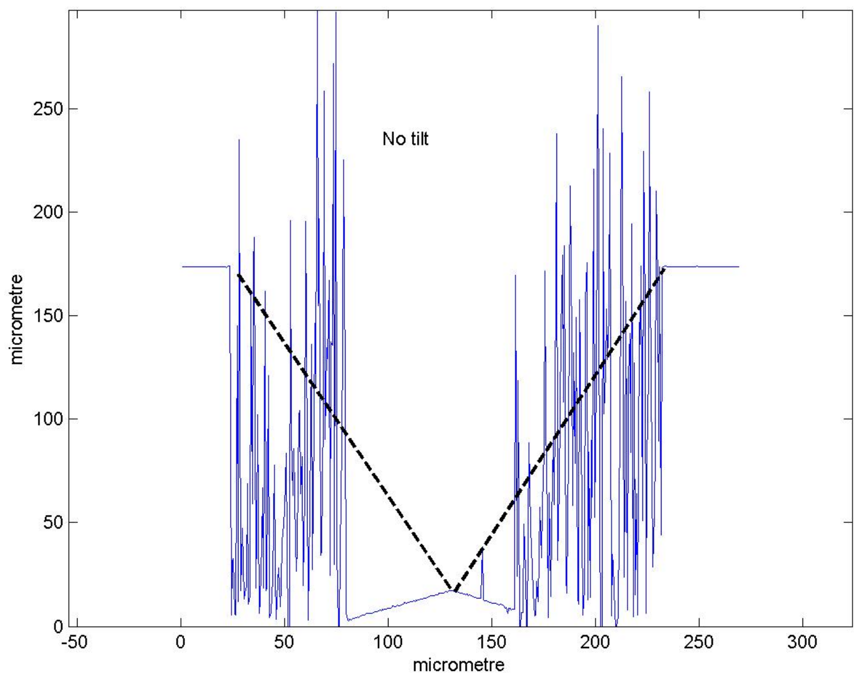

Figure 51 V-groove initial measurement

At the edge of the profile the top surface of the silicon substrate appears at the expected position. At the top of the V-groove the signal quality is poor and the measurement produces noise (blue spiked signal). This might be expected because the walls of the V-groove are smooth and inclined at 54.74 degrees to the horizontal, i.e. outside the acceptance cone of the objective lens and thus no valid data should be expected. However, a good signal is obtained and an apparently valid measurement is made at the bottom of the V-groove where a clear peak profile is shown, where in reality there should be a trough.

A basic ray analysis of the problem in Figure 52 shows that this error is caused by multiple reflections inside the V-groove, which cause the light emitted by the CSI instrument to be reflected three times from the groove walls, before being imaged by the microscope objective. This is then interpreted by the CSI instrument as an overly deep measurement in essence because a single scattering event is assumed. Many examples of this type of signature may be found on measured surfaces, where surface scratches are seen with no wall sides, and an inverted profile at the bottom of the scratch.

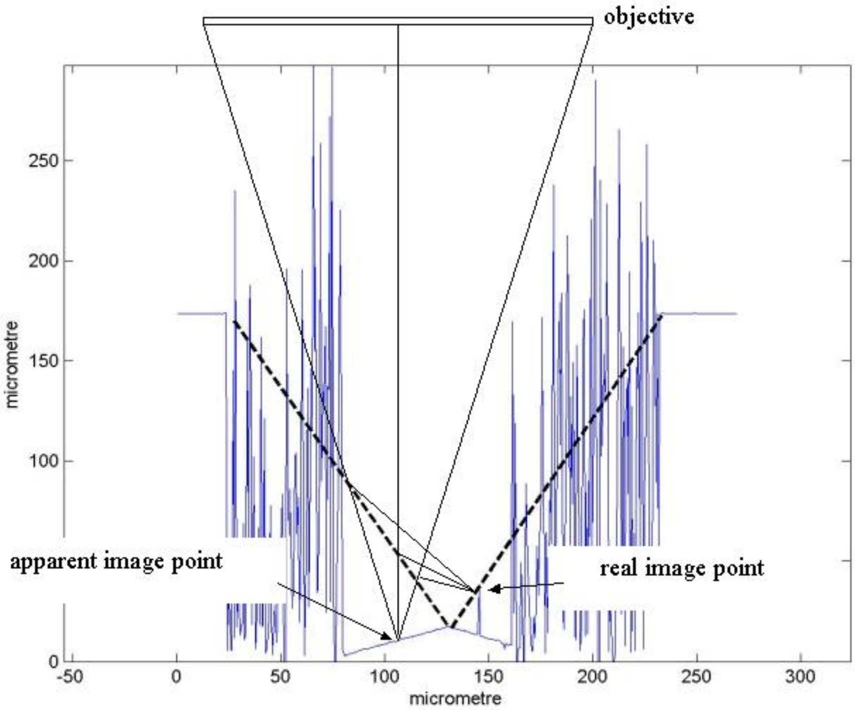

Figure 52 Ray tracing of the light in the V-groove

An engineering surface is often characterized by a range of scratches or grooves with varying internal angles. If the multiple reflections occur during measurement, the surface plots will include many examples of incorrect surface representation, and surface roughness quantification could be over estimated. In the same way, other artefacts such as pits (a conic profile is a straight forward example) would show as a blank sided hole with a small nipple, pyramid or inverted cone at the bottom. These issues are illustrated in Figure 53, which shows an aluminium surface with two intersecting scratches on the surface (Figure 53(a)) and a copper surface with a scratch (Figure 53(b)).

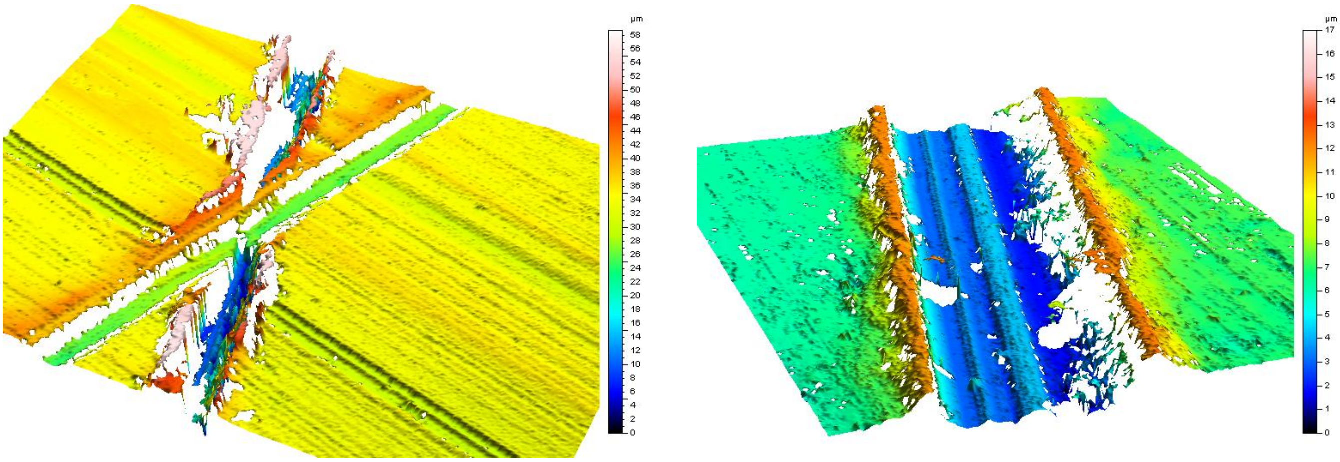

(a) **(b)**

Figure 53 Scratches in surfaces

In all cases it is noted that although measurements with significant modulation are usually returned from indented or grooved artefacts, the bottom always appears quite smooth. For this reason estimates of surface roughness parameters are likely to be overestimated.

Consequences of error sources

In this chapter the main limitations of CSI have been identified. Although modern well setup CSI instruments are able to measure a step height with an accuracy of better than 1 nm, this can rarely be repeated for more general surfaces. In practice, it is noticeable that data dropout increases as the gradient or tilt of the surface increases, and for a given objective lens, a cut-off angle exists beyond which data is not reported. Before this angle is reached however, it is often possible to see rapid jumps in the data that often correspond to a multiple of half the mean effective wavelength. These are 2π or fringe order errors that occur when the instrument identifies the central or zero order fringe incorrectly.

The mechanisms responsible for these errors are varied. They occur in part because neighbouring points in the image cannot be viewed as independent interferometers, their response is coupled and mixed by the optical transfer function of the imaging system. The effect of this mixing is noticeable when the surface gradient changes quickly and is exemplified by the batwing effect that is observed at step discontinuities. The coupling effect is also responsible for fringe order errors that have been observed in the measurement of periodic surfaces more noticeably as the pitch of the structure becomes comparable with the lateral resolution of the objective. Of course, optical aberrations that decrease resolution, exacerbate the mixing process and, when the aberration is field dependent, can result in ghost steps that have been observed at a well defined positions in the image.

More fundamental errors occur because light is scattered more than once from the surface of interest before it is collected at the detector. Current CSI instruments assume a single scattering event and can report significant errors when this is not the case. The effects of multiple scattering are most apparent when measurements are attempted on multifaceted steep sided surfaces such as V-grooves but are also present on most artefacts with scored or scratched surfaces.

In most cases errors occur in areas that return fringe data with poor modulation and for this reason most instruments will only report data that is above a certain modulation threshold. As the modulation rolls off with increasing surface tilt, however, merely setting a high threshold often removes undesirable quantities of valid data and an experienced user will identify errors and set the threshold accordingly. Frequently errors change or disappear in certain regions if the sample is tilted. In the case of surface structures with multiple facets this is particularly noticeable as the reflections between facets change their nature rapidly with surface tilt. However, tilting a surface to reduce error terms in one area, may increase error terms in another area.

More generally errors, also depend strongly on the algorithms used to analyse the fringe data. Often, the most noticeable difference is switching between surface measurements derived from the position of the fringe envelope (CSI mode) and that obtained from the phase of the fringes (PSI mode).

Changes in the reported measurements that occur as a result of modifications in the instrument parameters provide the best indication of measurement errors. For this reason it is good practice to repeat measurements under varying conditions whenever possible. Future development of CSI instruments may eventually lead to the ability to correlate results with an appropriate theoretical model or surface response in order to better estimate measurement uncertainty.

For the user, it is very difficult to estimate how these errors will influence the values of any areal parameters generated from the analysis of a surface. In some geometrically simple examples (for instance when surfaces are composed of very regular features) then it may be possible to systematically reduce the error terms present in the measurement and refine the confidence in the parameter values.

For surfaces that are geometrically complex (randomly rough surfaces) then many error sources may be simultaneously present and it may not be possible to remove, compensate for them, or estimate their combined influences. Therefore, currently the best advice for the user is to compare results with the known limitations of CSI as outlined in this chapter, and make a more qualitative estimate of validity.

Appendix

Links to other useful sources of information

National and international organizations

National Physical Laboratory

The National Physical Laboratory (NPL) is the UK's National Measurement Institute and is a world-leading centre of excellence in developing and applying accurate measurement standards, science and technology. For more than a century NPL has developed and maintained the nation's primary measurement standards. These standards underpin an infrastructure of traceability throughout the UK and the world that ensures accuracy and consistency of measurement.

NPL ensures that cutting edge measurement science and technology have a positive impact in the real world. NPL delivers world-leading measurement solutions that are critical to commercial research and development, and support business success across the UK and the globe.

Good measurement improves productivity and quality; it underpins consumer confidence and trade and is vital to innovation. NPL undertakes research and shares its expertise with government, business and society to help enhance economic performance and the quality of life.

NPL's measurements help to save lives, protect the environment, enable citizens to feel safe and secure, as well as supporting international trade and companies to innovation. Support in areas such as the development of advanced medical treatments and environmental monitoring helps secure a better quality of life for all. NPL is a world-leading centre in the development and application of highly accurate measurement techniques. As the UK's national standards laboratory, NPL underpins the National Measurement System (NMS), ensuring consistency and traceability of measurements throughout the UK. NPL offers a unique range of measurement services, contract research, consultancy and training services. Other areas of expertise include the design and characterisation of engineering materials, and mathematical software, especially its application to measurement and instrumentation.

For more information on the wide range of metrology services, facilities and research work carried out at NPL either visit the NPL web site at www.npl.co.uk or contact the NPL Helpline: +44 20 8943 6880

EURAMET - European Association of National Metrology Institutes

The European Association of National Metrology Institutes (EURAMET) is the Regional Metrology Organisation (RMO) of Europe. On 1st July 2007 EURAMET e.V. became the successor to EUROMET – the previous RMO which had coordinated European metrology needs for over twenty years. EURAMET coordinates the cooperation of National Metrology Institutes (NMIs) of Europe in fields like research in metrology, traceability of measurements to the SI units, international recognition of national measurement standards and of the Calibration and Measurement Capabilities (CMC) of its members.

EURAMET currently has thirty-two members (including NPL), five associate members and operates twelve Technical Committees, one for each physical metrology subject field, plus committees dealing with interdisciplinary metrology and quality matters. More details and information about the many cooperative projects run by EURAMET and its members can be found on the EURAMET web site: www.euromet.org.

NPL Measurement Network

The network is for anyone with an interest in measurement. It enables measurement knowledge to be shared between NPL scientists and network members by providing a forum for the exchange of information and advice between members and other measurement experts. It does this through a programme of seminars and conferences and by involving members in working groups or other activities tailored to their own particular interests.

Network members include people from a range of business sectors, including energy, transport and manufacturing, defence and security, healthcare, instrument manufacturers, calibration laboratories and academic institutions. If measurement is important for your job or organisation, then becoming a member will give you access to measurement information and contacts relevant to you.

There are six special interest groups within the network:

• Engineering & optical
• Materials & surface analysis
• Ionising radiation
• Communications & electromagnetics
• Environment & energy
• Biotech & healthcare

These groups provide a focus on a particular area of technology or interest. They ensure that we hold events that are relevant to the needs of our members, build links with partner organisations, and seek input to NPL's scientific work from members.

For further information about the Network:
Our website: www.npl.co.uk/measurement-network
Email: measurement_network@npl.co.uk
Phone: 020 8943 8742/6005

Traceability

Traceability in measurement is the concept of establishing a valid calibration of a measuring instrument or measurement standard, by a step-by-step comparison with better standards up to an accepted or specified standard. In general, the concept of traceability implies eventual reference to an appropriate national or international standard.

The National Physical Laboratory is the United Kingdom's national measurement institute. It operates at the heart of the National Measurement System (NMS) which is the infrastructure designed to ensure accuracy and consistency in every physical measurement made in the UK. Chains of traceability link UK companies' measurements directly to national standards held at NPL.

For the majority of industrial applications, companies can establish a link to national measurement standards through the calibration and testing services offered by United Kingdom Accreditation Service (UKAS) accredited laboratories, which are in turn traceable to NPL. However, for challenging or novel measurements to the highest standards of accuracy, which are not catered for by UKAS accredited laboratories, NPL can often provide a traceable measurement solution directly to industry.

UKAS is the sole national body recognised by government for the accreditation of testing and calibration laboratories, certification and inspection bodies. A not-for-profit company, limited by guarantee, UKAS operates under a Memorandum of Understanding with the government through the Department of Business, Innovation and Skills .

UKAS accreditation demonstrates the integrity and competence of organisations providing calibration, testing, inspection and certification services. Further information on UKAS can be found at www.ukas.com

Training courses

Good measurement supports the technical infrastructure, which leads to new and competitive products with efficient processes. However, knowing how to use a measurement tool is not the same as knowing how to use measurement as a tool. Measurement is a science to be applied with skill, not a manual.

Understanding the principles of measurement can lead to better decisions on product purchasing, reduced need for expensive technical support and reduced operational mistakes with expensive consequences. A better understanding of measurement will reduce the risks to your business.

NPL is able to provide a variety of practical application-based bespoke training courses from optical and laser technology to statistical modelling. The majority of our courses are organised to meet the specific requirements of the customer. To enquire about NPL developing you a bespoke course please contact the NPL Helpline.

NPL also has a training framework for Dimensional Metrology. The NPL-Training for Dimensional Metrology is divided into four levels, covering measurement users to measurement strategy definers, always through a practical hands-on approach:

Level 1 – Measurement User:
Uses measurement knowledge and expertise
Level 2 – Measurement Applier:
Applies measurement knowledge and expertise
Level 3 – Measurement Developer:
Develops and extends measurement knowledge and expertise
Level 4 – Measurement Definer:
Defines new and leading edge application of measurement knowledge

For further information visit the NPL training at www.npl.co.uk/training or contact the NPL Helpline: +44 20 8943 6880.

International standards

International Organization for Standardization

The International Organization for Standardization (ISO) is a worldwide federation on national standards bodies from some 140 countries.

The mission of ISO is to promote the development of standardisation and related activities in the world with a view to facilitating the international exchange of goods and services, and to develop cooperation in the sphere of intellectual, scientific, technological and economic activity.

ISO's work results in international agreements that are published as International Standards. Further information of ISO can be found at www.iso.ch

ISO surface texture standards

The following ISO specification standards relate to the measurement of profile using stylus instruments and are included in this guide for completeness.

ISO 3274 (1996) Geometrical product specifications (GPS) – Surface texture: Profile method – Nominal characteristics of contact (stylus) instruments
ISO 4287 (1997) Geometrical product specifications (GPS) – Surface texture: Profile method – Terms, definitions and surface texture parameters
ISO 4288 (1996) Geometrical product specifications (GPS) – Surface texture: Profile method – Rules and procedures for the assessment of surface texture
ISO 5436 (2000) Geometrical product specifications (GPS) – Surface texture: Profile method – Measurement standards – Part 1 Material measures
ISO 11562 (1996) Geometrical product specifications (GPS) – Surface texture: Profile method – Metrological characteristics of phase correct filters
ISO 13565 (1996) Geometrical product specifications (GPS) – Surface texture: Profile method; Surface having stratified functional properties – Part 1: Filtering and general measurement conditions

ISO 13565 (1996) Geometrical product specifications (GPS) – Surface texture: Profile method; Surface having stratified functional properties – Part 2: Height characterization using the linear material ratio curve
ISO 13565 (2000) Geometrical product specifications (GPS) – Surface texture: Profile method; surfaces having stratified functional properties – Part 3: Height characterization using the material probability curve
ISO 12085 (1996) ISO 13565 (1996) Geometrical product specifications (GPS) – Surface texture: Profile method – Motif parameters

The areal specification standards are at various stages of development. The plan is to have the profile standards as a subset of the areal standards (with appropriate re-numbering). Hence, the profile standards will be re-published after the areal standards (with some omissions, ambiguities and errors corrected) under a new numbering scheme that is consistent with that of the areal standards. All the areal standards are part of ISO 25178 which will consist of at least the following parts, under the general title Geometrical product specification (GPS) — Surface texture: Areal:

- Part 1: Areal surface texture drawing indications
- Part 2: Terms, definitions and surface texture parameters (published 2010)
- Part 3: Specification operators
- Part 4: Comparison rules
- Part 5: Verification operators
- Part 6: Classification of methods for measuring surface texture (published 2010)
- Part 70: Measurement standards for areal surface texture measurement instruments
- Part 71: Software measurement standards
- Part 72: Software measurement standards – XML file format
- Part 601: Nominal characteristics of contact (stylus) instruments (published 2010)
- Part 602: Nominal characteristics of non-contact (confocal chromatic probe) instruments
- Part 603: Nominal characteristics of non-contact (phase shifting interferometric microscopy) instruments

- Part 604: Nominal characteristics of non-contact (coherence scanning interferometry) instruments
- Part 605: Nominal characteristics of non-contact (point autofocus) instruments
- Part 606: Nominal characteristics of non-contact (variable focus) instruments
- Part 701: Calibration and measurement standards for contact (stylus) instruments (published 2010)
- Part 702: Calibration and measurement standards for non-contact (confocal chromatic probe) instruments
- Part 703: Calibration and measurement standards for non-contact (phase shifting interferometric microscopy) instruments
- Part 704: Calibration and measurement standards for non-contact (coherence scanning interferometry) instruments
- Part 705: Calibration and measurement standards for non-contact (point autofocus) instruments
- Part 706: Calibration and measurement standards for non-contact (variable focus) instruments

General interest

PD 6461 (1995) Vocabulary of metrology – Part 1. Basic and general terms (international)
PD 6461 (1995) Vocabulary of metrology – Part 2. Vocabulary of legal metrology – fundamental terms
PD 6461 (1995) Vocabulary of metrology – Part 3. Guide to the expression of uncertainty in measurement

Semiconductor Equipment and Materials International (SEMI)

SEMI is a volunteer-driven organisation for the exchange of information amongst users and suppliers in the semiconductor industry and flat panel display industries. Approximately 1300 technologists worldwide participate in the development of specifications and standards for these technologies. The documents are published as the SEMI Book of Standards and are available on the web at www.semi.org

Literature

Surface texture books

Blunt L, Jiang X 2003 Advanced techniques for assessment surface topography (Kogan Page Science)

Leach R K 2001 The measurement of surface texture using stylus instruments NPL Good Practice Guide No. 37 (available from www.npl.co.uk)

Leach R K 2009 Fundamental principles of engineering nanometrology (Elsevier: Amsterdam)

Leach R K, Blunt R, Conroy M, Mauger D 2008 Guide to the measurement of smooth surface topography using coherence scanning interferometry, NPL Good Practice Guide No. 108 (available from www.npl.co.uk)

Mainsah E, Greenwood J A, Chewynd D G 2001 Metrology and properties of engineering surfaces (Kluwar Academic Publishers)

Muralikrishnan B, Raja J 2008 Computational surface and roundness metrology (Springer)

Smith G T 2001 Industrial metrology: surface and roundness (Springer-Verlag)

Stout K J, Blunt L 2000 Three dimensional surface topography (Prenton Press)

Thomas T R 1999 Rough surface 2nd edition (Imperial College Press: London)

Whitehouse D J 1994 Handbook of surface metrology (Taylor & Francis)

Whitehouse D J 1993 Handbook of surface and nanometrology (CRC Press)

General measurement and instrumentation books

Bell S 2001 A beginner's guide to uncertainty of measurement NPL Good Practice Guide No. 11 (available from www.npl.co.uk)

Birch K 2001 Estimating uncertainties in testing NPL Good Practice Guide No. 36 (available from www.npl.co.uk)

Flack D R, Hannaford J 2005 Fundamental good practice in dimensional metrology NPL Good Practice Guide No. 80 (available from www.npl.co.uk)

Rastogi P K 1997 Optical measurement techniques and applications (Artech House Inc)

Smith S T, Chetwynd D G 1992 Foundations of ultraprecision mechanism design (Gordon & Breach Science Publishers)
Steel W H 1987 Cambridge studies in modern optics – interferometry (Cambridge University Press)
Williams D C 1993 Optical methods in engineering metrology (Chapman & Hall)